İSTANBUL TECHNICAL UNIVERSITY ★ INSTITUTE OF SCIENCE AND TECHNOLOGY

MULTIDIMENSIONAL MODELING OF HOMOGENEOUS CHARGE COMPRESSION IGNITION ENGINES

M.Sc. Thesis by
Alper KUTLUATA
(503001507)

Date of submission : 13 May 2002
Date of defence examination: 29 May 2002

Supervisor (Chairman): Prof. Dr. Cem SORUŞBAY
Members of the Examining Committee Prof.Dr. Metin ERGENEMAN(İ.T.Ü.)
Prof.Dr. Orhan DENİZ(Y.T.Ü.)

MAY 2002

İSTANBUL TEKNİK ÜNİVERSİTESİ ★ FEN BİLİMLERİ ENSTİTÜSÜ

HOMOJEN KARIŞIMLI SIKIŞTIRMALI ATEŞLEMELİ MOTORLARIN ÇOK-BOYUTLU MODELLENMESİ

YÜKSEK LİSANS TEZİ

Alper KUTLUATA
(503001507)

Tezin Enstitüye Verildiği Tarih : 13 Mayıs 2002
Tezin Savunulduğu Tarih : 29 Mayıs 2002

Tez Danışmanı : Prof. Dr. Cem SORUŞBAY
Diğer Jüri Üyeleri Prof.Dr. Metin ERGENEMAN(İ.T.Ü.)
Prof.Dr. Orhan DENİZ(Y.T.Ü.)

MAYIS 2002

ACKNOWLEDGEMENTS

This study has been performed under supervision of Prof. Dr. Cem Soruşbay. I would like to thank to him for his supervision.

I would like to thank also my family for their patience an support in everything all my life.

Finally and mostly I would like to thank my girlfriend for her support, energy and love.

May, 2002 Alper KUTLUATA

CONTENTS

ABBREVIATIONS vi
LIST OF TABLES viii
LIST OF FIGURES ix
LIST OF SYMBOLS xi
ÖZET xiii
SUMMARY xv

1. INTRODUCTION……. 1

2. HOMOGENEOUS CHARGE COMPRESION IGNITION ENGINES…….. 3
2.1. Description of HCCI Process…… 3
2.2. HCCI Engine Configurations……... 5
2.2.1. Port-injection or Fumigation…… 6
2.2.2. Early In-Cylinder Injection……. 7
2.2.3. Late In-Cylinder Injection…… 7
2.3. Development of HCCI Engines…….. 8
2.4. Drawbacks of the HCCI Engine…….. 11
2.4.1. Combustion Phasing and Control…… 11
2.4.2. Power Output…… 15
2.4.3. Homogeneous Mixture Preparation……16
2.5. Characteristics of HCCI Combustion……..16
2.5.1. Ignition Theory Related to The HCCI Concept……16
2.5.2. Emissions Behavior…… 24
2.5.2.1. Oxides of Nitrogen (NO_x)…… ……24
2.5.2.2. Particulate Matter (PM)…… 26
2.5.2.3. Hydrocarbons (HC) and Carbon Monoxide (CO)…… 26
2.5.3. Efficiency…… 27
2.6. Future Applications of HCCI……. 27

3. PHYSICAL MODELING……. 29
3.1. Zonal Models..…….. 29
3.2. Dimensional Models……. 32

4. CHEMICAL KINETIC MODELING……...… 34
4.1. Detailed Mechanisms…… 34
4.2. Skeletal Mechanisms……. 36
4.3. Reduced Mechanisms……... 37
4.4. Kinetic Analysis of Reaction Mechanisms…….. 40
4.4.1. Sensitivity Analysis……... 40
4.4.2. Reaction Flow Analysis…… 43

4.4.3. Chemical Lifetime Analysis……...…….. 45
4.4.4. Simplification and Reduction of Reaction Mechanisms…… 47

5. THE MODEL……... 51
5.1. The Physical Model……51
5.1.1. CFD Applications……51
5.1.2. The Governing Equations……...54
5.2. The Chemical Model……..….60
5.3. Simulation Parameters …… 61

6. RESULTS……. 63

7. CONCLUSION…… 78

8. REFERENCES…… 80

ABBREVIATIONS

3D	: Three Dimension
4SPACE	: 4-Stroke Powered Gasoline Auto-Ignition Controlled Combustion Engine
ABDC	: After Bottom Dead Center
A/F	: Air/Fuel
ALE	: Arbitrary Lagrangian Eularian
ARC	: Activated Radical Combustion
ATAC	: Active Thermo-Atmosphere Combustion
ATDC	: After Top Dead Center
BBDC	: Before Bottom Dead Center
BTDC	: Before Top Dead Center
CAD	: Crank Angle Degree
CAI	: Controlled Auto-Ignition
CFD	: Computational Fluid Dynamics
CHEMKIN	: Chemical Kinetics rate code
CI	: Compression Ignition
CIDI	: Compression-Ignition, Direct-Injection
CPU	: Central Processing Unit
CR	: Compression Ratio
CSP	: Computational Singular Perturbation
DI	: Direct Injected
EGR	: Exhaust Gas Recycling
HCCI	: Homogeneous Charge Compression Ignition
HCDC	: Homogeneous Charge Diesel Combustion
HCT	: Hydrodynamics, Chemistry and Transport code
IC	: Internal Combustion
ILDM	: Intrinsic Low Dimensional Manifolds
IMEP	: Integrated Mean Effective Pressure
IVC	: Inlet Valve Closure
LAG	: Avalanche Activated Combustion
PCCI	: Premixed Charge Compression Ignition
PCI	: Premixed Compression-Ignited
PGS	: Pressure Gradient Scaling
PM	: Particulate Matter
PREDIC	: Premixed Lean Diesel Combustion
PRF	: Primary Reference Fuels
QSOU	: Quasi-Second-Order Upwind
QSSA	: Quasi-Steady-State Approximations
RON	: Research Octane Number
RPM	: Revolution Per Minute

SI	: Spark Ignition
SIDI	: Spark-Ignition, Direct Injection
SGS	: Subgrid Scale
TDC	: Top Dead Center
VVA	: Variable Valve Actuation

LIST OF TABLES

	Page No
Table 5.1. Standard Values of k-ε Turbulence Model Constants……..	57
Table 5.2. Volvo TD100 Engine Geometry……	62
Table 5.3. Simulated Operating Conditions…….	62

LIST OF FIGURES

Page No

Figure 2.1. HCCI would use low-pressure fuel injection outside the cylinder, and no ignition system. If charge stratification is desired, it may be necessary to use in-cylinder injection..... 3
Figure 2.2. HCCI Engine Configurations..... 6
Figure 2.3. Methods for Controlling HCCI Combustion Phasing..... 12
Figure 2.4. Illustration of Ignition Limits in Accordance with Semenov's Thermal Ignition Theory..... 17
Figure 2.5. Schematic of the relative locations of explosive, non-explosive, and cool flame regions for a hydrocarbon-air mixture..... 18
Figure 2.6. The LAG Combustion System..... 19
Figure 2.7. Ideal modes of SI and HCCI heat release..... 20
Figure 2.8. HCCI Energy Release Model Illustration..... 21
Figure 2.9. Model of Combustion Regions and related engine conditions..... 22
Figure 2.10. Comparison of cylinder pressure histories for a) SI operation (gasoline), and b) HCCI (labeled ATAC) operation with methanol.. 22
Figure 2.11. Typical heat release curve from HCCI combustion of DF-2 Diesel fuel and a Fischer-Tropsch Naphtha..... 23
Figure 2.12. Typical heat release..... 24
Figure 2.13. Predicted NOx emissions vs. engine load for typical HCCI and DI Diesel combustion..... 26
Figure 6.1. The shaded view of the computational mesh..... 63
Figure 6.2. The computational mesh at crank angle 180^0 ATDC..... 64
Figure 6.3. Top view of the computational mesh..... 65
Figure 6.4. A perspective view that shows details of the valve lift region.... 65
Figure 6.5. The mesh view of the symmetry plane, plot across y=0. Both the valves and piston are at their BDC positions..... 66
Figure 6.6. The grid at TDC. Both valves are closed..... 67
Figure 6.7. The grid at 15 CAD ATDC. The intake valve (right) is open. The exhaust valve is closed..... 67
Figure 6.8. The grid at 90^0 ATDC, when the intake valve (right) is at its BDC and the exhaust valve (left) is closed..... 68
Figure 6.9. The gird at BDC**,** end of the intake stroke when the intake valve (right) is open and the exhaust valve (left) is closed..... 68
Figure 6.10. The gird at BDC**,** end of expansion stroke**,** when the intake valve (right) is closed and the exhaust valve (left) is open..... 69
Figure 6.11. The types of mesh structures according to the cell number..... 70
Figure 6.12. Crank angle-pressure diagram of the three kind of mesh structure according to cell numbers. The top diagram is full simulation history, and the bottom diagram is detailed view of history at high pressures... 71
Figure 6.13. Comparison of the simulated and measured cylinder pressure..... 72

Figure 6.14. Comparison of the engine speed effects on pressure-crank angle history……. 73
Figure 6.15. Comparison of the engine speed effects on temperature-crank angle history……. 74
Figure 6.16. Comparison of the inlet temperature effects on pressure-crank angle history……. 75
Figure 6.17. Comparison of the inlet temperature effects on temperature-crank angle history……. 76
Figure 6.18. Comparison of compression ratio effects on pressure-crank angle history……. 77
Figure 6.19. Comparison of the compression ratio effects on Temperature crank angle history…….. 77

LIST OF SYMBOLS

$\mathbf{A_{fr}}$	: forward pre-exponantial factor
$\mathbf{A_{br}}$	: backward pre-exponantial factor
$\mathbf{a_{mr}}$	: integral stoichiometric coefficient for reaction r
$\mathbf{a'_{mr}}$, $\mathbf{b'_{mr}}$	: reaction orders
B	: unity matrix
$\mathbf{b_{mr}}$	: integral stoichiometric coefficients for reaction r
$\mathbf{c^a_{ij}}$	: relative transfer of atom a through consumption of species i to species j
$\mathbf{c_i}$	: concentration of species i
$\mathbf{c_p}$	: total specific heat
$\mathbf{c_{pm}}$	: specific heat of species m
$\mathbf{c_{\varepsilon 1}}$, $\mathbf{c_{\varepsilon 2}}$, $\mathbf{c_{\varepsilon 3}}$	: k-ε turbulence model constants
$\mathbf{c_\mu}$	: empirical constant
D	: diffusion coefficient
$\mathbf{E_{br}}$	: backward activation temperature
$\mathbf{E_{fr}}$	: forward activation temperature
$\mathbf{f^a_{ij}}$	: relative transfer of atom a through formation of species i from species j
$\mathbf{h_m}$	: specific enthalpy of species m
$\mathbf{I_i}$	: relative importance of species i
$\mathbf{I_{i,0}}$	: initial value of I_i
I	: unit dyadic
$\boldsymbol{I_m}$	: specific internal energy of species m
$\boldsymbol{I}$	: specific internal energy
i	: species i
$\boldsymbol{J}$	: heat flux vector
J	: Jacobian matrix
$\mathbf{J_{ii}}$	: diagonal element of the Jacobian matrix
j	: species j
$\mathbf{K^r_c}$	: concentration equilibrium constant
k	: index for reactions, turbulent kinetic energy
$\mathbf{k_{fr}}$	: forward reaction rate
$\mathbf{k_{br}}$	: backward reaction rate
$\mathbf{k_k}$	: Arhenius rate constant of reaction k
m	: species m
$\mathbf{N_R}$	: number of reactions
$\mathbf{N_s}$	: number of species

n^a_j : number of atoms a in species j
n^a_k : number of atoms a transported in reaction k
Q^c : chemical heat release
Q_r : negative of heat of reaction at absolute zero
p : fluid pressure
R_0 : universal gas constant
r_k : reaction rate of reaction k
$S_{A,B}$: sensitivity of the species A on species B
Sc : input constants
T : temperature
T^c_i : chemical lifetime
t : time
t_0 : initial time
u : fluid velocity vector
v_0 : input constant
v'_{ik} : stoichiometric coefficient, reactant
v''_{ik} : stoichiometric coefficient, product
W_m : molecular weight of species m
w_r : kinetic reaction rate
x_m :mole of species m
Y_i : mole fraction of the species i
ε : turbulance disipation rate
λ : second coefficient of viscosity
ξ : temperature exponent
μ : first coefficient of viscosity
ρ : total mass density
ρ_m : mass density of species m
ρ^c_m : chemical source term
τ_i^c : cemical lifetime of species i
σ : viscous stress tensor
Δh^0_f : heat of formation of species m at absolute zero

HOMOJEN KARIŞIMLI SIKIŞTIRMALI ATEŞLEMELİ MOTORLARIN ÇOK BOYUTLU MODELLENMESİ

ÖZET

Homojen Karışımlı Sıkıştırmalı Ateşlemeli (HCCI) motorlar yanma modları tamamen farklı olmasına karşın kıvılcım ateşlemeli benzin motorlarıyla sıkıştırmalı ateşlemeli dizel motorlarının bir hibriti olarak düşünülen ve içten yanmalı motorlarda sağladığı verim ve emisyon değerleri açısından artan ilgiye sahip yeni bir teknolojidir. Bu tip motorlarda kıvılcım ateşlemeli motorlarda olduğu gibi hava yakıt karışımı ateşlenme öncesi homojen olarak emme sistemi veya silindir içinde oluşturulur ve sıkıştırma esnasında sıcaklığı yükselerek kendi kendine tutuşma sıcaklığına geldiğinde karışım sıkıştırmalı ateşlemeli motorlarda olduğu gibi herhangi bir dış ateşleme sistemi yardımı olmadan yanar. Yanma başlangıcı ateşleme prosesinin kendiliğinden gelişmesinden ötürü direk olarak kontrol edilemez. Sadece dolaylı olarak etken parametreler üzerinden kontrolü mümkündür. Çalışma parametreleri uygun olarak ayarlandığında yanma üst ölü nokta civarında gerçekleşir. Benzin motorlarında ön alev gelişimi önemli ölçüde değişim gösterdiği için çevrimden çevrime farklılıklar da olmaktadır. Ancak HCCI prensibinde homojen karışımın getirdiği aynı anda birçok noktadan ateşlemenin gerçekleşmesi ve yanmanın birçok noktadan eş zamanlı olarak başlaması sebebiyle çevrimden çevrime değişimler çok düşük mertebelerdedir ve bununla yanma hızı oldukça yüksektir.

HCCI dizel motorlarıyla karşılaştırıldığında ana avantajları düşük NO_x ve is emisyonlarıdır. Dizel motorlarında is zengin karışım bölgelerde NO_x ise sıcak stokiyometrik bölgelerde oluşmaktadır. Bu mekanizmalardan ötürü yanmanın iyileştirilmesiyle NO_x ve is miktarlarının her ikisini birlikte düşürmek oldukça zordur. Zengin ve stokiyometrik bölgelerle olan bu problemi gidermek homojen bir karışım kullanmakla mümkün olabilir.

Kıvılcım ateşlemeli benzin motorlarıyla karşılaştırıldığında ise avantajı kısmi yüklerde daha yüksek verim sağlamasıdır. Klasik stokiyometrik karışımlı ve katalizörlü bir benzin motoru emisyon değerleri açısından dizel motoruna göre daha temiz bir motor olarak gösterilmesine karşın HCCI motoruyla kıyaslandığında, HCCI motorunun sağladığı kısmi yüklerdeki verime ulaşamamaktadır.

Bütün bu avantajlara karşın HCCI'nın dez avantajları geniş yük ve hız aralıklarında ateşleme zamanının ve yanma fazının kontrolündeki zorluk, iki tip motora kıyasla daha fazla ürettiği HC emiyon değerleri ve çıkış gücünün sınırlı olmasıdır.

Son yıllarda, hesaplamalı akışkanlar dinamiğinin (CFD), yanma proseslerinin anlaşılmasında bir araç olarak kullanılması büyük ölçüde kabul görmüştür. Kullanımının yaygınlaşmasıyla beraber, yanmanın çok boyutlu olarak modellenmesi çalışmaları da hız kazanmıştır. Bu çalışmada da yenibir konsept olan Homojen Karışımlı Sıkıştırmalı Ateşlemeli Motorların çok boyutlu olarak modellenmesi amaçlanmıştır. Bu doğrultuda KIVA-3V kodu hesaplamalı akışkanlar dinamiği (CFD) programı olarak kullanılmış, fiziksel ve kimyasal modelleme hesaplamaları

tamamiyle bu kod yardımıyla yapılmıştır. Literatürden Homojen Karışımlı Sıkıştırmalı Ateşlemeli Motorlar üzerine yapılmış deneysel bir örnek referans alınarak modelleme sonuçları bu datalar ile karşılaştırılmıştır. Çalışmada methanın modellenmesi üzerinde durulmuş ve kimyasal kinetik modellenmesi iki adımlı global kinetik mekanizması ile sağlanmıştır. HCCI motorlarda yanma fazının ve yanma başlangıcının kontolünde etkin olarak kullanılan, emme sıcaklığı, sıkıştırma oranı ve devir sayısı parametrelerinin etkileri de bu çalışma kapsamında incelenmiştir.

Yapılan bu çalışma, deneysel sonuçlarla karşılaştırıldığında, Homojen Karışımlı Sıkıştırmalı Ateşlemeli Motorların çok boyutlu olarak modellenmesinin mümkün olduğunu göstermiştir.

MULTIDIMENSIONAL MODELING OF HOMOGENEUS CHARGE COMPRESSION IGNITION ENGINES

SUMMARY

With the increasing need to both conserve fossil fuel and minimize toxic emissions, much effort is being focused on the advancement of current combustion technology. One such research topic emerging in combustion society is the concept of Homogeneous Charge Compression Ignition (HCCI). This process is often considered a hybrid of the conventional spark plug ignited and the compression ignition proceses. As in a spark-ignited engine, the air-fuel mixture is homogeneous however as in compression ignited combustion the mixture is auto-ignited by compression heating.

Homogeneous Charge Compression Ignition (HCCI) combustion is achieved when a mixture of air, fuel and recycled combustion products is compressed until it auto-ignites. This results in heat releasing reactions that initiate simultaneously at multiple sites within the combustion chamber and occur at the global equivalence ratio. Unlike Diesel (diffusion-controlled) combustion, HCCI reactions are not necessarily limited by the mixing rate at the interface between the fuel jet and oxidizer. HCCI combustion differs from spark-ignited combustion in that it has no discernible flame front and is devoid of a localized high-temperature reaction region. Thus, HCCI combustion is generally characterized by distributed, low-temperature reactions that occur relatively fast.

HCCI combustion technology offers the possibility of having advantages of both Diesel and gasoline engines. The major advantages with Homogeneous Charge Compression Ignition compared to the diesel engine are low NOx emissions and fewer problems with smoke. Diesel engines are widely used in heavy-duty vehicles and in other commercial applications, due to its high efficiency and durability. In the diesel engine soot is formed in the fuel rich regions and NOx in the hot stoichiometric regions. Due to these mechanisms, it is difficult to reduce both NOx and soot simultaneously through combustion improvement. To eliminate the problems with fuel rich regions and stoichiometric regions, a homogeneous charge can be used instead.

The benefit with HCCI compared to the Spark Ignition (SI) engine is the much higher part load efficiency.

The disadvantages of HCCI engines are including high hydrocarbon and carbon monoxide emission, high peak pressures, high rates of heat release, reduced operating range, lower power density than a Diesel engine, difficulty in controlling the combustion phase and timing. There is increasing hope that these advantages will be solved through various means with the advancement of HCCI research.

Over the past several years, computational fluid dynamics (CFD) has been increasingly accepted as an adjunct to understanding of practical combustion

systems. Since the use of CFD, multi-dimensional studies with combustion have become commonplace in the literaure.
This study concentrates on multi-dimensional modelling of Homogeneous Charge Compression Ignition Engines. The impacts of engine speed, intake temperature, and compression ratio are also investigated in this study. As a CFD software tool for the modelling of combustion process, KIVA-3V code is used. Both the physical and chemical modelling calculations are done by KIVA-3V code. An experimental study is taken as a reference from the literature and releated to the experiment engine geometry a three-dimensional model is generated. For the chemical kinetic modelling a two-step kinetic mechanism is used. The first of the two global rate equations controls the disapperance of methane, and the second the oxidation of carbon monoxide. This work shows that three-dimensional modelling of methane HCCI engine is possible with good agreement to the experimental data.

CHAPTER 1

INTRODUCTION

Homogeneous Charge Compression Ignition (HCCI) combustion is achieved when a mixture of air, fuel and recycled combustion products is compressed until it auto-ignites. This results in heat releasing reactions that initiate simultaneously at multiple sites within the combustion chamber and occur at the global equivalence ratio. Unlike Diesel (diffusion-controlled) combustion, HCCI reactions are not necessarily limited by the mixing rate at the interface between the fuel jet and oxidizer.

HCCI combustion differs from spark-ignited combustion in that it has no discernible flame front and is devoid of a localized high-temperature reaction region. Thus, HCCI combustion is generally characterized by distributed, low-temperature reactions that occur relatively fast.

The operation of piston engines on a compression ignition cycle using a lean, homogeneous charge has many potential attractive features. These include the potential for extremely low NOx and particulate emissions while maintaining high thermal efficiency and not requiring the expensive high pressure injection system of the typical modern diesel engine.

In the ideal Diesel cycle, heat is added to the working fluid at constant pressure. This is approximated in real diesels by the injection of a high cetane fuel spray into the compressed air mass where auto-ignition occurs. Ignition delay after the start of injection is controlled by the cetane number of the fuel. The rate of heat release is controlled by the rate at which fuel is injected and the rate at which fuel vaporization and mixing occur. NOx production is inherently high in Diesels because of the high temperatures in the combustion regions where the mixing brings about near stoichiometric conditions which produces high temperatures. Engine power is controlled by the quantity of fuel injected.

In the ideal Otto cycle, heat is added to the working fluid at constant volume. This process is approximated by igniting a premixed high octane fuel and air mixture. The

fuel air mixing is accomplished either before the mixture is introduced into the cylinder by carburetion or more recently by inlet port injection of the fuel into the air flows. The fuel air mixture is usually assumed to be homogeneous. Ignition is initiated by a spark plug. The heat release rate is controlled by flame propagation from the spark gap through the mixture at a rate that is dependent primarily on the turbulent mixing of the hot products behind the flame front with the unburned mixture ahead of the flame front. NOx formation is high if stoichiometric mixtures are used, but three-way catalysts are currently used to reduce the NOx to low levels. The HCCI combustion process uses the same auto-ignition process as a Diesel but results in rapid heat release and therefore better approximates an Otto cycle than a Diesel cycle.

CHAPTER 2

HOMOGENEOUS CHARGE COMPRESSION IGNITION ENGINES

2.1. Description of HCCI Process

Homogeneous Charge Compression Ignition (HCCI) technology is receiving increased attention for its potential to improve both the efficiency and emissions of IC engines. HCCI is a hybrid of the well-known Spark Ignition (SI) and Compression Ignition (CI) engine concepts. As in an SI engine, a homogeneous fuel-air mixture is created in the inlet system. During the compression stroke the temperature of the mixture increases and reaches the point of auto ignition; i.e. the mixture burns without the help of any ignition system, just as in a CI engine. In some regards, HCCI incorporates the best features of both spark ignition (SI) and compression ignition (CI), as shown in Figure 2.1.

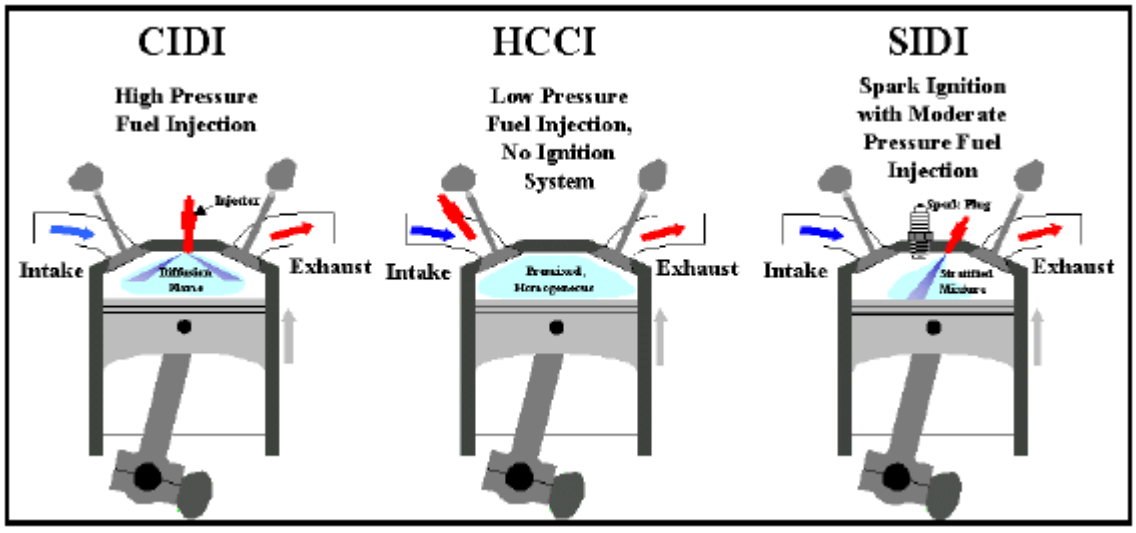


Figure 2.1. HCCI (as most-typically envisioned) would use low-pressure fuel injection outside the cylinder, and no ignition system. If charge stratification is desired, it may be necessary to use incylinder injection.

Most engines employing HCCI to date have dual mode combustion systems in which traditional SI or CI combustion is used for operating conditions where HCCI operation is more difficult.

Typically, the engine is cold-started as an SI or CIDI engine, and then switched to HCCI mode for idle and low- to mid-load operation to obtain the benefits of HCCI in this regime, which comprises a large portion of typical automotive driving cycles. For high-load operation, the engine would again be switched to SI or CIDI operation. Research efforts are underway to extend the range of HCCI operations.

The major advantages with Homogeneous Charge Compression Ignition, HCCI, compared to the diesel engine are low NOx emissions and fewer problems with smoke. Diesel engines are widely used in heavy-duty vehicles and in other commercial applications, due to its high efficiency and durability. In the diesel engine soot is formed in the fuel rich regions and NOx in the hot stoichiometric regions. Due to these mechanisms, it is difficult to reduce both NOx and soot simultaneously through combustion improvement. To eliminate the problems with fuel rich regions and stoichiometric regions, a homogeneous charge can be used instead.

The benefit with HCCI compared to the Spark Ignition (SI) engine is the much higher part load efficiency. The conventional (stoichiometric charge) SI engine fitted with a three-way catalyst can be seen as a very clean engine compared to the diesel engine. But it suffers from poor part load efficiency.

The major drawback with HCCI is the problem of controlling the ignition timing over a wide load and speed range. Another drawback compared to the Spark Ignition (SI) engine and the diesel engine is higher emissions of unburned hydrocarbons.

In an HCCI engine the fuel is injected into the (preheated) air in the intake manifold to create a homogeneous charge. During the compression stroke the charge is further heated to attain auto-ignition close to Top Dead Center (TDC). With HCCI, there is no direct control of the onset of combustion, as the ignition process relies on a spontaneous auto-ignition. The ignition timing can only be controlled indirectly. By adjusting the operating parameters correctly, ignition will occur near TDC. In SI engines, large cycle-to-cycle variations occur since early flame development varies significantly [1]. With HCCI, cycle-to-cycle variations of combustion are very small since combustion initiation takes place at many points at the same time. HCCI has no flame propagation; instead the whole mixture burns close to homogeneous at the

same time [2]. As the whole bulk burns almost simultaneously the combustion rate becomes very high. Therefore highly diluted mixtures have to be used to limit the rate of combustion. This can be achieved by much excess air (that gives the [3], [4] and/or with Exhaust Gas Recycling (EGR) [5]. Water injection can also be used to slow down the combustion rate [6].

2.2. HCCI Engine Configurations

A number of promising engine concepts using HCCI combustion are being developed, including free piston designs [35], and two-stroke engines [21]. In this section, only conventional 4-stroke engine designs suitable for over the road applications are included.

Figure 2.2 shows a schematic breakdown of HCCI engine configurations. The first distinction in this illustration is for full-time HCCI engines vs. dual combustion mode engines. Full-time HCCI engines have the largest benefit potential. Highly boosted, fuel-lean, dedicated HCCI Engines may be attractive for some stationary or marine applications. Future development of HCCI-specific fuels and combustion phasing control may also expand the air/fuel ratio operating range.

An alternative way of obtaining full power output, at the expense of additional benefits, is to operate an engine on HCCI combustion at low and part loads and on either spark-ignition or conventional Diesel combustion at full load. Obviously, this approach is only attractive for applications that experience significant part load engine operation and would benefit from emissions reductions over this operating range. Dual-mode spark-ignition/HCCI engines have not been discussed much in the literature, but appear attractive for light-duty vehicle applications.

Dual-mode Diesel/HCCI engines, on the other hand, are being pursued by several research groups around the world.

The next level of classification for HCCI engines is comprised by the method of fueling. This represents an important distinction because it has a profound effect on the engine characteristics and confines the combustion control methods that can be employed.

Three fueling methods will be described in more detail: port-injection, early in-cylinder injection, and late incylinder injection.

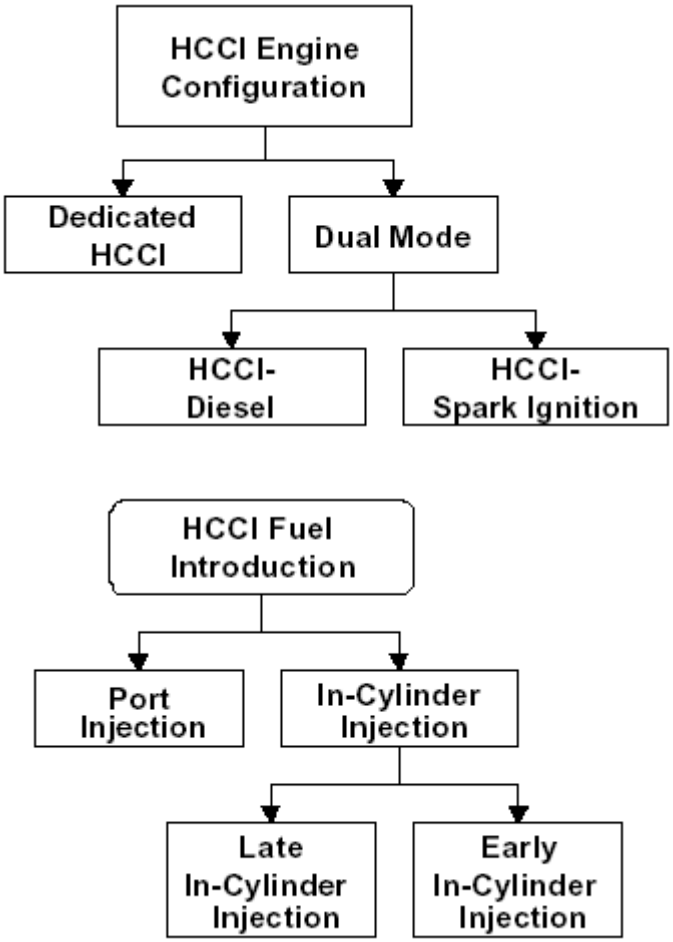


Figure 2.2. HCCI Engine Configurations.

2.2.1. Port-Injection or Fumigation

The simplest way of promoting a homogenous incylinder pre-mixed charge is by introducing fuel upstream of the intake valves, and inducting the mixture into the cylinder during the intake stroke. This method takes advantage of the turbulence generated as the intake flow rushes past the intake valves to promote mixing. However, the fuel air mixture is exposed to the entire time-temperature history of the cylinder, and thus injection timing cannot be used to control the start of reaction. Port-injection or fumigation is the most common configuration used in HCCI engines, and a number of researchers have used it with varying degrees of success [4], [5], [6], [8], [13], [16], [36], [37], [38], [39].

Port-injection or fumigation of heavy fuels can result in high HC and CO emissions, and in increased fuel consumption and oil dilution. Most of these problems can be attributed directly to poor fuel vaporization and fuelwall interactions within the

combustion chamber. Port-injection may be attractive for gaseous and high volatility fuels, but is more problematic for Diesel fuel.

2.2.2. Early In-Cylinder Injection

Another method of promoting a homogeneous fuel-air mixture within the cylinder is through early (well in advance of TDC) in-cylinder injection of a portion or all of the fuel. (PREDIC-Premixed Lean Diesel Combustion, PCI-Premixed Compression-Ignited). By this way a partly homogeneous mixture is then formed. This can be done through the same nozzles used for Diesel combustion [40] or through separate direct-injectors [41]. Interestingly, this method provides ineffective control of the reaction phasing by varying the fuel introduction time. This occurs because the fuel vaporization process significantly affects the time-temperature history to which the mixture is exposed and limits the range over which control can be attained.
HCCI operation with in-cylinder injection is only reported in the literature for Diesel fuel. However, fuel wall impingement is a severe problem when injecting heavy fuels into the low-density air charge. Some researchers have expended significant effort in minimizing wall impingement by developing low-penetration fuel injectors [42], [43] and have obtained significant improvements. However, wall impingement is likely to remain a problem for in-cylinder injection of Diesel fuel into low-density environments. Incylinder fuel injection is likely to become the preferred method for fueling HCCI engines in the future as better mixture preparation techniques are developed.

2.2.3. Late In-Cylinder Injection

This concept, also use a premixed charge, created in the inlet system. But the charge here is ignited by the fuel injected directly into the combustion chamber, the near or after TDC, (HCDC-Homogeneous Charge Diesel Combustion). The ignition delay is extended through the use of large amounts of cooled EGR, a reduction in the engine compression ratio, and vigorous swirl. The net result is that the combustion reactions begin well after the end of injection, and a diffusion-limited combustion jet is not established. Despite the significant mixture inhomogeneity that exists within the cylinder, low NOx and soot emissions are obtained that is proportional to the amount

of fuel being injected. Late in-cylinder injection of Diesel appears to avoid most of the problems associated with fuel wall impingement and provides some control of the combustion phasing, but the short ignition delay of Diesel limits this approach to low engine loads. Further developments of the late in-cylinder injection approach are likely to be applied to other classes of Diesel engines in the near future.

2.3. Development of HCCI Engines

The theoretical and practical roots of HCCI combustion concepts are ultimately credited to the Russian scientist Nikolai Semenov and Gussak in 1930s. Their approach to HCCI mode is given in Section 2.6.1.

HCCI has been widely observed in two stroke engines in the past and has been given various names such as Controlled Auto-Ignition (CAI), Activated Radical Combustion (ARC) or Active Thermo-Atmosphere Combustion (ATAC) and Premixed Charge Compression Ignition (PCCI). Onishi et al. were among the first to study this peculiar combustion mode in a two-stroke engine with a compression ratio of 7.5:1. They observed HCCI over a wide speed range and showed that there is no flame propagation and that the entire cylinder charge burns at the same time [2]. Soon after Onishi, Noguchi et al. demonstrated the same combustion mode in a two-stroke engine with a 6.7:1 compression ratio and conducted radical concentration measurements during combustion. These measurements identified the CHO, HO2 and O radicals as responsible for the ignition of the homogeneous charge [20]. Following Noguchi, Iida showed that the HCCI operating range of a two-stroke engine with a compression ratio 6:1 could be significantly expanded if methanol was used instead of gasoline [14]. No-load HCCI was possible between 2000 to 3500 rpm with methanol. When gasoline was used, HCCI occurred above 3000 rpm and combined HCCI and conventional combustion would take place between 2500 and 3000 rpm. Iida also investigated a low heat rejection variant of his engine and conducted radical concentration measurements during combustion, identifying the OH radical as important for HCCI operation in contrast to Noguchi's experiments [20]. After Iida, Ishibashi et al. demonstrated a hybrid HCCI-SI two-stroke engine with a compression ratio of 6.4:1 [21]. HCCI was used to improve part-load combustion stability, reduce HC emissions and improve part-load fuel economy for a wide speed range. The main feature of the engine and the mechanism responsible for

the change between normal SI combustion and HCCI was a special valve, positioned very close to the exhaust ports, which controlled the self-EGR rate. Following Ishibashi, Gentili et al. investigated HCCI in a two-stroke engine with a 9:1 compression ratio over a wide speed range and performed optical visualization studies [22]. They indicated that HCCI may not necessarily require complete mixing of the residual and the fresh mixture, and confirmed the small cyclic pressure variation of HCCI. In another publication, Gentili at al. investigated HCCI in combination with direct fuel injection in a two-stroke engine with a 10.5:1 compression ratio [23]. Two injection strategies were examined, air-assisted direct fuel injection and liquid-only direct fuel injection. Air-assisted fuel injection expanded the HCCI load range compared to the indirect injection case while direct injection limited the HCCI speed and load range with respect to the indirect injection case.

In the area of four-stroke engines, Najt and Foster demonstrated HCCI in a four-stroke engine [7]. They used a variable compression ratio engine operating with a mixture of isooctane and heptane and inlet air heating. Among other interesting points, they indicated that high compression ratios lead to violent heat release rates. A 10:1 compression ratio lead to knocking combustion while 7.5:1 was selected as the best compromise. Soon after, Thring demonstrated HCCI in a four-stroke variable compression ratio engine using both gasoline and diesel fuels [12]. A 15:1 compression ratio was unsuitable for HCCI as it led to knocking combustion, so it was reduced to 8:1. Then, by heating the intake air the engine would operate in HCCI mode within a small speed and load range. Thring investigated various combinations of λ and EGR and suggested a hybrid HCCI-SI engine in which HCCI would be used under part-load conditions and normal SI operation would only be used close to full load conditions. Following Thring, Ryan and Callahan came to similar conclusions with regard to the compression ratio of four-stroke engines for HCCI operation [13]. They used a variable compression ratio engine with inlet air heating running on diesel fuel and covered a range from 7.5:1 to 17:1. Acceptable HCCI operation was achieved with compression ratios in the range 8:1 to 11:1. Later on, Aoyama et al. demonstrated HCCI in a four-stroke engine with a 17.4:1 compression ratio [8]. They also compared HCCI with diesel and gasoline direct injection operation using the same experimental arrangement and investigated the effects of intake air heating and super-charging. Christensen et al. continued the super-charging investigation of

Aoyama. They used a four-stroke engine with two compression ratios, 17:1 and 19:1, and three different fuels: iso-octane, ethanol and natural gas [4]. They found that supercharging dramatically increases the attainable IMEP for HCCI. In another publication, Christensen and Johansson examined the effect of different EGR rates, A/F ratios and inlet mixture temperatures on HCCI in a four-stroke engine with an 18:1 compression ratio, again using isooctane, ethanol and natural gas [5]. They identified a limited load and speed range of HCCI operation together with the lack of control over the timing of heat release as the two major problems prohibiting further exploitation of HCCI. Yet another investigation by Christensen et al. was made with a four-stroke variable compression ratio engine equipped with two port injectors, allowing alterations to the fuel properties on the fly [17]. Satisfactory operation was observed within a wide compression ratio range (11:1 to 21.5:1), with various fuels and inlet air temperatures. However, the problem of a limited HCCI operating range remained, together with the problem of heat release phasing.

From the above presentation of previous research on HCCI, many interesting points arise. The first thing to note is that HCCI can be achieved in both two-stroke and four-stroke engines. In two-stroke engines, HCCI has been observed under a variety of part-load conditions, in engines with compression ratios between 6:1 and 10.5:1, running at speeds between 2000 and 4000 rpm. The fuel used in the majority of the studies was gasoline while methanol was shown to extend the range of HCCI. No external aids were necessary in order to obtain HCCI (e.g. inlet air heating). On the other hand, HCCI in four-stroke engines is problematic. The speed and load ranges are limited and it is necessary to preheat the inlet air and/or use a high compression ratio. Particularly as far as four-stroke compression ratios are concerned, there appear to be two different approaches: some [7], [12] suggest low compression ratios (8:1) and inlet air heating, while others [8] rely on unusually high compression ratios for gasoline engines (18:1 and higher) in order to induce HCCI. However, both concepts complicate the development of a hybrid HCCI-SI engine for automotive applications. Another area of disagreement in the literature concerns the HCCI combustion mechanism itself. In most papers, the presence of radicals in the residual gas is considered fundamental for HCCI to occur. However, it has been suggested that for auto-ignition charge temperature is the fundamental governing factor [7]. Furthermore, there seems to be a disagreement even between those who have performed in-cylinder radical concentration measurements with respect to which

radicals are the most influential in inducing HCCI [20,14]. As far as exhaust emissions are concerned, there is general agreement that NO_x emissions are significantly reduced while HC emissions are higher for HCCI four-stroke engines and lower for HCCI two-stroke engines compared to SI combustion. Small cyclic pressure variation is another point of general agreement in the literature, while another interesting and unclear point is why methanol, a fuel with a high octane number considerably expands the HCCI operating range instead of reducing it [14].
At this point it is worth noting that there are certain details which differentiate HCCI in two-stroke versus four-stroke engines, such as the considerably shorter port timings of two-stroke engines versus the valve timings of four-stroke engines, the difference in the amount of residual gas trapped inside the cylinder after combustion, the two-stroke oil which is pre-mixed with the fuel in the case of two-stroke engines and last but not least the backflow, which may occur in a four-stroke engine but it is not very obvious in two-stroke engines since the intake process is forced. Furthermore, it is extremely important to note that in two-stroke engines, the residual gas is mainly responsible for auto-ignition. Whether HCCI is triggered by increased radical concentrations in the residual gas or by heat transfer from the residual gas to the fresh mixture or by both radicals and heat transfer is still unknown and open to investigation. However, using residual gas to trigger HCCI has been successfully demonstrated as a concept [21] and proven in practice for two-stroke engines.

2.4. Drawbacks of the HCCI Engine

There are a number of obstacles that must be overcome before the potential benefits of HCCI combustion can be fully realized in production applications. This section describes the main difficulties with this technology.

2.4.1. Combustion Phasing and Control

One of the principal challenges of HCCI combustion is control of the combustion phasing over a wide speed/load range. Unlike in spark ignition or conventional Diesel engines, a direct method for controlling the start of combustion is not available. Instead, the start of combustion is established by the auto-ignition chemistry of the air-fuel mixture. Auto-ignition of a fuel-oxidizer mixture is

influenced by the properties of the mixture and by the time-temperature history to which it is exposed. Hence, combustion phasing of HCCI engines is affected by:

- Auto-ignition properties of the fuel
- Fuel concentration
- Residual rate and, possibly, reactivity of the residual
- Mixture homogeneity
- Compression ratio
- Intake temperature, latent heat of vaporization of the fuel, and engine temperature
- Heat transfer to the engine
- Other engine-dependent parameters

Several approaches for controlling the combustion phasing have been attempted, but a fundamental distinction can be made between those methods attempting to control the time-temperature history to which the mixture is exposed, and methods aimed at altering the propensity for auto-ignition of the mixture, as illustrated on Figure 2.3.

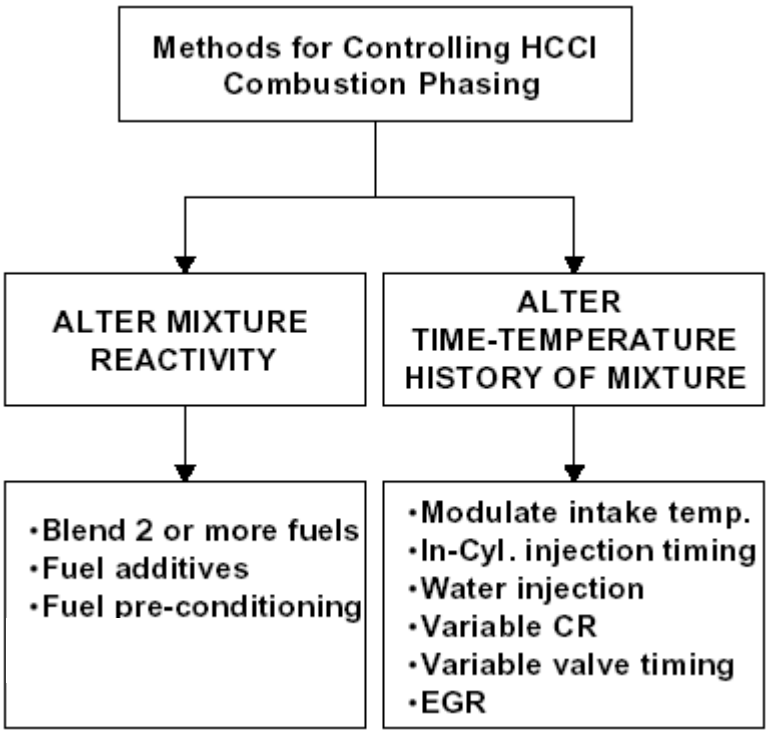


Figure 2.3. Methods for Controlling HCCI Combustion Phasing.

In laboratory experiments, the most popular method for controlling the start of reaction is by modulating the intake air temperature. The effects of initial charge temperature have been widely reported, ever since Najt and Foster [7] showed that Homogenous Charge Compression Ignition (HCCI) combustion could be achieved in a SI 4-Stroke engine under lean fuelling and elevated inlet charge temperatures (~300-500°C). In all cases, the effect of increasing inlet charge temperature is to advance auto-ignition timing and decrease combustion duration.

Aoyama et. al. [8] also showed that the lean-burn limit, defined by hydrocarbon emissions and combustion efficiency, can be extended with increased initial charge temperature. However, this strategy is generally not considered as a practicable method for achieving combustion control due to the high thermal inertia of heating systems.

Compression ratio effects on ignition timing are also widely understood. Increasing compression ratio has a similar effect as raising the inlet charge temperature; to increase the end-of-compression temperature above that required for spontaneous ignition. Systems that achieve combustion-timing control through changes in compression ratio can be divided into two types:

i. Ones that vary the combustion chamber geometry,
ii. Ones that vary the cylinder volume at Inlet Valve Closure (IVC).

Type (i) was investigated by Nakano et. al. [9]. They used a combination of a piston mounted in the cylinder head (to vary the combustion chamber geometry) and varying quantities of external EGR as two tools for timing control. Type (ii) requires the use of a Variable Valve Actuation (VVA) system so that control over IVC timing can be independently varied with respect to the other valve timing events. These types of systems are under development and are only just becoming commercially available, explaining why little work has been done to date. The effect of boosting the intake pressure has a similar effect as increased compression ratio – to raise the end-of-compression pressure, and temperature depending on whether intercooling is employed. However, boosting is more versatile because it allows one to increase the density of the charge without changing its overall composition. Thus, higher engine loads can be achieved with a minimal effect on exhaust NOx emissions, as shown by Aoyama et. al. [8].

Control over the recycling of burned gases can include variations of both the prompt residual rate and external EGR rate to achieve proper combustion phasing. The effect

of changes in the residual gas rate was investigated by Lavy et. al. [10], who presented preliminary results from the collaborative 4SPACE (4-Stroke Powered gasoline Auto-ignition Controlled combustion Engine) project, investigating all aspects of Controlled Auto-Ignition (CAI) combustion. 3D CFD analyses on a suitable 2-stroke engine were undertaken to determine the global and local in-cylinder conditions necessary for CAI combustion. They found that the occurrence of CAI is dominated by the degree of mixing between fresh charge and exhaust gas residuals. 4-stroke concepts were developed to mimic the internal fluid dynamic and mixing effects of the 2-stroke when running in CAI mode, resulting in the first 4-stroke engine able to achieve CAI over a limited load and speed range without the use of external charge heating or high compression ratio. This was achieved using altered valve timing, lift, and duration. Law et. al. [11] presented two methods of controlling the EGR rate. The first was similar to Lavy et.al. [10], and the second involved the storage of exhaust gas in the exhaust manifold prior to readmission to the combustion chamber during the intake stroke. They have shown that both methods are effective in controlling combustion timing and duration. The method of varying residual gas rate has been shown to work using both mechanical [10] and electro-hydraulic [11] valve actuation.

Although the use of burned gas residuals has so far proven to be the most practicable for achieving HCCI, there has been a limited amount of detailed work investigating the effects of exhaust gas dilution on HCCI combustion [7], [12], [13], [5], [9]. Thring [12] investigate the effects of A/F ratio, EGR rate, fuel type, and compression ratio on the attainable HCCI combustion region and engine-out emissions. He found that 4-stroke HCCI maximum loads could not approach those of 2-stroke HCCI engines under the conditions chosen. He also identified that detailed analyses of the heat-release characteristics over the HCCI range would be useful for further understanding. For the most part, papers that investigate EGR dilution effects do so by either fixing the A/F ratio or the fuelling rate. The authors believe that the effect of air and EGR dilution should be investigated simultaneously so that the relative contributions of each type can be quantified in terms of effects on combustion parameters.

Fuel-injection timing (in direct injected applications) has proven to be an ineffective method for controlling the combustion phasing [44], [45] as the fuel vaporization process significantly affects the time-temperature history of the mixture.

Water injection has been attempted as a method for delaying the start of reaction, but this approach was also found to be largely inadequate [6].

Beyond the time-temperature history, the properties of the mixture, reactivity of the mixture, can also be altered by blending two or more fuels, using fuel additives or fuel pre-conditioning.

The effects of fuel blends have been studied by a number of authors [14], [15], [16], [17], [18]. Christensen et. al. [17] achieved HCCI with a number of Primary Reference Fuels (PRFs) and mixtures of Gasoline and Diesel, operating at various compression ratios and intake temperatures. Combustion efficiencies were adversely affected by increasing compression ratio, reducing the expected rise in fuel conversion efficiency. On the whole, the HCCI combustion efficiencies of mixtures containing Diesel fuel were seriously affected by poor combustion due to poor fuel vaporization. Under ambient intake conditions, gasoline fuel (95 RON) was surprisingly more difficult to force into HCCI combustion (through increased compression ratio) than Isooctane (100 RON). Olsson and Johansson [19] demonstrated how the composition of a PRF (Isooctane/Heptane) fuel can affect ignition timing so that combustion can be controlled over a wide load range with additional inlet boost pressure. All of these types of systems add complexity to engine control and require additional ancillaries, which may make them unsuitable for certain types of vehicles.

2.4.2. Power Output

A current drawback of HCCI combustion is that it is presently limited in power output. Stable HCCI combustion can generally be achieved for lean A/F ratios and/or large amounts of EGR. However, as the A/F ratio approaches stoichiometric values (without EGR dilution), the combustion stability degrades, heat release rates increase, knock-like oscillations in the cylinder pressure appear, and the emissions benefits vanish [36], [8], [3], [46]. Fuels with inherently lower heat release rates, like methane, can be combusted at lower A/F ratios and achieve higher specific engine outputs [3].

Given this apparent limitation in A/F ratio for HCCI combustion, power increases can be obtained by augmenting the airflow through the engine. Supercharging has proven to be effective in this respect, and it also has a beneficial influence on

reducing the heat release rate [8], [4], [44]. Christensen and coworkers have achieved HCCI operation up to an IMEP of 14 bar, using an externally boosted engine fueled with methane. Increasing the engine speed may also be an effective method of increasing HCCI power output and reducing the heat release rate in crank-angle space, but this approach is not well documented. A high-speed, supercharged engine may be the most viable configuration for lean HCCI combustion.

Another approach to overcome the limitations in power output has been to pursue the development of "dual-mode" engines that employ HCCI combustion at low loads and Diesel combustion or spark-ignition at high loads. Although attractive, HCCI/spark-ignition engines have not been discussed much in the literature. HCCI/Diesel engines are being pursued by a number of researchers.

2.4.3. Homogeneous Mixture Preparation

Effective mixture preparation, and avoiding fuelwall interactions is crucial for achieving high fuel efficiency, reducing HC and PM emissions, and preventing oil dilution. Impingement of fuel on the surfaces of the combustion chamber has been proven detrimental to HC emissions even for moderately volatile fuels such as gasoline [47]. Mixture homogeneity has an effect on the auto-ignition reactions that control the HCCI combustion phasing [43], [6], but there is significant evidence that low NOx emissions can be produced even with a large degree of mixture inhomogeneity within the combustion chamber [48], [49], [50], [51]. Homogeneous mixture preparation is most difficult for fuels with reduced volatility such as Diesel, which requires elevated intake air temperatures for low-smoke operation when port-injected [46].

2.5. Characteristics of HCCI Combustion

2.5.1. Ignition Theory Related to The HCCI Concept

Homogeneous Charge Compression Ignition (HCCI) has emerged as a technology with potential for reducing engine-out emissions and significant research efforts have been directed at understanding the fundamental mechanisms of this combustion mode in recent years. The theoretical and practical roots of the HCCI combustion

concepts are ultimately credited to the Russian scientist Nikolai Semenov, who began pioneering work in the field of ignition in the 1930s. Two relevant aspects of these efforts are Semenov's Thermal and Chemical ignition theories [24], [25], [26].

The Thermal ignition theory postulates that the combustion process in air/fuel mixtures can be initiated only when sufficient molecular collisions are occurring (sufficient temperature, pressure conditions) [26]. Figure 2.4 depicts generalized plots of the "Semenov Equation", showing typical predicted boundaries which separate non-igniting and spontaneously igniting regimes for air/fuel mixtures within vessels, in terms of pressure vs. temperature, and temperature/pressure vs. concentration (fuel/ air ratio).

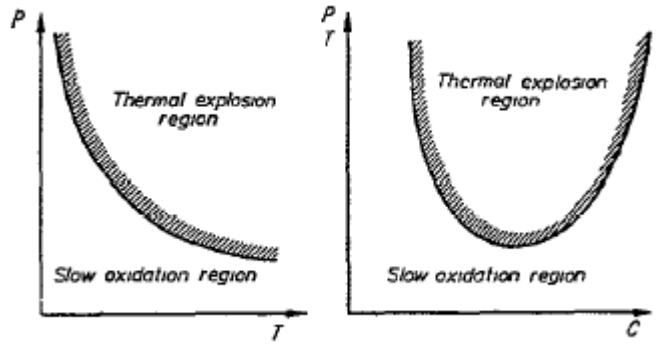


Figure 2.4. Illustration of Ignition Limits in Accordance with Semenov's Thermal Ignition Theory.

The Semenov Equation proved to be a useful qualitative tool, yet experimental results were not in strictest agreement.

Thereafter Semenov developed his Chemical, or Chain theory of ignition, wherein he hypothesis that combustion involves a process of branching chemical reaction chains, initiated at active chemical centers. According to this theory, spontaneous ignition occurs whenever the number of chains being initiated exceeds the number being terminated. This theory helped to explain some differences between predicted spontaneous ignition trends (as shown in Figure 2.4), and those determined experimentally, as shown in Figure 2.5.

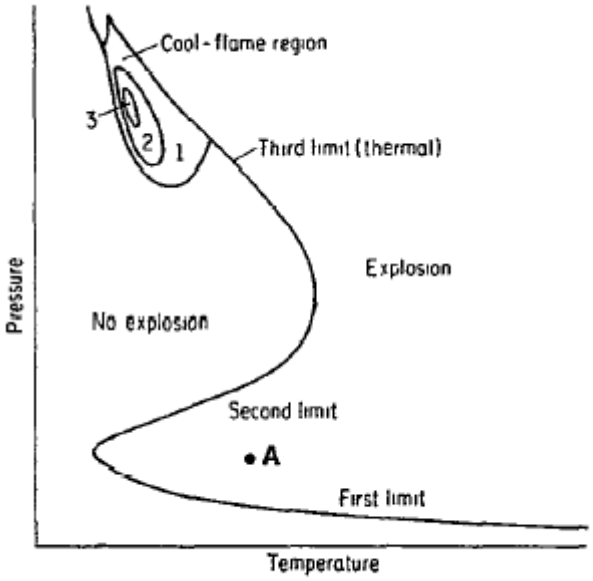


Figure 2.5. Schematic of the relative locations of explosive, non-explosive, and cool flame regions for a hydrocarbon-air mixture.

In Figure 2.5, the experimental ignition/non-ignition boundary shows a curious peninsula, which is absent in the plot of the Semenov Equation in Figure 2.4a. The chain theory provides an explanation, in terms of the 3 limits of non-ignition as labeled in Figure 2.5. Approaching the first limit from point A (which is within the explosive regime), increasing numbers of chains are destroyed at the vessel wall with respect to those formed in the gaseous state. Approaching the second limit, or lower pressure boundary of the peninsula, chain formation process become slower with respect to chain destruction processes due to pressure increases. At the high pressure side of the peninsula, mixtures rapidly explode, due to a high frequency of molecular collision. Regions to the right of the peninsula and above the first limit are all within the explosive regime.

Cool flames comprise an additional non-explosive, yet light emitting /exothermic condition, as observed in Figure 2.5. They are characterized by the presence of radical species, such as OH, CH, C_2, H, CHO, HO_2, and O [7], [27], [28], [8], [29], [30], [31]. As their name would suggest, cool flames occur at lower than conventional combustion temperature (below 950 K for gasoline) [7]. Their occurrence is believed to be closely related to the low-temperature kinetics which occur prior to the high temperature energy release reactions occurring in normal engine combustion processes, during the period termed ignition delay [26]. Research

of gasoline auto-ignition using rapid compression machines has demonstrated similar phenomena [7], [31]. Thus the kinetics of knock initiation and ignition delay are considered to be related to cool flames [26], [30].

As such Somonov, seeing the limitations imposed by the physical-dominating processes of SI and CI engines, sought to exploit a chemical-kinetics controlled combustion process for IC engines. By subjecting entire IC engine intake charges to the thermodynamic and chemical conditions similar to those of cool flames, a more uniform heat release process should be realized.

The first controlled-combustion engine, developed by Semenov, Gussak, et al, utilized the LAG (Avalanche Activated Combustion) concept [25]. This system employed a lean intake charge (to limit the rate of heat release), supplemented by a high temperature and partially burned rich discharge from a separate pre-chamber. As this rich mixture traversed in to the main combustion chamber, it was extinguished, and became thoroughly mixed with the main charge, providing active species and thermal energy for more homogeneous combustion. Figure 2.6 shows a schematic of this process. The LAG process, considered a successful variation of HCCI combustion attainment, has undergone significant study and development since its introduction [32], [33].

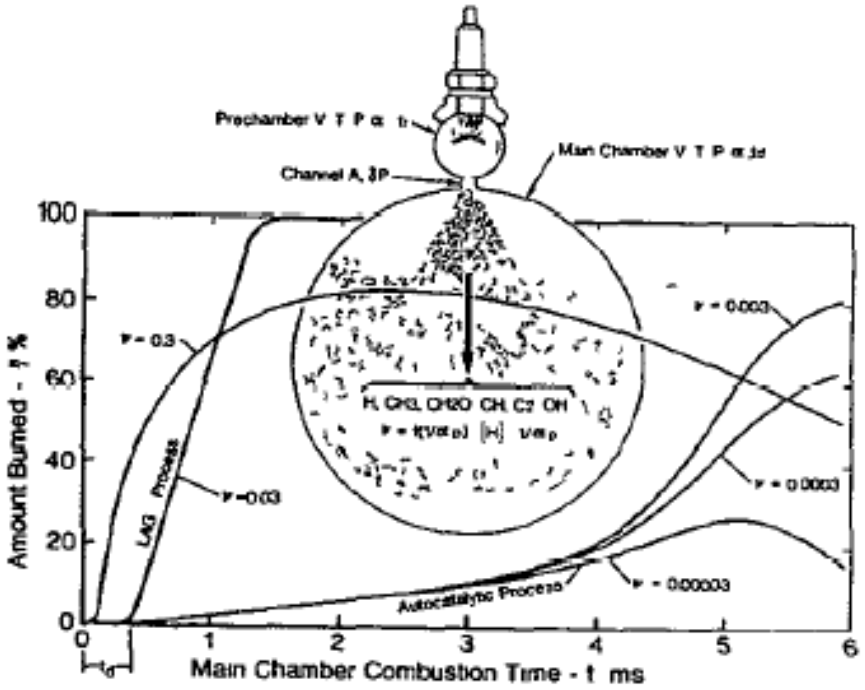
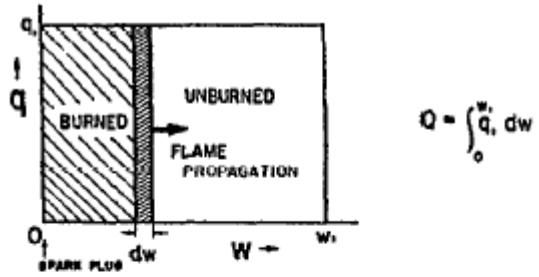
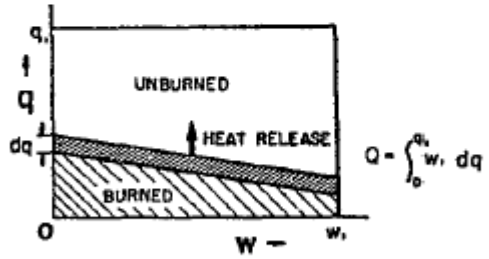


Figure 2.6. The LAG Combustion System.

Since these studies and recent studies, it is known that the ideal HCCI process in IC engines involves the simultaneous reactive envelopment of entire intake charges, allowing a more uniform and repeatable processing of fuel to proceed with respect to that of SI or CI engines. Figure7 illustrates the fundamental difference between SI and HCCI engine heat release.



(a) Spark Ignition Combustion



(b) HCCI Combustion

Figure 2.7. Ideal modes of SI and HCCI heat release [2].

The x-axis represents the fraction of total mixture weight, w, while the y-axis represents q, the heating value per unit weight of charge in the cylinder. Whereas the entire heating value of each minute parcel of mixture must be released during the finite duration spent in the SI engine active zone, HCCI combustion more slowly and uniformly releases heat from the entire charge. This is further illustrated in Figure 2.8, where simultaneous reactions are depicted with thermal equilibrium existing in the mixture of combustion products and unconsumed air.

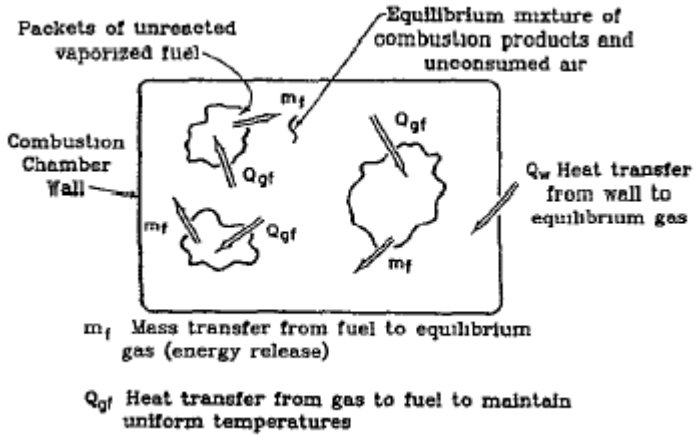


Figure 2.8. HCCI Energy Release Model Illustration [7].

The achieve HCCI combustion in IC engines, temperatures must be sufficient to initiate and support the active sites yet a means must exist to prevent runaway energy releasing conditions (explosive energy release), as occurs during SI engine knocking. In addition to the LAG type combustion system, which utilizes a lean main mixture fed by an extinguished rich charge, these goals have been accomplished with exhaust gas recirculation (EGR). Two stroke engines are particularly conducive to supplying prompt EGR, which offers more thermal energy to the intake charge than external EGR, and have thus been utilized in several investigations [2], [14], [27], [20].

Figure 2.9 illustrates relative combinations of mean charge temperature, new charge quantity and residual gas quantity suited to HCCI, SI or neither combustion-operating mode. Delivery ratio, the x-axis in this figure, is similar in meaning to the volumetric efficiency of SI engines, defined as the ratio of entering of delivered air mass to the ideal air mass (unthrottled) at ambient density. The presence of residual gas or EGR, lowers the delivery ratio. In Figure 2.9, HCCI is not stable or possible in region A, as mean charge temperature is too low due to excessive EGR. Region B is best suited for HCCI combustion, with relatively high charge temperatures and quantity of residual gases present. In C, both HCCI and SI can occur interchangeably, while SI operation is optimal in D, where temperature is low enough to prevent knocking and residual gas is low enough to prevent misfiring.

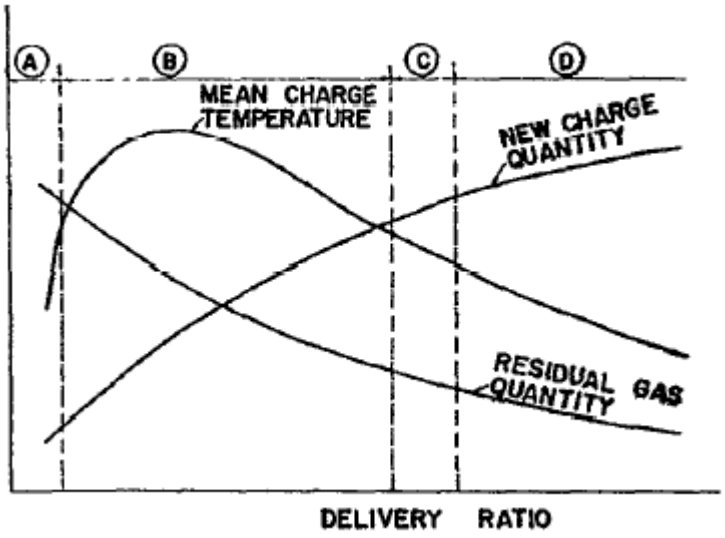


Figure 2.9. Model of Combustion Regions and related engine conditions [2].

HCCI operation, when optimized, has been shown to provide efficient, smooth operation [7], [2], [14], [34], [27], [12], [20]. The smoothness of HCCI combustion is attributed to an extreme repeatability of pressure profiles from cycle to cycle. Figure 2.10 compares the pressure history for 50 cycles from SI and HCCI engines, operating at similar steady state conditions of speed, load, and equivalence ratio.

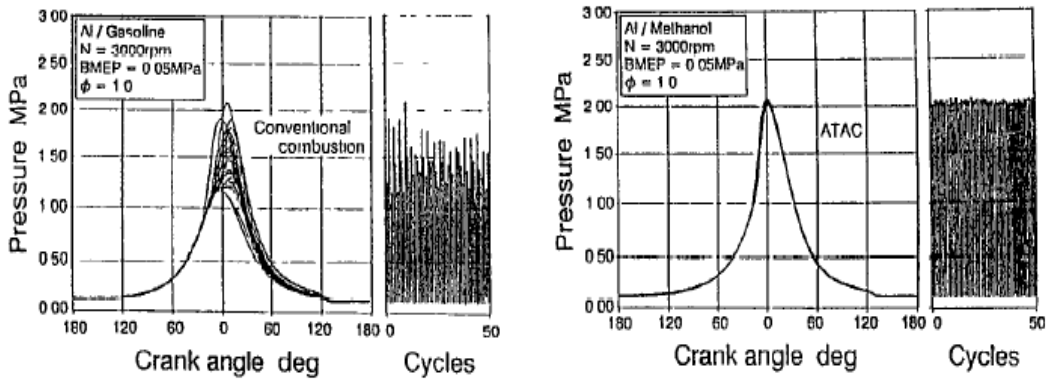


Figure 2.10. Comparison of cylinder pressure histories for a) SI operation (gasoline), and b) HCCI (labeled ATAC) operation with methanol [14].

HCCI combustion of most fuels displays a peculiar two-stage heat release, as shown in Figure 2.11.

The first stage of the heat release curve is associated with low-temperature kinetic reactions (cool and/or blue flames), and the time delay between the first and main

heat releases is attributed to the "Negative Temperature Coefficient Regime" of these reactions [52], [53]. Low-temperature kinetics has been studied for some time, as this chemistry is responsible for knock in spark-ignition engines [54], [55]. Research conducted with the use of optical diagnostics has shown that HCCI combustion initiates simultaneously at multiple sites within the combustion chamber and that there is no discernable flame-propagation [52], [14], [8]. It has been reported that, despite the absence of a flame front, the HCCI heat release rate is not controlled purely by chemical reaction rates. One group has postulated that turbulent mixing may play an important role in limiting the heat release rate [56], although this view is not embraced by all researchers in the field. Since the combustion reactions are not initiated by a spark and are not limited by traditional flame-sheet physics, leaner mixtures can be consumed by HCCI combustion than is possible through other methods. In general, HCCI combustion consists of distributed, fuel-lean reactions and is devoid of localized high-temperature regions or flame fronts.

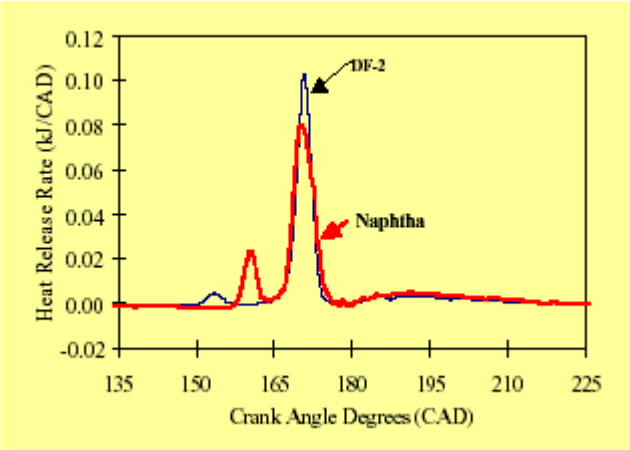


Figure 2.11. Typical heat release curve from HCCI combustion of DF-2 Diesel fuel and a Fischer-Tropsch Naphtha.

The experimental results of the study of Christensen et al. are seen in Figure 2.12. For these experiments a Volvo TD-100 series diesel at 10:1 compression value. The engine is an in-line six cylinder engine, modified to operate on one cylinder only. In this figure the two stage of heat release can be seen.

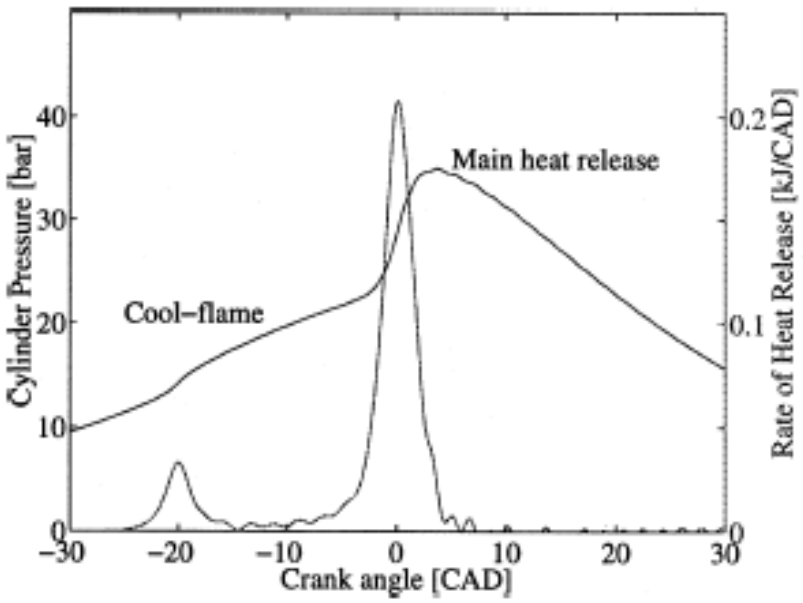


Figure 2.12. Typical heat release [142].

HCCI combustion initiation is not sensitive to incylinder fluid mechanics, and generally displays very low cyclic variability [36]. However, under some conditions, bi-modal cylinder pressure distributions have been obtained [21]. This bi-modal, or irregular, combustion characteristic is believed to be associated with the gas exchange process and the retention of residual exhaust products from previous cycles [21], [54].

2.5.2. Emissions Behavior

The main motivation for studying HCCI combustion stems from its potential for significant reductions in exhaust emissions in comparison to conventional Diesel or spark-ignition combustion. A brief overview of the emissions characteristics from HCCI engines is provided in this section.

2.5.2.1. Oxides of Nitrogen (NO_x)

Perhaps the single largest attraction of HCCI combustion is that it can reduce NOx emissions by 90 –98 % in comparison to conventional Diesel combustion [46], [45], [50], [57]. The underlying mechanism responsible for this reduction in NOx emissions is the absence of high-temperature regions within the combustion chamber. HCCI combustion reactions occur at the global air-fuel ratio, which is

typically quite lean, and at a temperature significantly below those encountered within the reaction zone in Diesel or spark-ignition engines. Several numerical models of NOx emissions from HCCI combustion have documented this effect [7], [58], [3], [59]. HCCI combustion is currently practical only at low mixture equivalence ratios. Peak combustion temperatures within HCCI engines are related directly to the engine load (if controlled by stoichiometry), and NOx emissions from HCCI combustion are known to increase considerably with increasing engine load. A quasi-dimensional engine model (Alamo Engine) was used to model the NOx emissions from HCCI combustion of Diesel fuel in comparison to conventional direct-injection Diesel combustion. This model requires the crank-angle resolved heat release as an input and uses the Zeldovich reaction set and a correlated contribution from prompt NO kinetics to predict NOx [60], [61]. Figure 2.13 shows the heat release rates used as inputs to the model and the predicted NOx emissions from HCCI combustion of Diesel fuel compared to a direct-injected Diesel engine (DI-Diesel) and DI-Diesel with aggressive EGR levels. The compression ratio for all cases was 16:1, and the prescribed heat-release curve for HCCI represents a typical scenario at this compression ratio. These results show that HCCI combustion can result in large NOx reductions at part engine load, but that the potential NOx advantage of HCCI combustion vs. DI-Diesel diminishes at higher equivalence ratios.

The numerical model was also used to study the effects of combustion phasing on HCCI performance. It was found that premature HCCI ignition at high loads causes dramatically increased BSFC and NOx levels. However, at low to medium load conditions, premature.

HCCI ignition increases BSFC without a large penalty in NOx emissions. The model also predicts that optimizing the combustion phasing can extend the low-NOx region of HCCI combustion to lower air/fuel ratios, but this has been difficult to achieve in practice so far.

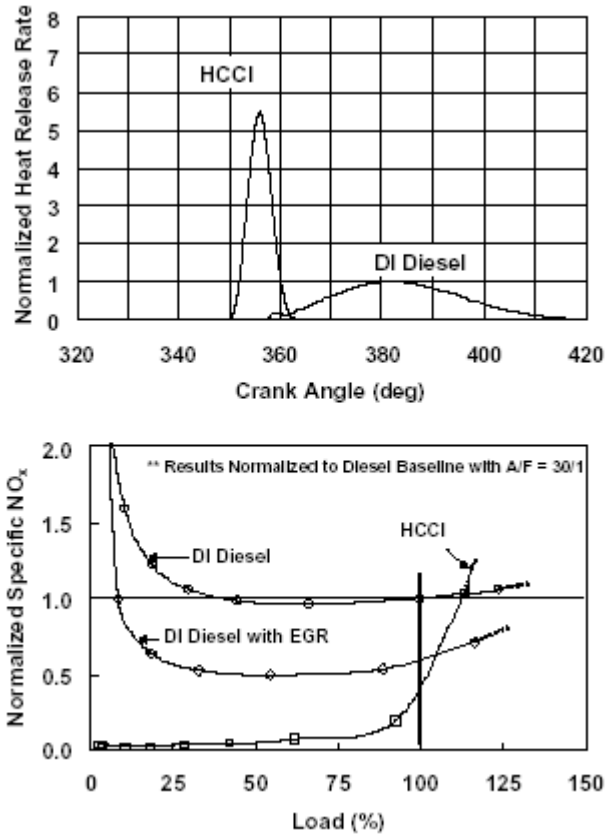


Figure 2.13. Predicted NOx emissions vs. engine load for typical HCCI and DI Diesel combustion.

2.5.2.2. Particulate Matter (PM)

HCCI combustion has also been reported to produce low levels of smoke and PM emissions [38], [48], [49], [51]. The mechanism for these smoke reductions is not as well documented, but it is thought that the absence of diffusion-limited combustion and localized fuel-rich regions discourages the formation of soot. One exception to this can occur when poor mixture preparation leads to liquid fuel deposition on the combustion chamber and localized fuel-rich regions of combustion.

2.5.2.3. Hydrocarbons (HC) and Carbon Monoxide (CO)

In contrast to NOx and PM emissions, HCCI combustion typically results in higher HC and CO emissions than conventional Diesel combustion [38], [45], [5]. One factor that contributes to these observed levels of HC and CO emissions is the low incylinder temperature due to the lean mixtures and/or high levels of EGR, which are

necessary for satisfactory HCCI operation. It is well known that reduced burned gas temperatures lead to decreased post-combustion oxidation rates within the cylinder [62] and increased levels of HC and CO in the exhaust. Mixture preparation is of great importance to HC emissions for HCCI combustion of liquid fuels, for it is well known that liquid fuel deposition on combustion chamber surfaces can result in dramatic increases in HC emissions [47]. This problem is exacerbated for heavy fuels such as Diesel.

2.5.3. Efficiency

HCCI combustion is generally characterized by high heat-release rates, which can approximate the ideal Otto cycle when properly phased in relation to the engine cycle. The distributed low-temperature reactions and nonluminous combustion result in reduced heat rejection to the engine. Hence, HCCI combustion is, in itself, conducive to high thermodynamic cycle efficiencies.

HCCI fuel efficiencies comparable to those of conventional diesel combustion at part load have been reported by several researchers [8], [57], [38], [5], [42]. However, reduced fuel efficiencies (higher BSFC) are reported for Diesel engines employing partial fumigation [37] and for some direct-injected HCCI engines running on Diesel fuel [38], [63]. Difficulties in mixture preparation, fuel impingement on the walls, and poor combustion phasing are thought to be predominantly responsible for these reduced efficiencies.

2.6. Future Applications of HCCI

There are a number of obstacles, which must be overcome in order to realize a fuel-efficient, low emissions HCCI engine. A full-time HCCI engine appears desirable, but its ability to produce power comparable to conventional Diesel or stoichiometric engines is still in question. Computational and experimental results suggest that, even if stoichiometric air-fuel ratios were possible under HCCI combustion, there would be no NOx benefit over spark-ignited combustion. Highly boosted, fuel-lean HCCI engines appear to be a promising option for producing full power output in stationary and marine applications. Future development of HCCI-specific fuels and improvements in combustion phasing control may enable Diesel-like air/fuel ratios

and power output. For near-term mobile applications, however, HCCI combustion may be best suited to “dual-mode” engines, which take advantage of HCCI benefits at low loads and operate on either spark-ignition or conventional Diesel combustion at full load. An attainable goal may be to operate on HCCI mode up to 75% of the peak load. Accordingly, the nearest-term application of HCCI combustion is likely to be in those engine applications, which experience substantial low and part load operation during their useful life.

HCCI combustion has received most attention for Diesel engine applications, because future NOx reductions due to pending emissions legislation is more severe for these engines. However, HCCI combustion may be an attractive method for reducing low-load NOx emissions from spark-ignited engines. Full-time HCCI engines are not limited to Diesel or gasoline, and may require HCCI-specific fuels or additives.

CHAPTER 3

PHYSICAL MODELLING

The modeling of combustion, which goes to the early days of internal combustion engine development in nineteenth century, is an important problem in most practical combustion systems. This development is the result of research to develop both more realistic approximations for real engine processes, and more accurate methods for calculating the parameters of combustion in an engine [64]. The computer simulations of combustion models of engine processes are now valuable tools for predicting and analyzing engine performance.

The HCCI engine operates under regimes where compression heating of the charge results in ignition throughout the bulk mixture that is considered highly homogeneous. To predict the combustion mechanism in HCCI the approaches for the combustion modeling can be used. These models for combustion may be classified in three main categories: zonal models, one-dimensional models and multidimensional models.

3.1. Zonal Models

Zonal models are zero dimensional and generally used in studies of thermodynamic cycle analysis. These models may be divided in three parts: single-zone, two-zone and multizone models. By the use of these models, it is possible to study the transient behavior of temperature, pressure and concentrations. The combustion chamber is divided into a number of zones, which is assumed as a homogeneous mixture with the same temperature history, mole fraction and mass fraction of species, to compensate the spatial variation of combustion parameters. The pressure is assumed to be the same throughout out the combustion chamber at each moment. The advantage of zonal models is that the computation of detailed mechanisms and different phenomena such as flame propagation is possible [90].

In this approach the combustion in the cylinder is taken globally, and cylinder pressure and temperature changes by the crank angle degree and cylinder volume are calculated via the thermodynamic first law. The flame propagation ratio is calculated related to the temperature, pressure, mixture concentrations ratios and some other parameters to get the burned fuel amount in unit time from the global combustion model. In calculations the effect of kinetic and equilibrium reactions are taken in to account chemically.

Single zone models predict only pressure, temperature and fuel concentration in the combustion chamber. These models have many empirical correlations when they are used to predict autoignition onset.

Recent analyses of HCCI engines have used detailed chemical kinetics codes [80,81] in either single zone mode [4, 82], or multi-zone mode [83,84]. Single zone models assume that the combustion chamber is a well-stirred reactor with a uniform temperature, pressure and composition. This model is applicable to homogeneous charge engines, where mixing is not a controlling factor. Single zone analyses can predict start of combustion with good accuracy if the conditions at the beginning of the compression stroke are known, and therefore can be used to explore ranges of operation for different fuels and conditions [69]. On the other hand, single zone models cannot take into account the effect of temperature or concentration gradients that exist inside the cylinder. The assumption of uniform charge temperature inside the cylinder results in all the mass igniting at the same time when the ignition temperature is exceeded. Therefore, a single zone model underpredicts the burn duration, and also overpredicts both peak cylinder pressure and NOx, and it poorly predicts HC and CO emissions, because HC and CO emissions result from cold mass in crevices and boundary layers, which are too cold to burn to completion. A multi-zone model [83] can take better account of temperature gradients inside the cylinder, and therefore can do a much better job at predicting peak cylinder pressure, NOx and burn duration, and generates much improved predictions for HC and CO emissions. These benefits are obtained at the cost of a much-increased time for computation compared with a single zone model. Both models are valuable when judiciously applied [85].

A one-zone model has already been investigated and described in literature to model the behavior of natural gas HCCI engines [65], [66], [67], [68]. Despite its simplicity

it reproduces the overall engine performance trends and gives very good agreement with experimental data, and is therefore often applied in similar simulations.

One of the studies of thermo-kinetic one-zone model was done by Fiveland et al [87] to capture the fuel composition effects seen in the experiments. CHEMKIN libraries was used in this study for modeling combustion. Martinez-Frias also use a single-zone detailed chemical kinetics code HCT (Hydrodynamics, Chemistry and Transport) in his investigation of a control system for HCCI engines, where thermal energy from exhaust gas recirculation (EGR) and compression work in the supercharger are either recycled or rejected as needed [100]. In another research to investigate a control system for HCCI engines, where equivalence ratio, fraction of EGR and intake pressure are adjusted as needed to obtain satisfactory combustion, a one-zone model was used [85].

Two-zone model is used mostly in autoignition and knock studies in several studies in the past. A two-zone model was developed for the prediction of the onset of autoignition and knock in several engines with different fuels by Karim [70], [71], [72]. The burned products and unburned reactants in the cylinder charge assumed as separated zones and generated important performance parameters such as pressure history and power output. A dimensionless knock criterion was developed to provide an indication of the knock intensity [70]. A two-zone model of the whole cycle of a SI engine for knock prediction was also used by Moses et al. The effect of methanol admixture on gasoline knocking also was investigated by them. It is found that 9% methanol cancels out knocking for the engine.

A simplified two-zone zero-dimensional model for the end gas in an SI engine by applying principles from classical thermodynamics is used by Hajireza [73]. The end-gas is assumed to be compressed by the progressing flame front and the piston movement in their first model. In the second model, it is assumed that the unburned gas is affected by both flame front propagation and the piston movement [74]. A zero-dimensional, three-zone model for the investigation of gas behavior in the combustion chamber of SI engines was also developed by them [75]. The first zone is modeled as the zone behind the flame front like the burned gas products, the second zone for unburned gas ahead of the flame front and the third zone for the end gas adjacent to the wall. In the model, flame front velocity, convective heat transfer coefficient and the thickness of the boundary layer is determined by three empirical equations [90].

For predicting combustion and emissions in a Homogeneous Charge Compression Ignition (HCCI) Engine generally a methodology that judiciously uses a fluid mechanics code followed by a chemical kinetics code is used to achieve great reduction in the computational requirements; to a level that can be handled with current computers. Such a methodology had developed by Aceves et al [86] for prediction of Iso-Octane HCCI combustion. The procedure is based upon a two-step sequence. First, a fluid mechanics code (KIVA3V) is used, without any chemical kinetics, to calculate temperature histories during the compression stroke. The engine geometry-specific information calculated by KIVA3V in the form of the temperature histories is then handed off to a detailed chemical kinetics code (HCT; Hydrodynamics, Chemistry and Transport). HCT operates in multi-zone mode, with geometry-independent zones. While many thousands of spatial grid nodes are needed in KIVA3V to resolve the fluid mechanical features of the compression stroke, the spatial resolution of HCT is only about 10 nodes or "zones," while great resolution of the numerous chemical species is now demanded. This procedure achieves the benefits of linking the fluid mechanics and the chemical kinetics with a great reduction in the computational effort, to a level that can be handled with current computers.

A similar study is done by Ogink et al [87] to combine detailed chemistry and gas exchange processes. The simulation tool was constructed by connecting the SENKIN code of the CHEMKIN library to the AVI BOOST engine cycle simulation code. In this study a single-zone model was used.

3.2. Dimensional Models

Multidimensional models contain the real gas-dynamic flow, turbulence, flame propagation and autoignition in the combustion chamber and solve these quantities by numerical methods for control volumes. The prediction of the gas inhomogeneity is better with multidimensional models. These models need reduced chemical mechanisms and semiemprical models of multidimensional turbulence. Thus, their universality to more complicated flows like one in an engine is doubtful. Furthermore, computer resources are not enough to combine multidimensional models with detailed chemical kinetics calculations in most cases.

In this approach the combustion chamber is formed with computational planes and

solved for laminar or turbulent flows by the mass, momentum, and energy equations spontaneously with the chemical reactions equations.

One-dimensional models can be used to calculate the inhomogeneity of pressure, temperature, species concentrations and gas flow field. The flame front propagates in one direction normal to the wall surface in the one-dimensional models [76].

A quasi-one-dimensional model for predicting the onset of end-gas autoignition is used by Jenkin [77]. It has been coupled with a chemical kinetic model for the low temperature, pre-flame reactions of hydrocarbon fuel and air mixtures. It can predict the onset of autoignition without any knowledge of the cylinder pressure history. The model was used also to investigate the effect of the flame propagation rate on the knock onset time.

Two- and three-dimensional models have been developed in last twenty years. A low-temperature kinetics model (Shell autoignition model) was integrated by Natarajan and Bracco [78] with an two-dimensional engine model and applied to cool-flames in a stirred reactor, to spatially uniform mixtures in a constant volume bomb and to a rapid compression machine. They found that the autoignition chemistry was activated in front of the main flame and autoignition occurred in the low-temperature region of the propagating flame.

A two-dimensional model for the simulation of combustion in SI engines is employed for knock prediction by Schapertons and Lee [79] using modified shell model for low temperature reactions and a single global reaction for main combustion in the flame front. They also investigated the effects of engine geometry, exhaust gas recirculation and swirl on knock. Their model provides some details related to the pattern of flow in the engine but needs some information about the chemistry of combustion.

In recent years, some researchers use both zonal and multidimensional models. It is easier to use zonal models for the understanding and the explanation of knock mechanism. However, one- and multi-dimensional models give information about the inhomogeneity of quantities and the properties of the gas in detail [90].

CHAPTER 4

CHEMICAL KINETIC MODELLING

The modeling of the HCCI engines requires a detailed knowledge of the chemical kinetics of combustion system. In recent years, chemical kinetic modeling has become important for the analysis of combustion systems i.e. internal combustion engines.

In general, a reaction mechanism gives a description of the elementary steps occurring during the conversion of reactants (fuel and oxidizer) to final products and consists of all the chemical species related to combustion event together with the elementary reactions among them. It provides a combination between the variety of chemical species concentrations and the energy equation through the heat of reaction [135].

This chapter is prepared from the [90], [91].

4.1. Detailed Mechanisms

Kinetic modeling of combustion using detailed mechanisms presents a powerful method for investigating the key elementary reactions discussed previously. Detailed mechanisms consist of a few hundred elementary reactions involving many tens of intermediate species that make up the combustion process that has to be accounted for. They include all the important elementary reactions and species, and as much fundamental information as which is known.

The generation of a detailed mechanism has come a long way from the early developments in the hydrogen oxygen scheme. It is a highly effort concentrated, time consuming and iterative task. As a result of hard work over several decades, detailed reaction mechanisms have been developed for alkane fuels up to iso-octane based on fundamental understanding of the chemical mechanisms involved by a number of different groups of workers [92], [93], [94], [95]. Detailed reaction mechanisms are

also available for the combustion of other simple fuels such as hydrogen and alcohols.

The generation of reaction mechanisms manually starts with the estimation of necessary species and with assessing in which reactions they are likely to occur under the appropriate conditions. Reactants and main products with their large number of intermediate species must be included in the mechanism. Thus, an enormous number of reaction steps have to be evaluated. Although this procedure can be automated, producing a general program for a detailed mechanism generation is very difficult.

In recent years, programs for the automatic generation of the detailed reaction mechanisms have been prepared [96], [97], [98]. These programs generally consist of the following steps:

1. Storing the structures of chemical species in a form which can be used easily by the reaction generator,
2. Producing a feasible set of elementary reactions for a reaction generator,
3. Searching for kinetic parameters of the generated reactions in a database,
4. Producing possible reactions in the reaction generator.

After these steps, a detailed sensitivity analysis of the global parameter against all chemical rate coefficients is performed for the resulting mechanism to get a set of reactions, which are most important in the combustion process. Then an iterative process is applied to adjust the rate coefficients as accurate as possible up to the first set of optimized rate coefficients is reached. Next, controlling local parameters instead of global ones will refine the mechanism. Finally, an improved reaction mechanism is generated using the same iteration procedure [97].

There are some computer codes developed for mechanism generation such as Mamox (automatic reaction generation for low temperature oxidation), Reaction (X-window based program), Exgas (automatic reaction generation) and Thergas (kinetic parameters and thermodynamic data estimation).

The difficulty of using detailed mechanisms such as the most recent detailed mechanism for iso-octane which consists of 3445 elementary reactions and 805 species used by Curran [99], is related to the computational demands of the large set of nonlinear equations used to simulate reactions.

The main problem in these computations is that with the differences in reaction time-scales between each of the species is great. The existence of short time-scales

associated with intermediate species within a long overall time-scale increases the computational time. This problem is a feature of the detailed mechanisms and called "stiffness". The stiffness of the equation system also is increased by the low concentration species appearing in the reaction mechanism. Because of stiffness problem, too small time-steps are necessary to achieve stability and the use of standard integration methods like explicit Runge-Kutta methods become inapplicable in detailed mechanisms. It is therefore necessary to reduce the chemical system for using in simulations of practical engines with the commercial software products.

4.2. Skeletal Mechanisms

The principal difficulty in modeling the combustion of practical fuel molecules in computer simulations is the requirement large amounts of computer time and memory. Introduction of the detailed chemical mechanisms into complex multi-dimensional fluid dynamics problems for large hydrocarbon molecules is very difficult for these reasons. Thus, simplified mechanisms based on these detailed mechanisms validated against experimental data must be developed to be used in real engine conditions. A useful technique in modeling is reducing the detailed mechanisms first to a skeletal mechanism and then to reduce mechanism as long as the predictability of the kinetic models is still acceptable [100].

Detailed mechanisms, which are constructed by automatic mechanism generation, have some species that don't play any practical role for the computation conditions. These species and reactions are defined as redundant. The calculation of redundant species concentrations with very little mass fraction increases the computation time without any gain. The redundant species and reactions from a chemical reaction system are identified and eliminated for different pre-set levels of minimum reaction flow and sensitivity. In this approach species such as fuel, oxidizer and some products are predefined as non-redundant.

The species, which have sensitivity more than a maximum predefined value of all sensitivities for the combustion process under consideration, are defined also as non-redundant species during the range. They are obtained by means of a detailed sensitivity analysis. The non-redundant species are not removed from the mechanism.

It is possible to compute the relative importance of each species and reactions with the detailed reaction flow analysis, which is performed for each reactive atom in the system such as C, H and 0. The species and reactions which have a minimum flow less than predefined value of relative importance are selected as redundant. The details of the sensitivity and reaction flow analyses will be explained in the Section 4.4.

The skeletal mechanism, which is the first step of reduction procedure from detailed mechanism to reduced one, is constructed by excluding the redundant species from detailed mechanism without loss of information and is valid just for the situation that the chemical analysis is performed for. Its basic idea is to focus on a problem oriented mechanism.

With using this procedure, approximately 50% of the species from a detailed mechanism for laminar flames were removed by Warnatz [101]. A skeletal mechanism with simultaneous use of reaction flow and sensitivity analysis has been generated from a detailed mechanism for autoignition process of primary reference fuels by Soyhan et al [102]. In this study, the number of species was reduced from *75* to 64 without any significant loss of information. This skeletal mechanism was used as the input for a further reduction procedure base on the Quasi Steady State Approximation [103].

4.3. Reduced Mechanisms

Applying detailed kinetic models with large number of reactions in practical internal combustion engines is very difficult as the chemical models combined with multi-dimensional fluid dynamic models consume large amounts of computational time and memory. It is also difficult to see how detailed chemistry can be coupled to computational fluid dynamics (CFD) calculations of practical engines within predictable time.

Reduced mechanisms, which consist of a few steps and involve only a small number of chemical species, have been developed to overcome the limited range of applicability of the detailed mechanisms and to shorten the CPU time of computations. A successful reduced mechanism is faster and can reproduce essential features of combustion in comparison to the detailed mechanism [104].

There are numbers of approaches to generate the reduced mechanisms. They can be classified in two main categories as static and dynamic approaches, which will be discussed later.

Analyses such as reaction flow and sensitivity analysis are used to investigate the static influence of a species or a reaction in the detailed mechanism in the static approaches. Sensitivity analysis gives the reactions and species with high sensitivities and defines them as non-redundant which cannot be removed from detail mechanism. After adding fuel, oxidizer and products to this non-redundant list, reaction flow analysis gives the atomic mass flow through the given reactions. This is used to detect redundant species that are considered unimportant for the mechanism, due to the very small amounts of formation and destruction, for differently defined levels of mass flow.

The second one is to take a detailed or skeletal mechanism as reference and then to select only the most important species and reactions for the reduced mechanism [105]. Reduced mechanisms can be generated by applying the steady state assumptions to a detailed or skeletal mechanism without any significant loss of accuracy. A measure of species lifetimes is taken from the diagonal elements of the jacobian matrix of the chemical source terms. The species with the lifetime shorter than and mass-fraction less than specified limits are assumed to be in steady state and selected for removal from the skeletal or detailed mechanism. The details of species lifetime analysis will be discussed in the Section 4.4.

The first global model called Shell Model was developed at the Shell Thornton Center [106]. This model was refined by Cox and Cole [107] and then by Hu and Keck [108]. Autoignition is controlled by generic reactions in the Shell Model. They included only those reactions, which have a direct effect on time of occurrence of autoignition and needed only a few species to simulate the two stage phenomena of autoignition in hydrocarbon fuels.

A global mechanism that was constructed by introducing only the key reactions leading to autoignition of mixtures of air, fuel and diluents is used by Hu and Keck. It is based on the work of Benson [109] and similar to that proposed by Cox and Cole. It consists of 19 reactions essentially has a feature of producing two-stage ignition characteristics in high-pressure region. These two models are developed from the Shell model and give more accurate results for alkane oxidation at low temperature range. They are limited in their ability to show the transition of the

autoignition process for low to high temperature regime.

Hu and Keck's model was used by Chun et al. [110] to predict knock occurrence in a SI engine and obtained good agreement with experiments. The global model of Chun was also used by Brussovansky et al [111] to predict the effects of air and coolant temperature, deposits, spark timing and engine speed on knock occurrence.

The Chun model was applied by Cowart to predict the knock onset in an SI engine for iso-octane and n-pentane and the predictions were in a good agreement with experimental results. He also applied the reduced mechanism to predict knock intensity [112].

The global kinetic model described by Hu and Keck was used by Li et al. [113] to investigate the ability of a reduced chemical kinetic model in calculating heat release at low and intermediate temperature and to predict the heat release generated under motored engine conditions for a PRF fuel. The Hu and Keck model were also extended to include carbon monoxide formation and aldehyde, olefin and carbony] oxidation with 5 new species and 11 additional reactions.

A reduced mechanism for combustion of methane with special emphasis on formation and destruction of hydrocarbon radicals using steady state and partial equilibrium assumptions for minor species was developed by Paczko et al. [114]. The results of the reduced mechanism were validated by Glarborg et al. [115] by comparing perfectly stirred reactor calculations. It was shown that the reduced mechanism generally provides a good description of the methane oxidation process.

A reduced kinetic model very similar to Hu and Keck's was employed by Nakano et al. [116] to investigate the knock limited torque limit of engines. These works show that reduced models are able to predict the onset of knock. The reduced model contains 19 reactions and 17 species, and has ability to predict the two-stage ignition characteristics of paraffinic hydrocarbon fuels.

The reduced chemical kinetic models were discussed by Wang et al. [117]. The applicability of the reduced chemical kinetic model by Li et al. [118] was explored to predict autoignition time of primary reference fuels. It is found that this model is a useful tool to predict the autoignition time and a reasonable reduced kinetic mode. for butanes. This model is analyzed and modified by Wang et al. [119] to reflect the different oxidation chemistry between PRF's and butanes and refined b. comparing with experimental data.

A reduced mechanism for the autoignition of iso-octane by identifying paths to

formation of the stable species measured during experiments and eliminating paths to formation of species which were not measured was developed by Roberts et al. [120]. The mechanism, which consists of 103 species and 131 reactions, includes low, intermediate and high-temperature reactions and enhances the production of carbonyls during low to intermediate temperature oxidation of iso-octane.

The reduced chemical models for alkane oxidation, their development and application to predictions of combustion characteristics were reviewed by Griffiths [121] in detail. The reduction methods are also briefly explained in this review.

4.4. Kinetic Analysis of Reaction Mechanisms

A chemical kinetic mechanism can be analyzed by several methods. The influence of a parameter uncertainty on the final solution is calculated by means of a sensitivity analysis. The flux from the reactants to the final products is calculated by a reaction flow analysis. Further analysis for the dynamic characteristics of species and reactions can be examined by lifetime analysis.

For the analysis of chemical kinetic mechanisms, species and reactions of chemical kinetic mechanisms can be classified as important, necessary and redundant. Important species might be initial reactants and final products of the combustion process. Species, which have sensitivity more than a maximum predefined value of all sensitivities for the combustion process under consideration, are referred as the necessary species. They must be included in the mechanism for accurate reproduction of concentration of important species and temperature profiles. The species, which have a flow less than a pre-defined value of relative importance, are defined as redundant. First two types of species can be called as non-redundant species and identified by sensitivity analysis. Redundant species are detected by reaction flow analysis.

4.4.1. Sensitivity Analysis

Sensitivity analysis is a method for the studying the parametric information in kinetic models. It investigates the relation between the parameters and the results of the model. This technique provides information, which is difficult to control for complex mechanisms by using traditional methods. Through sensitivity analysis the species

that need to be calculated accurately for the desired result and which needs to be kept in the mechanism are found.

The simplest method for the calculation of the sensitivities is perturbing each individual parameter by a small amount at a time and after re-running the model, defining the sensitivities by differences at a later time. This method is slow and less accurate but it can be used if there is no better method.

Here, the task is to identify the species that are most sensitive on the entire combustion process, i.e. has the highest impact on the heat release and the pre-set none redundant species. Therefore a sensitivity analysis is performed:

$$S_{A,B} = \frac{\partial[A]}{\partial[B]} \approx \sum_{k=1}^{N_R} \frac{d[A]}{dr_k} . \frac{dr_k}{d[B]} \tag{4.1}$$

where $S_{A,B}$ is the sensitivity of the species A on species B, and higher order effects are not included giving rise to the approximation sign. Letters in brackets denote chemical species in units of a concentration. The last factor in the sum in equation 4.1 becomes

$$\frac{\partial r_k}{\partial c_j} = \nu'_{jk} c_j^{(\nu'_{jk})} \prod_{i \neq j}^{N_s} c_j^{(\nu'_{ik})} k_k = \frac{\nu'_{jk}}{c_j} r_k \tag{4.2}$$

resulting in the following expression for the species sensitivity that is used in the computations

$$S_{A,j} = \sum_{k=1}^{N_R} \left| \frac{d[A]}{dr_k} \frac{\nu'_{kj}}{c_j} r_k \right| \tag{4.3}$$

The species sensitivity analysis is then performed for entire parameter ranges. The different parameter sets give different ratings of the most sensitive species.

The relative importance that a species needs in order to be included in the reaction mechanism, I, is defined as

$$I_i = \max(I_j f_{ij}^a, I_j c_{ij}^a, I_i; j = 1, N_s, a = 1, N_a) \tag{4.4}$$

Equation 4.4 needs to be solved iteratively. The initial value, $I_{i,o}$ for this process is given by the relative species sensitivity coefficients:

$$I_{i,o} = \frac{S_{ji}}{\max_{k=1,N_s}(S_{jk})} \tag{4.5}$$

This implies that the preset non-redundant species have a level of relative importance of 100%. If a species is found to be crucial for either formation or consumption of a non-redundant species, it is given a relative importance value according to its role in this process. The species is then classified as non-redundant if its importance is higher than a pre-set value. The procedure is repeated until the calculated importance of the species converges. At the end of the process, the remaining redundant species were eliminated from the original mechanism

A variational method has been developed by Grouset et al. [122] and applied to a set of non-linear equations describing a well-stirred reactors network for fast sensitivity analysis. It is used to show how it can help in reduction of chemical kinetic mechanisms and to predict combustion chamber performance. A complete sensitivity analysis for all parameters obtained in less time than needed for the solution calculation. This method gives an information about reduction possibility before reduction procedure and was used as a first step for a reaction scheme reduction in conventional chemical reduction techniques.

This analysis was used by Chevalier et al. [123] for OH-radical concentration in ignition of heptane-air mixture. Detailed sensitivity analyses of n-heptane and cetane for automatic generation of reaction mechanisms were also performed by them.

A sensitivity analysis, which is able to identify the rate-limiting steps in a reaction mechanism, have been used for homogeneous systems, stationary one-dimensional systems and combination with uncertainty consideration by Warnatz [92]. An example of sensitivity analysis for the ignition delay time in 112-02 mixtures at different temperatures with respect to rate coefficients was given where the integral property was the ignition delay time in a spatially homogeneous system in this paper. The other examples were performed for methane-air flame, propane-air flame, and

benzene-air flame. All these examples show that only a few elementary reactions determine the chemistry and reduction possibility.

A detailed sensitivity analysis based on the OH concentration in an n-decane-air mixture during ignition delay at high temperatures was performed by Nehse et al. [124] to generate an oxidation mechanism of large aliphatic hydrocarbons. It is found that there was sensitivity to reactions of fuel-unspecific small molecules with small contributions even from C_3- and C_4- species at high temperatures.

Sensitivity analysis can be used to analyze the effect of different levels of reduction for the application of steady state assumption by Somers and Goey [125]. The steady state sensitivities were used to analyze and to minimize the differences between the reduced mechanism and the original detailed mechanism.

4.4.2. Reaction Flow Analysis

Although the application of sensitivity analysis for mechanism reduction is completely correct, mechanism reduction can be done in an easier way by applying reaction flow analysis. It can be used with sensitivity analysis, which gives the most important species and reactions, simultaneously. The reaction flow analysis, which is performed for each reactive atom in the system such as C, H, 0 and N, determines the major and minor paths from fuel to products.

The theory of reaction flow analysis is based on the fact that if a species has no consuming reactions, a change in its concentration doesn't affect the concentration of other species. Thus, a species is redundant if the removal of all its consuming reactions doesn't cause significant effect on important futures comparing with detailed mechanism.

The next step is finding redundant reactions and elimination of them from the detailed mechanism. A comparison of the contribution of reaction steps to the production rate of necessary species gives the redundant reactions [92]. If the contribution of a reaction to each necessary species is small, this reaction is called redundant reaction according to this method. In this approximation, the reaction contributions must be calculated at several reaction times and all of the contributions to each necessary species must be considered. All reactions, which consume the redundant species, are redundant and can be removed from the detailed mechanism. The sensitivity for reaction rate coupled with reaction flow analysis can be used to

identify other redundant reactions.

The reaction flow analysis checks the formation and consumption of species at specific times in time-dependent problems in a process such as homogenous ignition. The following two net flow parameters f_{ij}^{a} and c_{ij}^{a} are used to describe the flow of atom a between species i and j through formation or consumption of the former:

$$f_{ij}^{a} = \frac{\sum_{k=1}^{N_R} r_k v'_{jk} v''_{ik} \frac{n_j^a}{\Delta n_k^a}}{\sum_{k=1}^{N_R} r_k v''_{ik}} \tag{4.6}$$

$$c_{ij}^{a} = \frac{\sum_{k=1}^{N_R} r_k v''_{jk} v'_{ik} \frac{n_j^a}{\Delta n_k^a}}{\sum_{k=1}^{N_R} r_k v'_{ik}} \tag{4.7}$$

where f_{ij}^{a} is the relative transfer of atom a through formation of species i from species j and c_{ij}^{a} is the relative transfer of atom a through consumption of species i to species j.

The number of atoms n_j^a are normalized to the total number of atoms transported in the reaction as

$$\Delta n_k^a = \sum_{i=1}^{N_s} v'_{ik} n_k^a \tag{4.8}$$

The flow parameters are also normalized to the total formation and consumption rate of species i in order to achieve range between 0 and 1 for the flow parameters.

Reaction flow analysis has been discussed by Tomlin et ai. [97] to find redundant species and reactions. It was applied to hydrogen oxidation system in continuously stirred batch and flow reactors. Redundant species, 11202 and 03, and redundant reactions, which consume these redundant species, were removed from the chemical reaction mechanism.

A reduction of redundant species for a natural gas mechanism has been performed, using reaction flow analysis simultaneously with sensitivity analysis by Soyhan et al.

[126]. Different levels of definition of the redundancy was used, namely 1.0%, 5.0% and 10.0%. The resulting mechanism consists of 46 species and 518 reactions, compared to 53 species and 590 reactions in the original mechanism. Validation of the mechanisms to shock tube experiments, and comparison of the skeletal mechanism to the detailed mechanism, shown that the practical difference between them is so small and can be considered unimportant for engine calculations.

A method for automatic reduction of detailed kinetic to skeletal mechanisms for complex fuels using sensitivity and reaction flow analysis simultaneously was presented by Soyhan et al. [102]. Redundant species, not relevant for the occurrence of autoignition in the end gas, were identified and eliminated for different pre-set levels. The resulting skeletal mechanism was validated for the parameter ranges of initial and boundary values, the analysis have been performed and good agreement with detailed mechanism was achieved.

4.4.3. Chemical Lifetime Analysis

The dynamics of the chemical system can be analyzed by taking the time dependence into account in Equation 4.9, as

$$\frac{dx}{dt} = f(x(t)) \tag{4.9}$$

The parameter of the system, k can be considered as constant in time. The system is non-linear and can be linearised around point x_0 by using Taylor series,

$$\frac{d}{dt}(x - x_0) = f_0 + J(x - x_0) \tag{4.10}$$

Here x_0 is a constant linearisation vector. The general form of this equation is

$$\frac{dx}{dt} = Jx + Bw \tag{4.11}$$

where B is the unity matrix and w is a constant input signal formulated as,

$$w = (f_0 - Jx_0) \tag{4.12}$$

[127]. The solution of the system equation 4.11 can be written as;

$$x(t) = e^{j(t-t_0)}x(t_0) + \int_{t_0}^{t} e^{j(t-\tau)}Bw(\tau)d\tau \tag{4.13}$$

where $X(t_0)$ is the vector for initial values at time t_0.

The Jacobian elements, J_{ii}, are measures of the rates of change as a result of perturbation in concentration. If the Jacobian element is inverted, its dimension will be time; thus the inverted Jacobian element can be used as a characteristic time scale for a species. So, a measure of the lifetime of species i can be written as

$$\text{Lifetime} = \tau_i^c = (J_{ii})^{-1} \tag{4.14}$$

where J_{ii} is the diagonal element of the Jacobian matrix of the chemical source terms. Since the lifetime of a species is related to the reciprocal of the diagonal Jacobian element, short lifetimes give small errors and tolerate quite large errors [105]. Many species in the chemical kinetic reaction systems have very short lifetimes and can be described well by quasi steady state approximations described in Section 4.4.

The lifetime analysis was used by Nilsson et al. [128] to reduce the complex fuel chemistry for simulation of combustion in an Homogeneous Charge Compression Ignition (HCCI) Engine. They detected equilibrated species with an overall mass fraction weighted lifetime measure as

$$\text{Lifetime} = \tau_i^c = (Y_i / J_{ii}) \tag{4.15}$$

where Y_i is the mole fraction of the species i. This approximation induced a penalty for species with high concentrations and applied it for automatic quasi-steady-state reduction (QSSA) of the reaction mechanisms. Temperature and pressure history and ignition delay times were compared to validate different reduced mechanisms generated for different time scales. They reduced the original mechanism containing

52 species to reduced mechanism, which has 32 species, with an error less than 1 crank angle degree (CAD) in ignition delay time. When the original mechanism was reduced to 17 species, the ignition delay error increased to approximately 10 CAD.

The lifetime analysis was used by Lovâs et al. [129] to generate reduced chemical mechanisms for nitrogen containing fuels with a measure of species lifetimes, which was taken from the diagonal elements of the Jacobian matrix of the chemical source terms. The species with lifetimes shorter than a specified limit were selected as removal and assumed to be in steady state. The 69 species original detailed mechanism is reduced to 23 species reduced mechanism. Their reduced mechanism consists of fuels (C_2H_4, CH_3NH_2), oxidant (02), stable products ($C0_2$, H_20, NO) and intermediates. Although the lifetime of some species such as HINO is within the limit of the steady state approximation, they were not removed from the detailed mechanism because of numerical reasons. It is also shown that using species lifetime as a measure is a good method in the reduction of detailed mechanism and the results in calculated NO mole fraction is within the accuracy of the detailed reaction mechanism.

4.4.4. Simplification and Reduction of Reaction Mechanisms

The methods for kinetic analysis of reaction mechanisms discussed can be used for simplification and reduction of detailed mechanisms. The main problem of using detailed reaction mechanisms, which have large number of reactions and species, is the difficulty in applying to practical engines where the chemical models are combined with multi-dimensional fluid dynamic models. The calculations with detailed mechanisms require large amounts of computational time, because too small time steps are necessary to achieve stability due to stiffness problem. The stiffness of a system depends on the ratio of the fastest to slowest time-scales. A less stiff system can be obtained by the removal of the fast species. Therefore, it is necessary to use simplified chemical kinetic schemes with less reactions and species.

The important reduction techniques are computational singular perturbation methods (CSP), intrinsic low dimensional manifolds (ILDM) and quasi steady state approximations (QSSA).

The CSP and ILDM methods are based on time-scale separation. They use the fact that a large number of chemical processes in detailed reaction systems are very fast.

Thus they are not rate limiting and can be decoupled.

The method of CSP separates the reaction system into slow and fast reaction groups. Solving of the stiff set of differential equations, which describe the complex reaction system, is possible by the decoupling of fast reaction groups. The information about these fast and slow reactions groups help to find if a species is in steady state or not. This is used to reduce the full schemes. One of the most important advantages of CSP method is this can be used automatically. In CSP method, the construction of reduced mechanism starts with defining the number of global steps and identification of the steady state species. Then, integration of the rate of each elementary reaction gives the fast reactions while the rest of the reactions are assumed to be slow reactions. Finally, the reduced mechanism, which consists of the global steps with major species and the global rates expressed as linear combinations of the slow elementary rates, can be generated.

The CSP method was used by Massias et al. [104] with the above steps to construct reduced mechanisms for methane-air and hydrogen-air combustion with NO formation. The reduced mechanisms were constructed with a pre-defined number of global steps and reduced the computational time within the accuracy range.

The ILDM method is based on the same basic ideas as CSP. The detailed reaction mechanism is separated into reaction groups of large and small time scales. The group with the smallest time scales is introduced by steady-state approximations to obtain the reduced mechanism [130]. The main objective of this method is to produce tables of species and system properties to be used in commercial codes. The most important advantage of this method is that it is not necessary to know the reactions in equilibrium and the species in quasi-steady-state. The inputs of this method are the detailed mechanism and the degrees of freedom for the reduced mechanism. Production rates for the selected variables are calculated using the original system of kinetic ordinary differential equations in each grid point and tabulated. The method looks up for the nearest values in the table and estimates the production rate in each step of the solution [131].

The ILDM method has been applied to homogeneous and reactive flow systems by Maas et al. [132] and Niemann et al. [133]. In these studies, the ILDM method was separated into following steps:

- Identifying the ILDM and obtaining information about the coupling of the chemical kinetics with flow and molecular transport
- Storing the information for subsequent use in the reacting flow simulation and
- Solving the projected partial differential equation system for the scalar field.

A new tabulation method using ILDM of a stoichiometric hydrogen-oxygen system was applied and verified. The computation time and the storage requirement are reduced by using ILDM-reduced chemistry. The theory of the ILDM method is explained in detail by Tomlin et al. [97].

The quasi-steady-state approximation is the oldest method in time-scale analysis. It depends on the existence of time-scale separation in the variables and involves finding the QSSA species which react on a short time-scale. The selection of these species can be done automatically and after their identification, they can be eliminated from the detailed mechanism by solving the QSSA expressions explicitly [134]. In the QSSA method, source terms and steady-state species concentrations are connected to the chemical parameters by numerical equations.

Detailed and skeletal mechanisms can be reduced with the steady state assumption for intermediate species, which are consumed by fast reactions compared to their production reactions. Additionally, if the consumption is much faster than the transport due to convection and diffusion, the chemical production rate is zero. This leads to numerical equations for these species, which has all the information of the detailed mechanism. For steady state species,

$$\sum_{k=1}^{N_R} (\nu''_{i,k} - \nu'_{i,k}) \varpi_k = 0 \tag{4.16}$$

can be written. This equation can be solved for concentration of a steady state species if it appears as a linear reactant, as

$$[c_i] = \frac{\sum_{k=1}^{N_R} \nu''_{i,k} \prod_{j=1}^{N_S} [c_j]^{\nu'_{j,k}} r_k}{\sum_{k=1}^{N_R} \nu'_{i,k} \prod_{\substack{j \neq i \\ j=1}}^{N_S} [c_j]^{\nu'_{j,k}} r_k}. \tag{4.17}$$

A second order equation have to be solved for the steady state expression when max (ν'_{ir}) = 2. The concentrations of QSSA species are calculated from the concentrations of non-QSSA species and the production rates of non-QSSA species are calculated using the original system of kinetic ordinary differential equations in each step of the simulation [131].

The application of the QSSA to general systems has two main problems: The numerical solution of non-linear equation systems and identification of QSSA species directly from the time-scales of the linear system. The optimum reduced mechanism may not be produced by the QSSA method when there are faster time-scales than QSSA species.

The details of QSSA are explained by Griffiths [121] and Tomlin et al. [97]. Some practical applications of the QSSA were also given by Tomlin et al. such as direct and numerical applications for hydrogen oxidation. This approximation for automatic reduction of detailed mechanisms with a lifetime measure was used by Nilsson et al. [128] and Lovâs et al. [129] to detect equilibrated species and implemented the chemical source terms in a Fortran subroutine.

CHAPTER 5

THE MODEL

The multidimensional combustion modeling for HCCI engines is proposed in this study. For this purpose KIVA-3V program is used as a CFD (computational fluid dynamics) program.

5.1. The Physical Model

5.1.1. CFD Applications

Over the past several years, computational fluid dynamics (CFD) has been increasingly accepted as an adjunct to experimentation in the design and understanding of practical combustion systems. A major goal in the engine modeling effort, the calculation of three-dimensional engine flows with sprays and combustion, was realized in 1987. Since that time, three-dimensional studies with sprays and/or combustion have become commonplace in the literature.

KIVA-3V is a computer program for the numerical calculation of transient, two- and three-dimensional, chemically reactive fluid flows with sprays. In this version of KIVA an effective approach to modeling moving valves became available, as it done for piston motion in recent applications. The KIVA-3V equations and numerical solution procedure are very general and can be applied to laminar or turbulent flows, subsonic or supersonic flows, and single phase or dispersed two-phase flows. Arbitrary numbers of species and chemical reactions are allowed. A stochastic particle method is used to calculate evaporating liquid sprays, including the effects of droplet collision and aerodynamic breakups. Although the initial and boundary conditions and mesh generation have been written for internal combustion engine calculations, the logic for these specifications can be easily modified for a variety of other applications. Indeed, KIVA has been used for numerous studies besides

internal combustion engines, including cold flow analysis in complicated geometries, continuous spray combustors, Bunsen burner flames, non reacting sprays, and hydrogen-oxygen flames propagating in long tubes, to name just a few.

KIVA-3V solves the unsteady equations of motion of a turbulent, chemically reactive mixture of ideal gases, coupled to the equations for a single component vaporizing fuel spray. The gas-phase solution procedure is based on a finite volume method called the

ALE (Arbitrary Lagrangian Eularian) method [136], [137]. Spatial differences are formed on a finite-difference mesh that subdivides the computational region into a number of small cells that are hexahedrons. The corners of the cells are called vertices, and positions of vertices may be arbitrarily specified functions of time, thereby allowing a Lagrarian, Eularian, or mixed description. The arbitrary mesh can conform to curved boundaries and can move to follow changes in combustion chamber geometry. A strength of the method is method is that the mesh need not be orthogonal. The spatial differencing is made conservative wherever possible. The procedure used is to difference the basic equations in integral form, with the volume of a typical cell used as the control volume, and with divergence terms transformed to surface integrals using the divergence theorem [136].

The Cartesian components of the velocity vector are stored at cell vertices, and the momentum equations are differenced in a strictly conservative fashion. In contrast to the original ALE method, however, cell faced velocities are used during a portion of the computational cycle. Their use greatly reduces the tendency of the ALE method to parasitic velocity modes, thereby largely eliminating the need for node coupler.

The transient solution is marched out in a sequence of finite time increments called cycles or time-steps. On each cycle of the values of the dependent variables are calculated from those on the previous cycle. As in the original ALE method, each cycle is divided into two phases - a Lagrangian phase and a rezone phase. In the Lagrangian phase the vertices move with the fluid velocity, and there is no convection across cell boundaries. In the rezone phase, the flow field is frozen, the vertices are moved to new user specified positions, and the flow field is remapped or rezoned onto the new computational mesh. This remapping is accomplished by convection material across the boundaries of the computational cells, which are regarded as moving relative to the flow field.

The temporal difference scheme in KIVA-3V is largely implicit. In the Lagrangian phase, implicit differencing is used for all the diffusion terms and the terms associated with pressure wave propagation.

Explicit methods are used to calculate convection in the rezone phase; but the convection calculation can be sub-cycled an arbitrary number of times, and thus the main computational time-step is not restricted by the Courant stability condition of explicit methods [138]. The convection time-step is a sub-multiple of the main computational time-step and does satisfy the Courant condition. In addition to the partial donor cell differencing, KIVA3V can use a quasi-second-order upwind (QSOU) scheme for convection. Based on the ideas of van Leer [139], this scheme is monotone and approaches second-order accuracy when convecting smooth profiles. While more accurate than partial donor cell differencing, QSOU is also more time-consuming, and thus it is included as an option.

The number of species and chemical reactions that can be accounted for in KIVA3V are arbitrary; they are limited only by computer time and storage considerations. The code distinguishes between slow reactions, which proceeded kinetically, and fast reactions, which are assumed to be equilibrium. Chemical rate expressions for the kinetic reactions, which are Arrhenius in form, are evaluated by a partially implicit procedure. Two implicit equation solvers are available to compute chemical equilibrium a fast algebraic solver for hydrocarbon/air combustion and an iterative solver for more general circumstances.

Two models are available to represent the effects of turbulence. The user has the option to use a standard version of the $k-\varepsilon$ turbulence model, modified to include volumetric expansion effects and spray/turbulence interreactions, or to use a modified version of the subgrid scale (SGS) turbulence model. The SGS model reduces to the $k-\varepsilon$ model near walls where all turbulence length scales are too small to be resolved by the computational mesh. Boundary layer drag and wall heat transfer are calculated by matching to a modified turbulent law of the wall.

Evaporating liquid sprays are represented by a discrete-particle technique, in which each computational particle represents a number of droplets of identical size, velocity and temperature. Probability distributions often govern the assignment of droplet properties at injection or the changes in drop properties at downstream locations. When this is the case, droplet properties are determined by using a Monte Carlo sampling technique. The particles and fluid interact by exchanging mass, momentum

and energy. The momentum exchange is treated by implicit coupling procedures to avoid the prohibitively small time-steps that would otherwise be necessary. Accurate calculation of mass and energy exchange is ensured by automatic reductions in the time-step when the exchange rates become large. Turbulence effects on the droplets are accounted for in one of two ways. When the time-step is smaller than the droplet turbulence correlation time, a fluctuating component is added to the local mean gas velocity when calculating each particle's mass, momentum and energy exchange with the gas. When the time-steps exceed the turbulence correlation time, turbulent changes in droplet position and velocity are chosen randomly from analytically derived probability distributions for these changes. Droplet collisions and coalescences are accounted for, and a new model for droplet aerodynamic breakup has been installed. Volume displacement and thick spray effects on the exchange rates are neglected.

Because of improvements to the code's ease-of-use and versatility, for many applications, all required geometrical specifications, initial conditions and boundary conditions may be specified using the standard input alone. This is particularly true for internal combustion engine applications. The mesh generation logic allows the computational region to include cupped pistons and domed cylinder heads and to offset these relative to the axis of the cylinder. This symmetry is often found in engine cylinders with multihole injectors. For initial conditions, one can specify an axisymmetric swirl-velocity field with a Bessel function profile and a specified swirl ratio. Standard boundary conditions and rezone logic allow the mesh to follow the motion of a piston.

5.1.2. The Governing Equations

In this section, the governing equation for the fluid face and the boundary conditions are given. The unit vectors in the x, y and z directions are denoted by i, j and k respectively. The position vector x is defined by

$$x = xi + yj + zk, \tag{5.1}$$

the vector operator ∇ is given by

$$\nabla = i\frac{\partial}{\partial x} + j\frac{\partial}{\partial y} + k\frac{\partial}{\partial z}, \tag{5.2}$$

and the fluid velocity vector **u** given by

$$\mathbf{u} = u(x,y,z,t)I + v(x,y,z,t)j + w(x,y,z,t)k, \tag{5.3}$$

where **t** is time.

The KIVA-3V equations can be used to solve for both laminar and turbulent flows. The mass, momentum and energy equations for the two cases differ primarily in the form and magnitude of the transport coefficients (i.e., viscosity, thermal conductivity and species diffusivity), which are much larger in the turbulent case because of the additional transport caused by turbulent fluctuations. In the turbulent case the transport coefficients are derived from a turbulent diffusivity that depends on the turbulent kinetic energy and its dissipation rate. In this study of k-ε turbulence model is used.

The continuity equation for species m is

$$\frac{\partial \rho_m}{\partial t} + \nabla.(\rho_m u) = \nabla\left[\rho D \nabla(\frac{\rho_m}{\rho})\right] + \rho_m^c, \tag{5.4}$$

where ρ_m is the mass density of species m, ρ the total mass density, and **u** the fluid velocity. Fick's Law diffusion is assumed with a single diffusion coefficient D. Equations for D and source terms due to chemistry ρ_m^c will be given later. By summing Equation 5.4 over all species, the total fluid equation is obtained.

$$\frac{\partial \rho}{\partial t} + \nabla.(\rho u) = 0, \tag{5.5}$$

since mass is conserved in chemical reactions.

The momentum equation for the fluid mixture is

$$\frac{\partial(\rho u)}{\partial t} + \nabla.(\rho u u) = -\nabla p - \nabla(2/3\rho k) + \nabla.\sigma + \rho g, \tag{5.6}$$

where **p** is the fluid pressure.
The viscous stress tensor is Newtonian in form:

$$\sigma = \mu\left[\nabla u + (\nabla u)^T\right] + \lambda \nabla . uI \ . \tag{5.7}$$

The first and second coefficients of viscosity, μ and λ are defined later. The superscript T denotes the transpose and I is the unit dyadic. The specific body force g is assumed constant.

The internal energy equation is

$$\frac{\partial(\rho I)}{\partial t} + \nabla .(\rho u I) = -p\nabla . u - \nabla . J + \rho\varepsilon + Q^c \ , \tag{5.8}$$

where I is the specific internal energy, exclusive of chemical energy. The heat flux vector J is the sum of contributions due to heat conduction and enthalpy diffusion:

$$J = -K\nabla T - \rho D \sum_m h_m \nabla(\rho_m / \rho) \, , \tag{5.9}$$

where T is the fluid temperature and h_m the specific enthalpy of species m. The source terms due to chemical heat release Q^c will be defined later.
Two additional transport equations are solved for the turbulent kinetic energy k and its dissipation rate ε:

$$\frac{\partial \rho k}{\partial t} + \nabla .(\rho u k) = -2/3 \rho k \nabla . u + \sigma : \nabla u + \nabla . \left[(\frac{\mu}{\mathrm{Pr}_k}) \nabla k \right] - \rho\varepsilon \ , \tag{5.10}$$

and

$$\frac{\partial \rho \varepsilon}{\partial t} + \nabla .(\rho u \varepsilon) = -(\frac{2}{3} c_{\varepsilon_1} - c_{\varepsilon_3}) \rho \varepsilon \nabla . u + \nabla . \left[(\frac{\mu}{\mathrm{Pr}_\varepsilon}) \right] + \frac{\varepsilon}{k} \left[c_{\varepsilon_1} \sigma : \nabla u - c_{\varepsilon_2} \rho \varepsilon \right]. \tag{5.11}$$

These are standard k-ε equations with some added terms. The source term $(c_{\varepsilon_3} - 2/3 c_{\varepsilon_1}) \nabla .u$ in the ε equation accounts for length scale changes when there is velocity dilatation.

The Quantities c_{ε_1}, c_{ε_2}, c_{ε_3}, Pr_k and Pr_ε are constants whose values are determined from experiments and some theoretical considerations. Standard values of these constants are often used in engine calculations and these are given in Table 5.1.

Table 5.1. Standard Values of k-ε Turbulence Model Constants

Constant	Number
c_{e_1}	1.44
c_{e_2}	1.92
c_{e_3}	1.0
P_{r_k}	1.0
P_{r_ε}	1.3

The state relations are assumed to be those of an ideal gas mixture. Therefore,

$$p = R_0 T \sum_m (\rho_m / W_m), \tag{5.12}$$

$$I(T) = \sum_m (\rho_m / \rho) I_m(T), \tag{5.13}$$

$$c_p(T) = \sum_m (\rho_m / \rho) c_{pm}(T), \tag{5.14}$$

and

$$h_m(T) = I_m(T) + R_0 T / W_m, \tag{5.15}$$

where R_0 is the universal gas constant; W_m , the molecular weight of species m; I_m (T), the specific internal energy of species m; and c_{pm}, the specific heat at constant pressure of species m. the values of $h_m(T)$ and $c_{pm}(T)$ are taken from the JANAF tables.

The chemical reactions occurring in the system are symbolized by

$$\sum_m a_{mr} x_m \Leftrightarrow \sum_m b_{mr} x_m , \tag{5.16}$$

where x_m represents one mole of species m and a_{mr} and b_{mr} are integral stoichiometric coefficients for reaction r. The stoichiometric coefficients must satisfy

$$\sum_m (a_{mr} - b_{mr}) W_m = 0 , \tag{5.17}$$

so that mass is conserved in chemical reactions. Chemical reactions are divided into two classes: those that proceed kinetically and those that are assumed to be in equilibrium. In this studt only the kinetic reactions are used. Kinetic reaction r proceeds at a rate ω_r given by

$$\omega_r = k_{fr} \prod_m (\rho_m / W_m)^{\alpha'_{mr}} - k_{br} \prod_m (\rho_m / W_m)^{b'_{mr}} . \tag{5.18}$$

Here the reaction order α'_{mr} and b'_{mr} need not equal α_{mr} and b_{mr}, so that empirical reaction orders can be used. The coefficients k_{fr} and k_{br} are assumed to be of a generalized Arrhenius form:

$$k_{fr} = A_{fr} T^{\xi_{fr}} \exp\{ - E_{fr} / T \},$$

and

$$k_{br} = A_{br} T^{\xi_{br}} \exp\{ - E_{br} / T \}, \tag{5.19}$$

where E_{fr} and E_{br} are activation temperatures.

The rates of equilibrium reactions are implicitly determined by the constraint conditions

$$\prod_m (\rho_m / W_m)^{b_{mr}-\alpha_{mr}} = K_c^r(T), \tag{5.20}$$

where $K_c^r(T)$, the concentration equilibrium constant, is assumed to be of the form

$$K_c^r = \exp\left\{A_r \ln T_A + B_T / T_A + C_r + D_r T_A + E_r T^2{}_A \right\}, \tag{5.21}$$

where $T_A = T/1000$ K.

With the reactions rates ω_r determined by equations 5.18 or 5.20, the chemical source term in the species continuity equation is given by

$$\rho_m^c = W_m \sum_r (b_{mr} - a_{mr})\omega_r \,, \tag{5.22}$$

and the chemical heat release term in the energy equation is given by

$$Q^c = \sum_r Q_r \omega_r \,, \tag{5.23}$$

where Q_r is the negative of the heat of reaction at absolute zero,

$$Q_r = \sum_m (a_{mr} - b_{mr})(\Delta h_f^0)_m \,, \tag{5.24}$$

and $(\Delta h_f^0)_m$ is the heat of formation of species m at absolute zero.

The transport coefficients in KIVA-3V are taken to be

$$\mu = (1.0 - A_0)\rho\nu_0 + \mu_{air} + A_0 c_\mu k^2 / \varepsilon \,,$$

$$\lambda = A_3 \mu \,,$$

$$K = \frac{\mu c_p}{pr} \,,$$

and

$$D = \frac{\mu}{\rho Sc}. \tag{5.25}$$

The diffusivity v_0 is an input constant and c_μ is an empirical constant with a standard value of 0.09. A Sutherland formula is used for μ_{air}:

$$\mu_{air} = \frac{A_1 T^{3/2}}{YT + A_2}, \tag{5.26}$$

where A_1 and A_2 are constants. The constant A_3 is taken to be –2/3 in calculations of turbulent flow but can be arbitrarily specified in laminar flows. The Prandtl and Schmidt numbers, P_r and S_c are input constants.

5.2. The Chemical Model

As it mentioned in Chapter 4 applying detailed kinetic models with large number of reactions in practical internal combustion engines is very difficult as the chemical models combined with multi-dimensional fluid dynamic models consume large amounts of computational time and memory. It is also difficult to see how detailed chemistry can be coupled to computational fluid dynamics (CFD) calculations of practical engines within time. So a reduced mechanism of methane is chosen for modeling a HCCI engine.

The reduced mechanism used in this study for methane is taken from Tsao et al [141]. According to study two-step kinetic mechanism to account for oxidation of methane was used. The first of the two global rate equations controls the disappearance of methane, and the second the oxidation of carbon monoxide. The reaction equations are:

$2CH_4 + 3O_2 \rightarrow 2CO + 4H_2O$

$2CO + O_2 \rightarrow 2CO_2$

The reaction rates are expressed in the Arrhenius form as follows:

$$\omega_1 = -\frac{d[CH_4]}{dt} = 2.0\times10^{13}\exp\left(\frac{-2.3668\times10^4}{T}\right)[CH_4]^{0.7}[O_2]^{0.8}$$

$$\omega_2 = -\frac{d[CO]}{dt} = 4.5\times10^{11}\exp\left(\frac{-1.9639\times10^4}{T}\right)[CO][O_2]^{0.25}[H_2O]^{0.5}$$

The coefficients of both the methane and carbon monoxide global reactions are modified to conform the data input requirement. Also to conform the experiment conditions the coefficient at value of 2.3668×10^4 in first reaction changed as 2.08×10^4 .

5.3. The Simulation Parameters

The engine specifications and operating conditions of the engine is determined from the study of Fiveland et al. that investigated the influence of natural gas composition on engine operation both experimentally and chemical kinetic based cycle simulation [88]. The results taken from the combustion modeling then will be discussed in Section 6.

The research engine originates from a Volvo truck engine. It has been used in numerous HCCI experimental tests. The inline, six-cylinder engine has been modified for single cylinder operation. The engine specifications are shown in Table 5.2.

The simulation cycle range is between 270 CAD (90 CAD ABDC) and 430 CAD (70 CAD ATDC) when the valves are closed. The related simulation parameters are given in Table 5.3.

Table 5.2: Volvo TD100 Engine Geometry

Combustion Chamber	Pancake
Bore(mm)	126.5
Stroke(mm)	140
Connecting Rod(mm)	260
Compression Ratio	19.8
Inlet Valve Diameter(mm)	50
Exhaust Valve Diameter(mm)	46
Exhaust Valve Open	501 CAD (39 CAD BBDC)
Exhaust Valve Close	710 CAD(10 CAD BTDC)
Inlet Valve Open	5 CAD (5 CAD ATDC)
Inlet Valve Close	193 CAD (13 CAD ABDC)

Table 5.3: Simulated Operating Conditions

Fuel	Methane
Equivalence Ratio	0.3
Engine Speed (RPM)	1000
Cylinder Wall Temperature (K)	400
Piston face temperature (K)	400
Cylinder head temperature (K)	400
Initial mixture temperature (K)	400
Initial incylinder pressure (Bar)	1.6

CHAPTER 6

RESULTS

Multi-dimensional modelling of Homogeneous Charge Ignition (HCCI) Engine is performed in this study. The first step was generating mesh geometry for physical modelling. The engine specifications and operating conditions of the engine is determined from the study of Fiveland et al. that investigated the influence of natural gas composition on engine operation both experimentally and chemical kinetic based cycle simulation [88]. The research engine originates from a Volvo truck engine. The inline, six-cylinder engine has been modified for single cylinder operation. The geometry of Volvo TD100 Engine is given in Table 5.2.

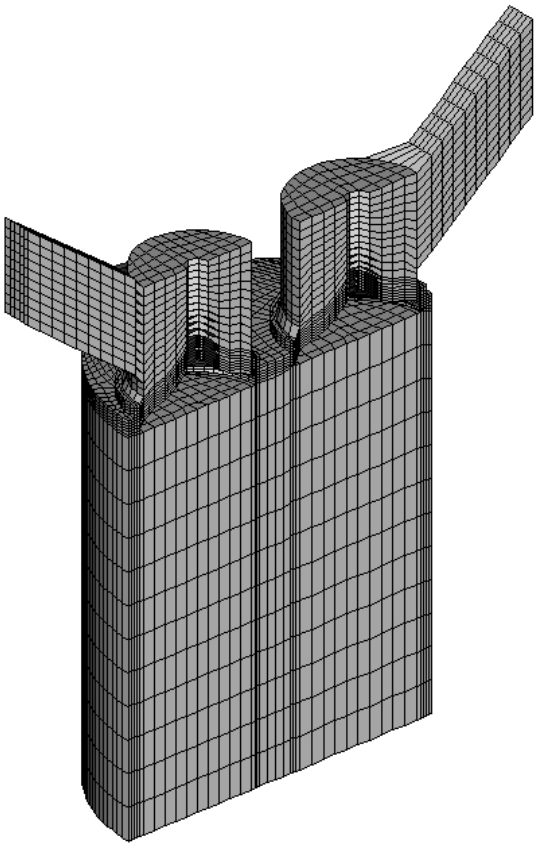


Figure 6.1. The shaded view of the computational mesh.

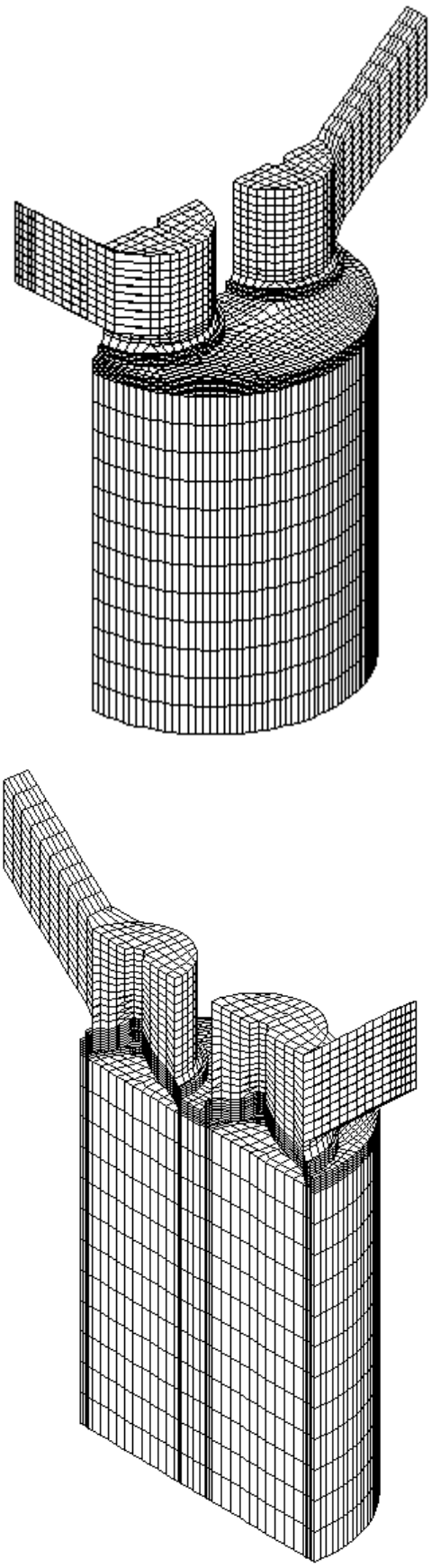


Figure 6.2.The computational mesh at crank angle 180^0 ATDC.

For mesh generating the own pre-processor of KIVA-3V named k3prep, is used. The generated pancake combustion chamber is consisting of two vertical valves, square runners and a flat piston crown. This computational volume is created from 41 blocks and the mesh contains 21426 vertices and 21337 cells. Figure 6.1-6.4 shows several views of the computing grid.

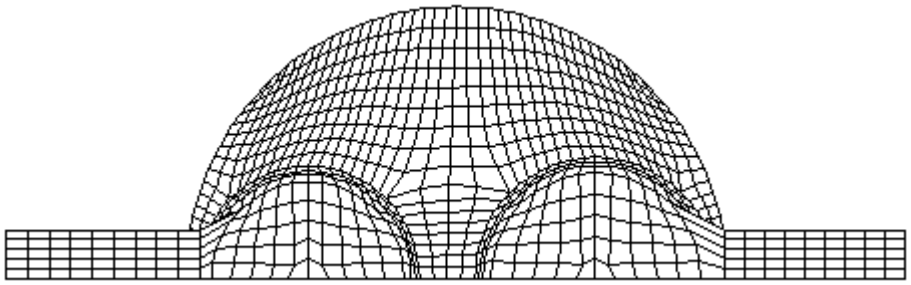


Figure 6.3. Top view of the computational mesh

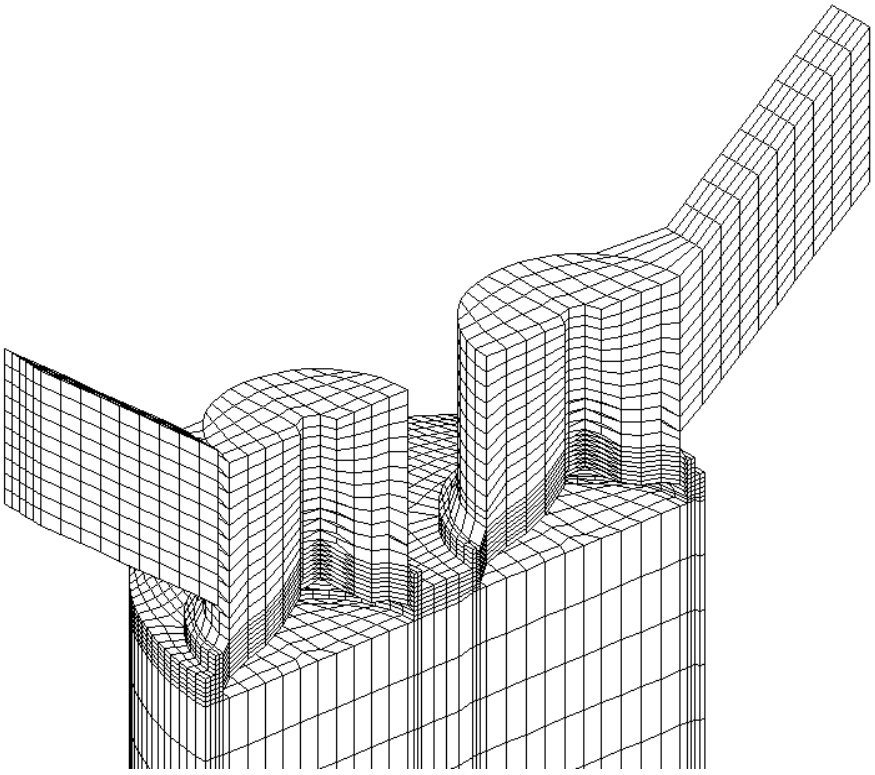


Figure 6.4. A perspective view that shows details of the valve lift region.

Figure 6.5 gives the plot across the symmetry plane where y=0. In this figure both the valves and the piston are at their BDC position.

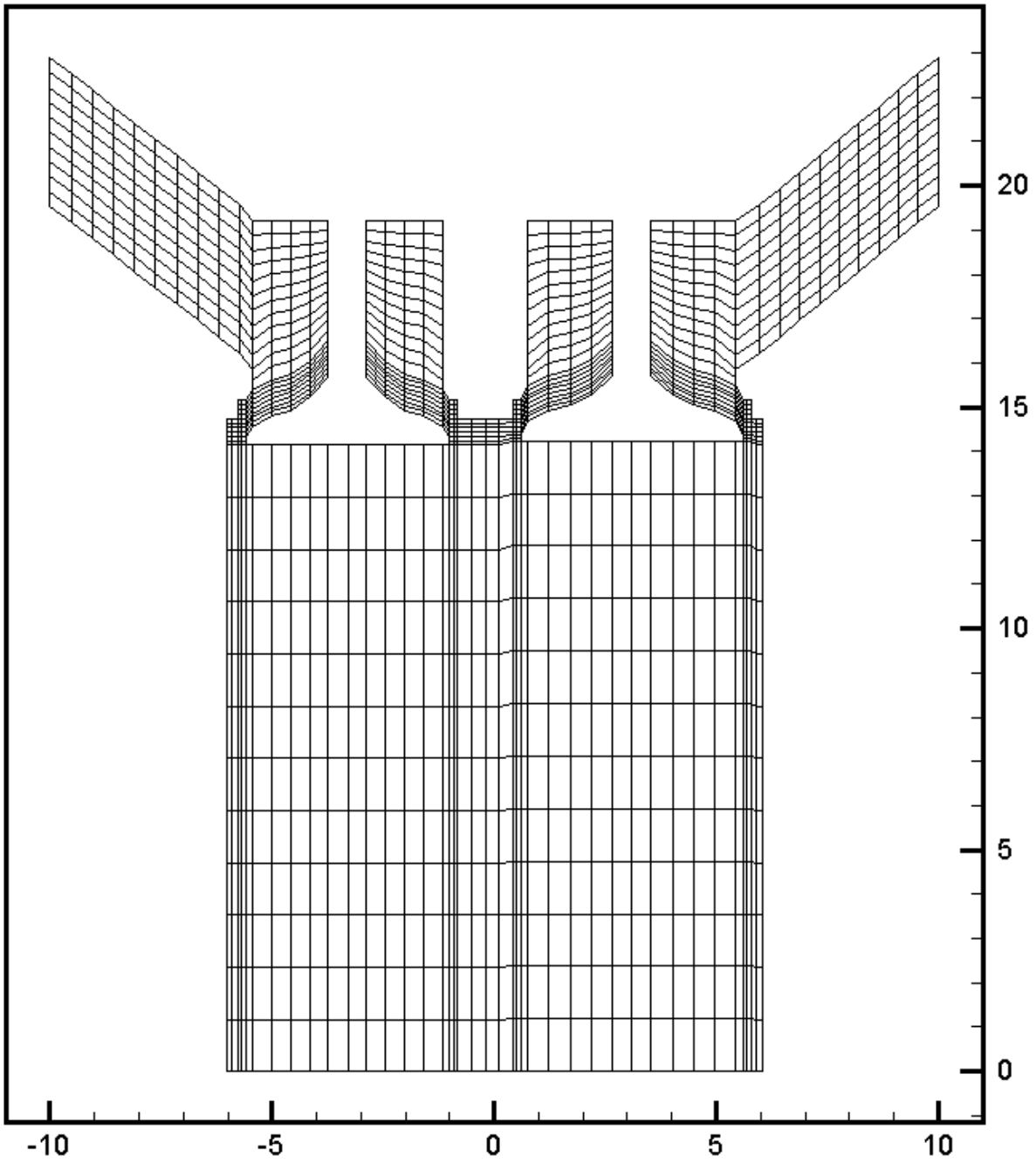


Figure 6.5. The mesh view of the symmetry plane, plot across y=0. Both the valves and piston are at their BDC positions.

In the below figures from Figure 6.6 to Figure 6.10, the valve position at several crank angles are shown for a full cycle simulation.

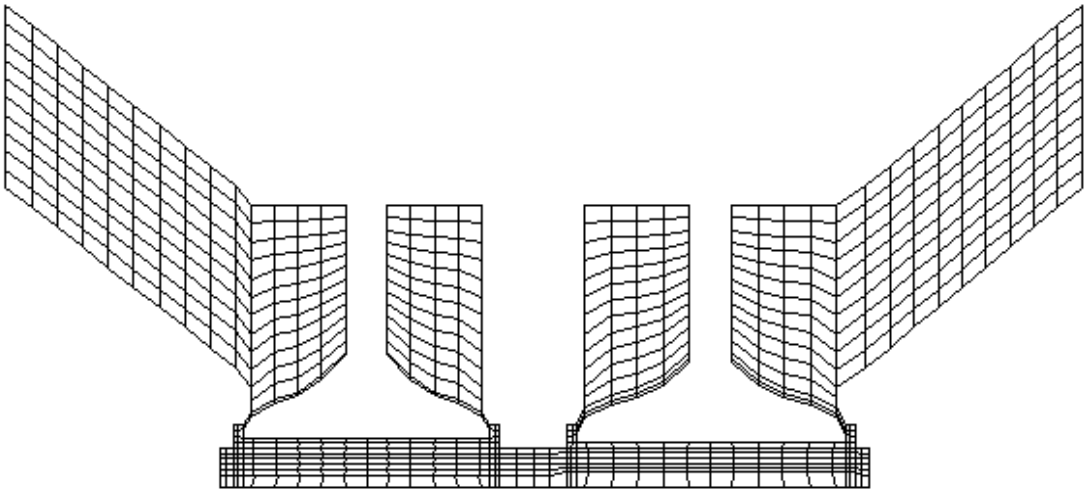


Figure 6.6. The grid at TDC. Both valves are closed**.**

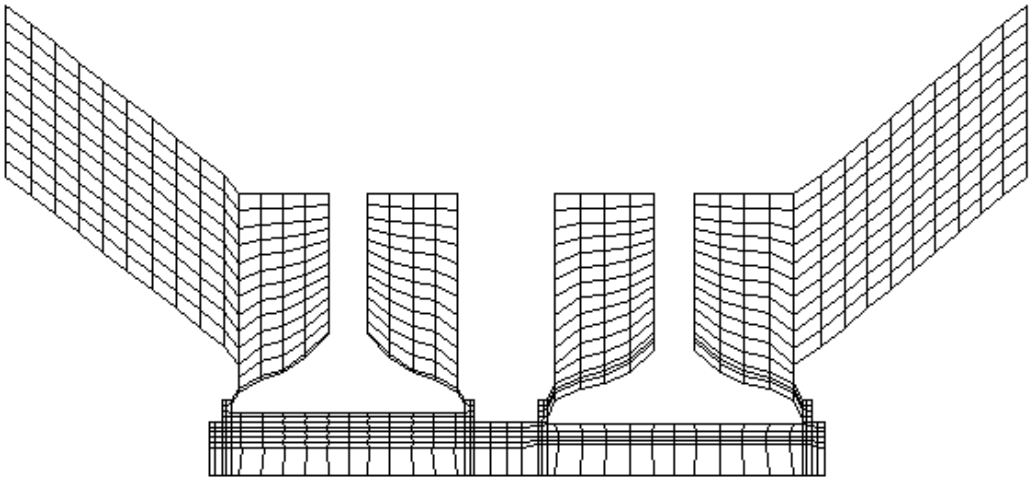


Figure 6.7. The grid at 15 CAD ATDC. The intake valve (right) is open. The exhaust valve is closed**.**

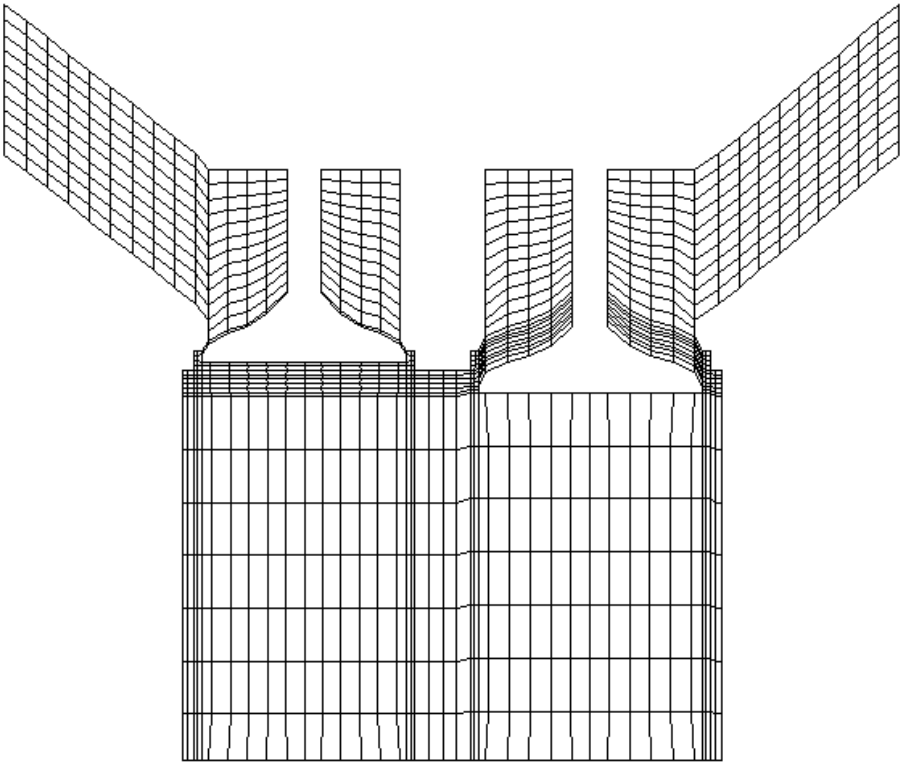


Figure 6.8. The grid at 90^0 ATDC, when the intake valve (right) is at its BDC and the exhaust valve (left) is closed.

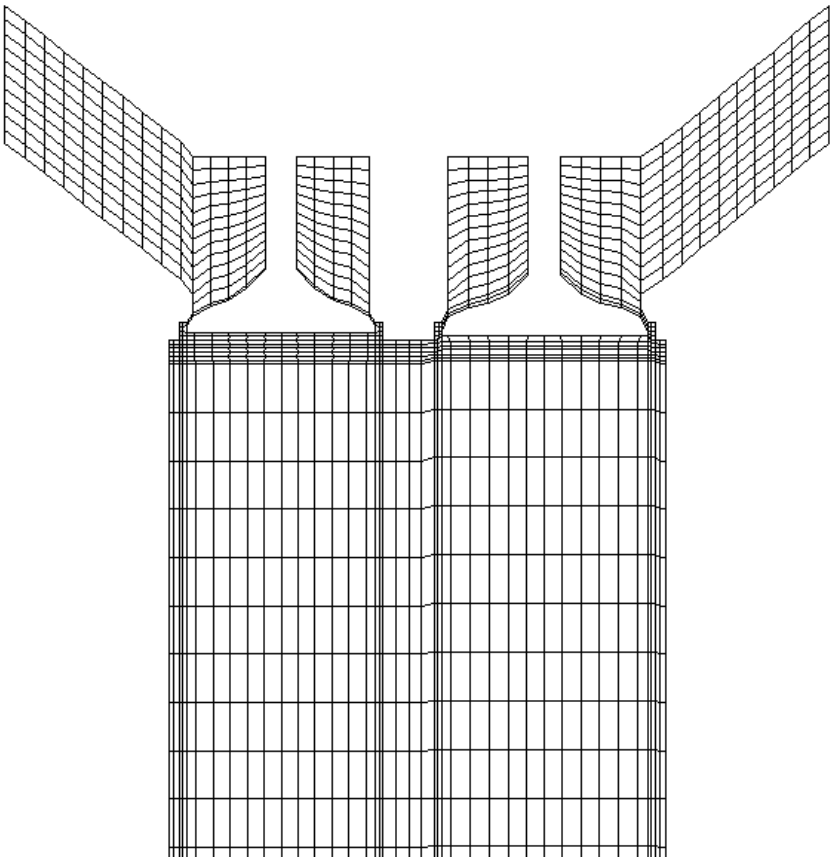


Figure 6.9. The gird at BDC**,** end of the intake stroke when the intake valve (right) is open and the exhaust valve (left) is closed.

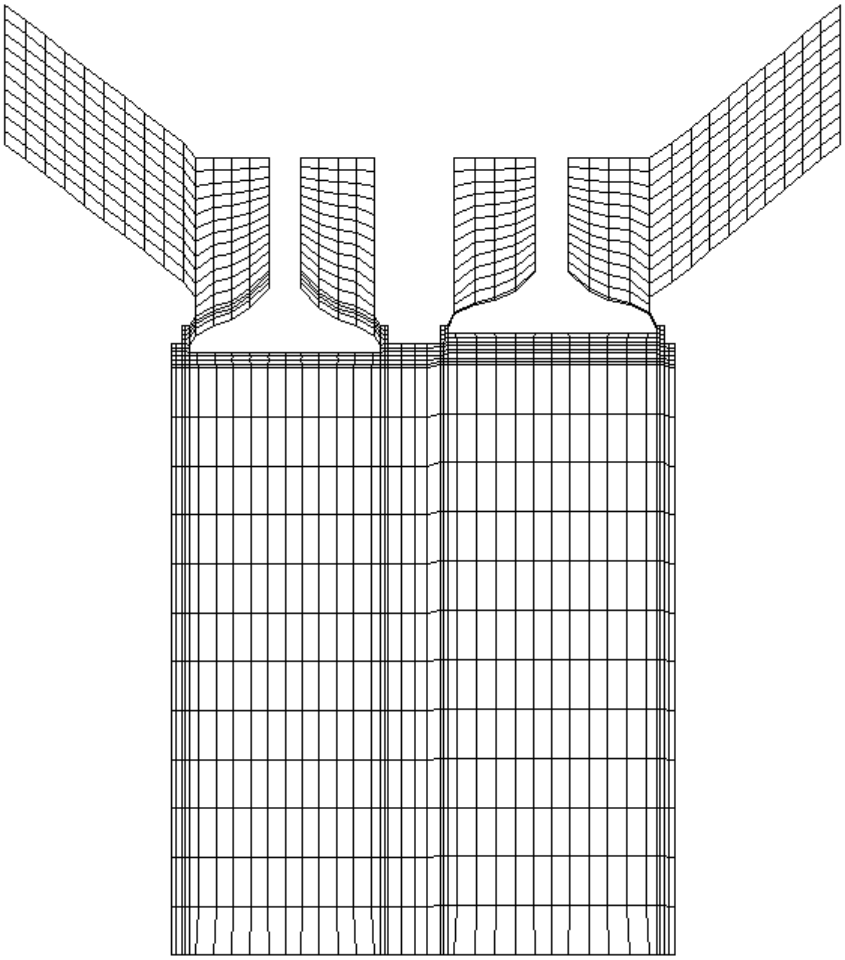


Figure 6.10. The gird at BDC**,** end of expansion stroke**,** when the intake valve (right) is closed and the exhaust valve (left) is open.

In this study to perform the effect of the mesh structure to the calculation, according to cell number, three kind of mesh generated as seen in Figure 6.11. The first one, the top view on the figure, includes 18289 cells and 18378 vertices. The second one, the middle view, includes 21337 cells and 21426 vertices. The third one, bottom view includes 30913cells and 31002 vertices.

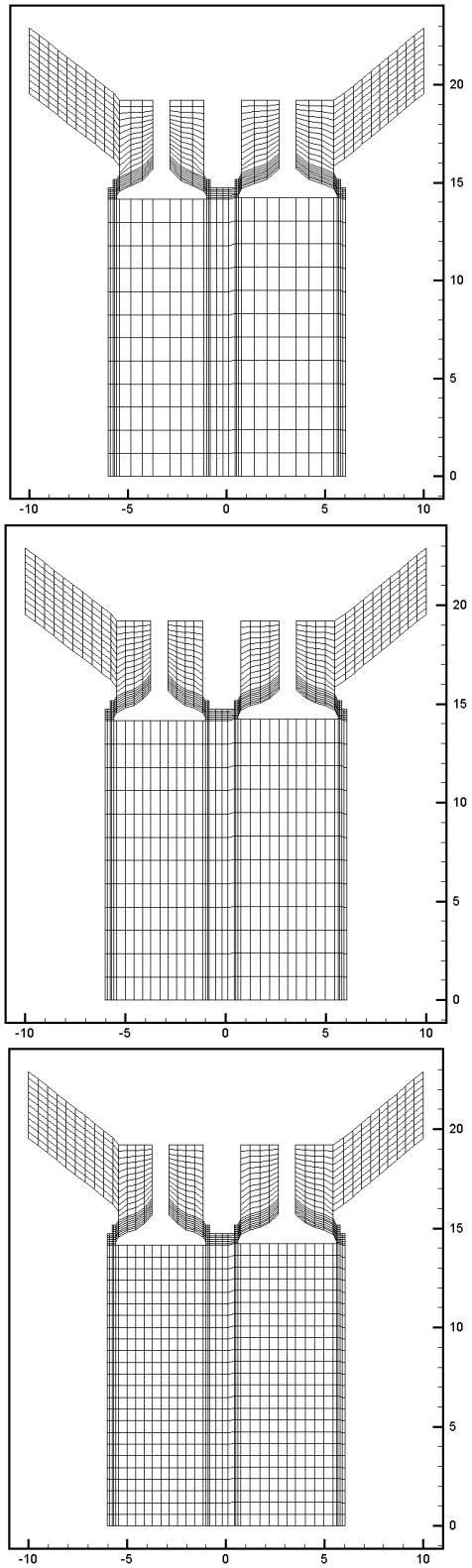


Figure 6.11. The types of mesh structures according to the cell number.

The results of the calculation for this three kind of mesh structure are so close to each other as seen in Figure 6.12. In the bottom view of the figure it is clear that for the mesh structures which have more cells then 21337, the results will be almost same. That means that after this limit, the mesh structure will be independent parameter for calculations. For this reason and to optimize the computational time in this study mesh structure that consists of 21337 cells is used.

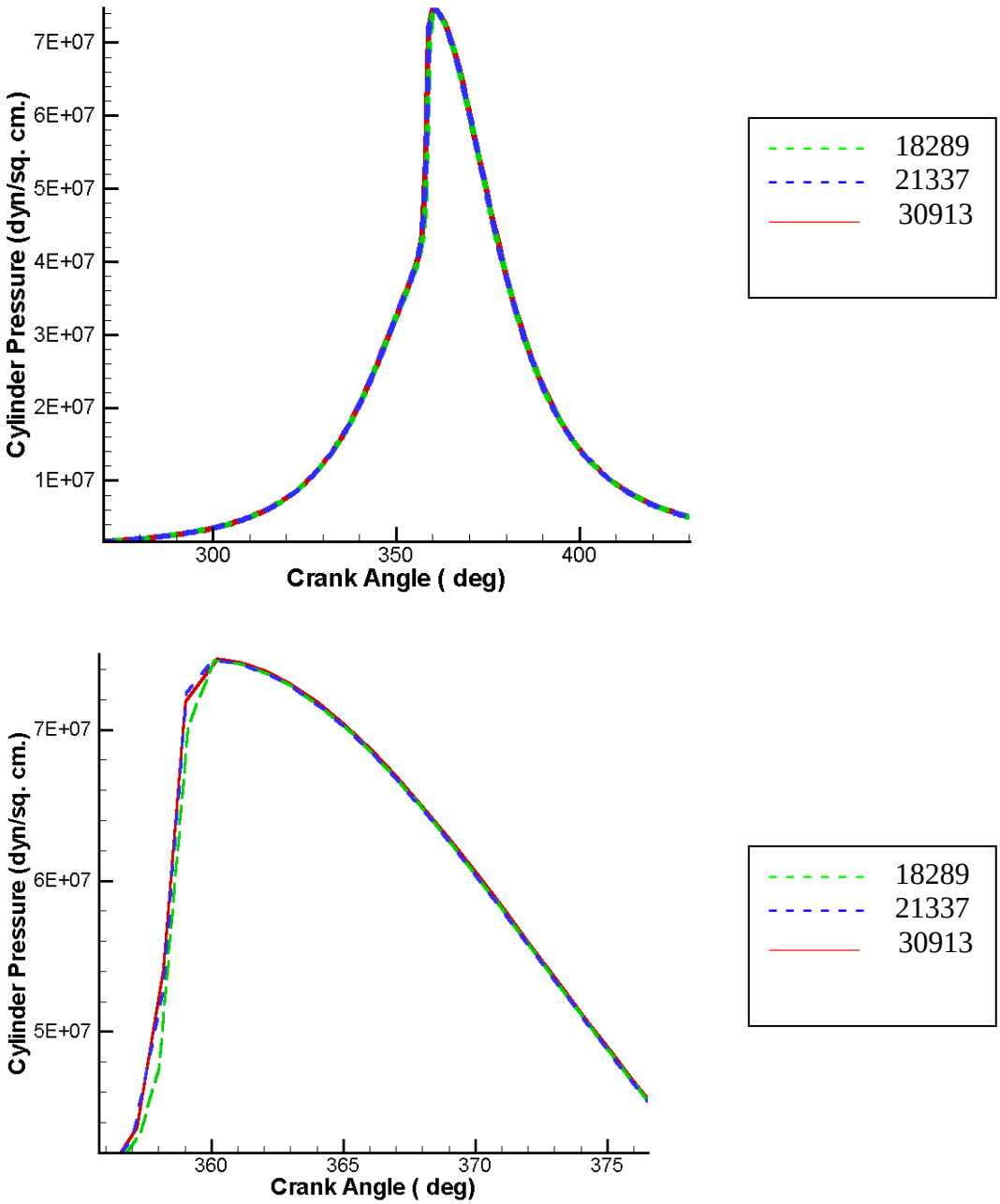


Figure 6.12. Crank angle-pressure diagram of the three kind of mesh structure according to cell numbers. The top diagram is full simulation history, and the bottom diagram is detailed view of history at high pressures.

Physical, chemical modeling and the simulation parameters of the study were given in Section 5. After the calculation of the simulation cycle between 270 crank angle degree (90 CAD BTDC) and 430 crank angle degrees (70 CAD ATDC), the diagram of cylinder pressure-crank angle history taken is seen in Figure 6.13. In this figure the simulated and the experimental pressures are compared. In both figure two stage of combustion inherent to HCCI engines, as explained in Section 2.5, can be seen. In the simulation cycle low-temperature kinetic reactions (cool flames), occurred nearly 24 CAD before the main combustion start. The main combustion started at 3 CAD BTDC and finished at 4 CAD ATDC. The main combustion period is nearly 7 CAD.

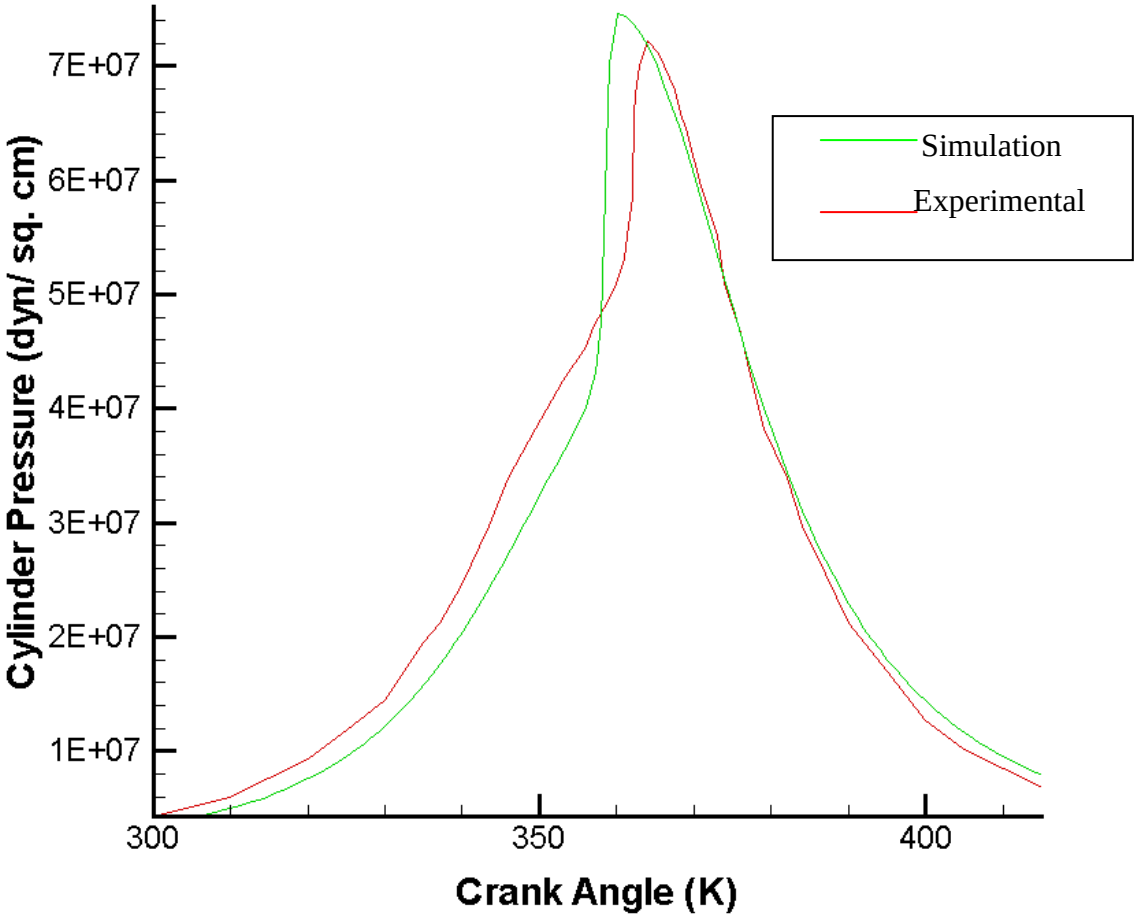


Figure 6.13. Comparison of the simulated and measured cylinder pressure.

Figure 6.13. also shows a comparison of the simulated pressure against the measured experimental data. The comparison is very reasonable considering that the average experimental conditions were used as simulation inputs. In the simulation cycle main combustion start occurred about 3 CAD before the experimental combustion start. It is noted that there is a little difference in the cylinder pressure experimental value and the simulated pressure near the end of compression. This is a result of the low temperature chemistry, in the simulation, releasing some energy near TDC. But as a result it can be said that the simulation were successful in predicting the pressure in cylinder.

In this study the impacts of the some parameters to the HCCI combustion are also investigated. The first of these parameters is the engine speed. The simulation cycle is performed at three different engine speeds at 600, 1000, 1600 rpm values. The related pressure and temperature history diagrams are shown in Figure 6.14-6.15.

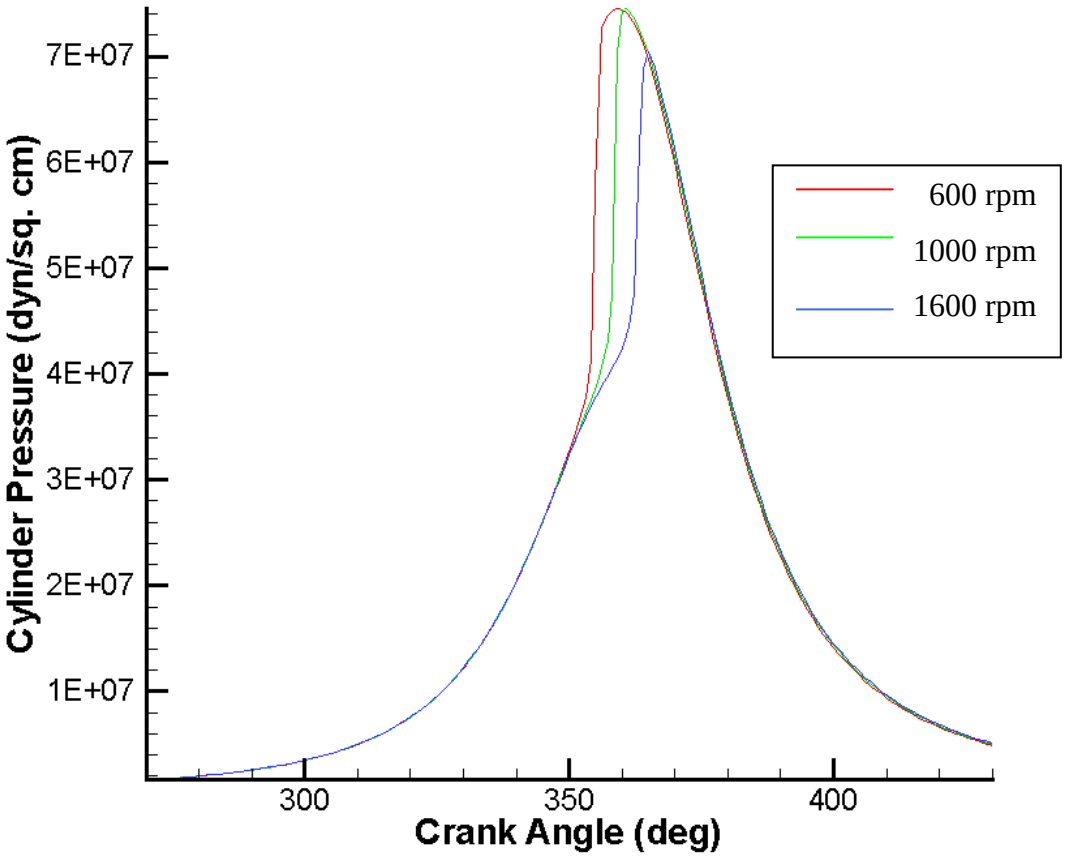


Figure 6.14. Comparison of the engine speed effects on pressure-crank angle history.

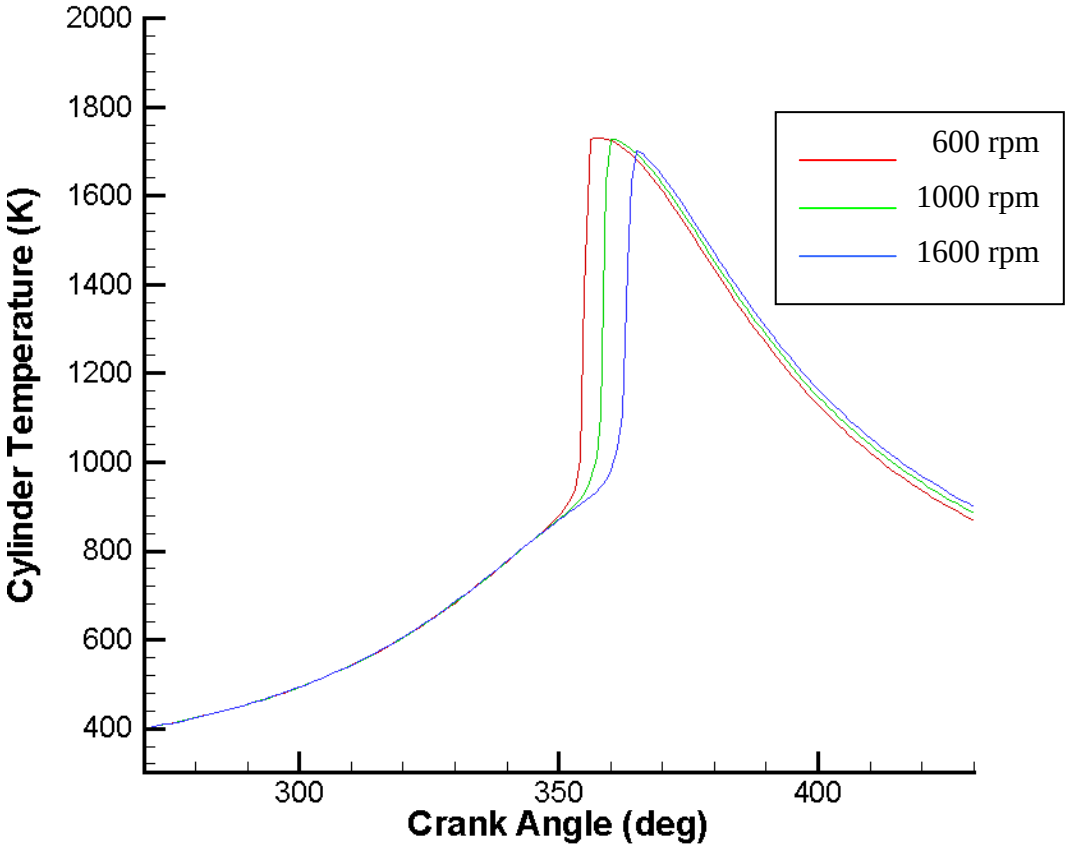


Figure 6.15. Comparison of the engine speed effects on temperature-crank angle history

As it seen in above figures, the lower kinetic reaction phase of the combustion are almost same. For each of the engine speed values, these reactions (cool flame) start approximately 26 CAD BTDC. For the second stage, main combustion begins 6 CAD BTDC at 600 rpm, 3CAD BTDC at 1000 rpm and 1 CAD ATDC at 1600 rpm. Combustion duration is 4 CAD at 600 rpm, 7 CAD at 1000 rpm and 8.5 CAD at 1600 rpm. When it is considered in real time in seconds it is seen that the main combustion begins earlier and the combustion duration decreases as the engine speed increase.

It is also seen from these figures that, the pressure and the temperatures at the end of the compression stroke are high at low engine speeds.

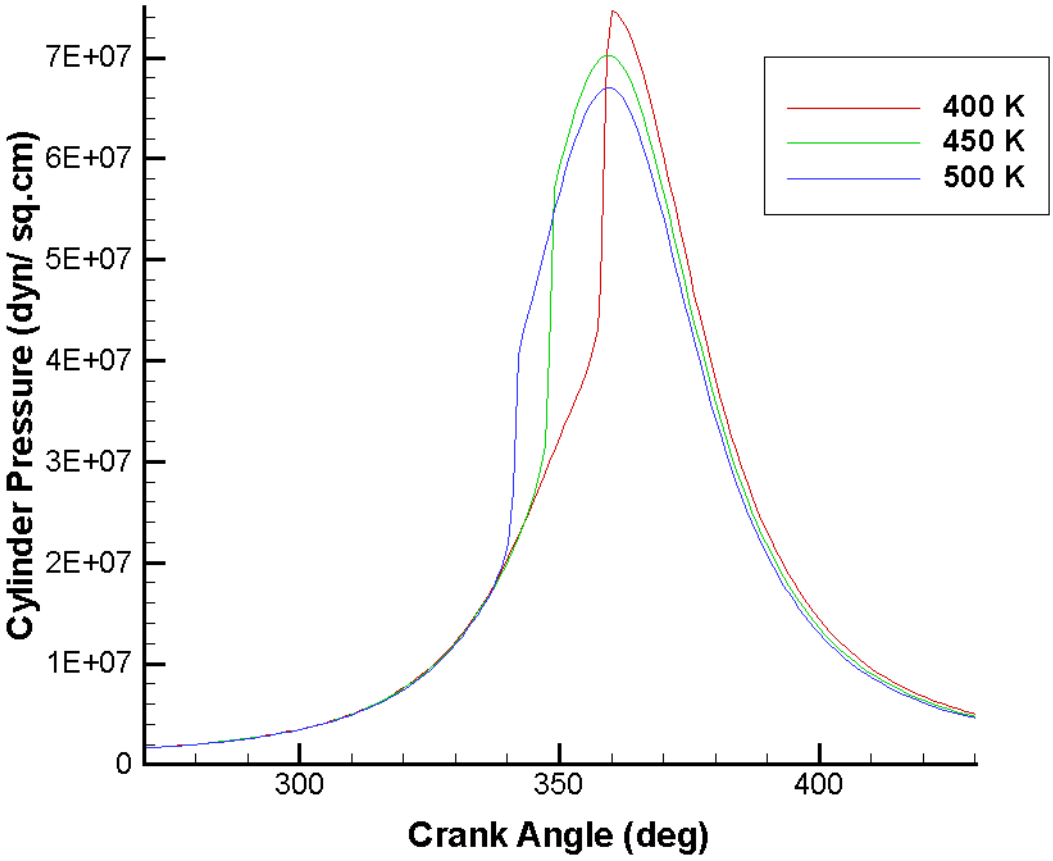


Figure 6.16. Comparison of the inlet temperature effects on pressure-crank angle history.

The other and the one of the most important parameters in controlling combustion phase and start of combustion is intake temperature values. It is known that in all cases, the effect of increasing inlet charge temperature is to advance auto-ignition timing and decrease combustion duration. This study is in good agreement in this decision. Both the low temperature reactions and main combustion begin earlier with increasing inlet temperatures. The low temperature reactions begins at 26 CAD BTDC at 400 K inlet temperature, 35 CAD BTDC at 450K and 43 CAD BTDC at 500 K. Similar to this the main combustion begins at 3 CAD BTDC at 400 K, 13 CAD BTDC at 450 K and 19 CAD BTDC at 500 K. Combustion duration values for 400 K inlet temperature is 7 CAD. This period decreases to 5 CAD at 450 K inlet temperature and 4 CAD at 500K temperature. These results can be seen in Figure 6.16-6.17.

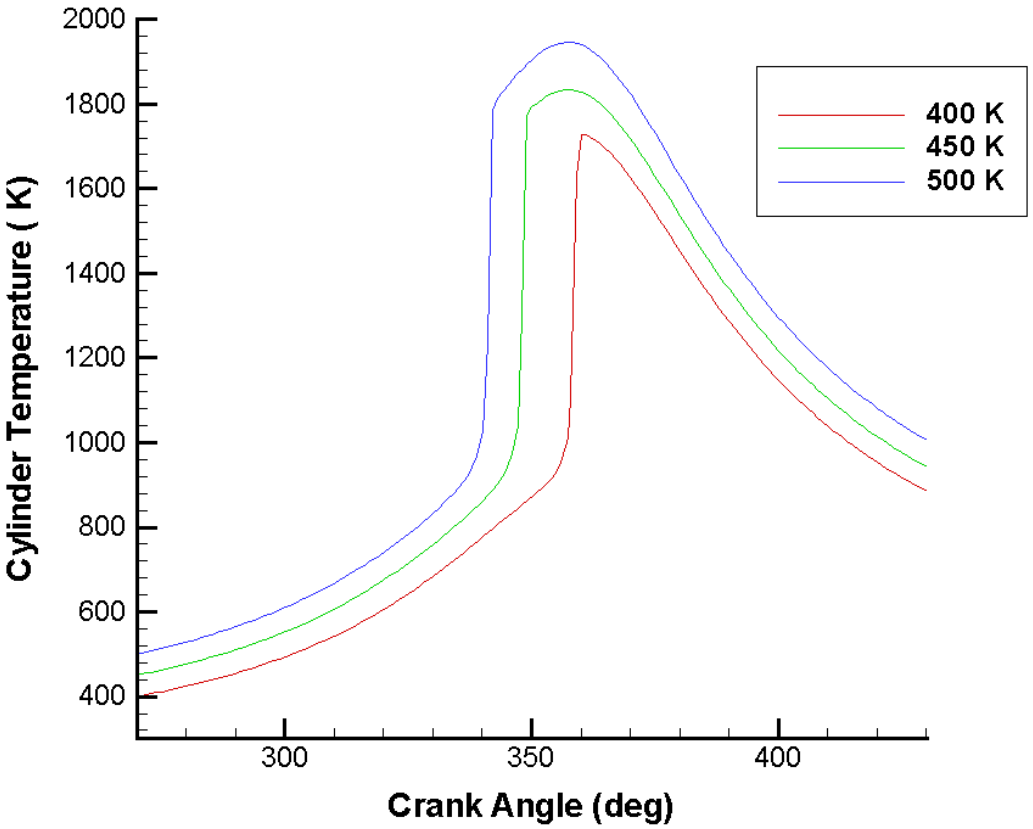


Figure 6.17. Comparison of the inlet temperature effects on temperature-crank angle history.

It is noted that increased intake temperatures also increase the cylinder temperature at the end of the compression stroke while decreasing the cylinder pressure.

Similar effects on combustion are seen in compression ratio parameter. The low temperature reactions begin in earlier time with increasing compression ratio. The simulated results showed that cool flames begin at 34 CAD BTDC at 23 :1, 26 CAD BTDC at 19.8:1 and 24 CAD BTDC at 18:1 compression ratios. Similar to this it is also shown that main combustion start get earlier as the compression ration increase. Main combustion begins 6 CAD BTDC at 23:1, 3CAD BTDC at 19.8:1 and 2CAD ATDC at 18:1 compression ratio increased. The main combustion duration values are 8 CAD, 7 CAD, 4 CAD relative to 18:1, 19.8:1. 23:1. This means that main combustion period get shorter at high compression ratios. It is also seen that increasing compression ration causes high pressure and temperature values at the end of compression stroke. The related values are seen Figure 6.18-6.19.

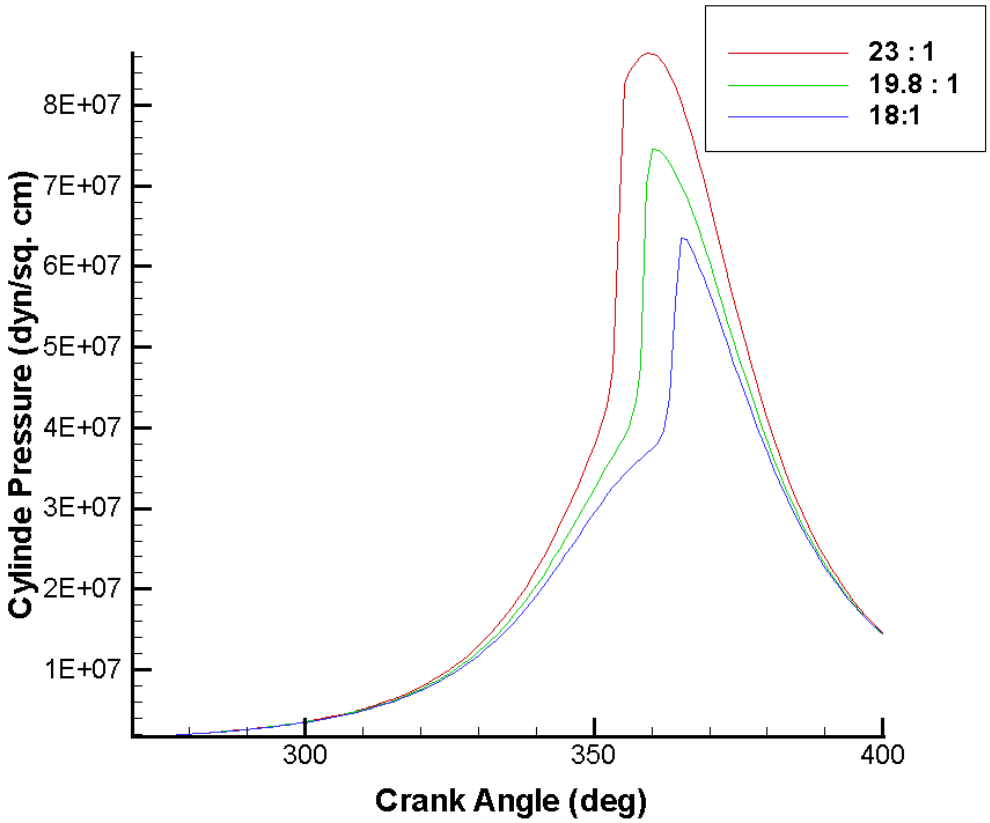


Figure 6.18. Comparison of compression ratio effects on pressure-crank angle history.

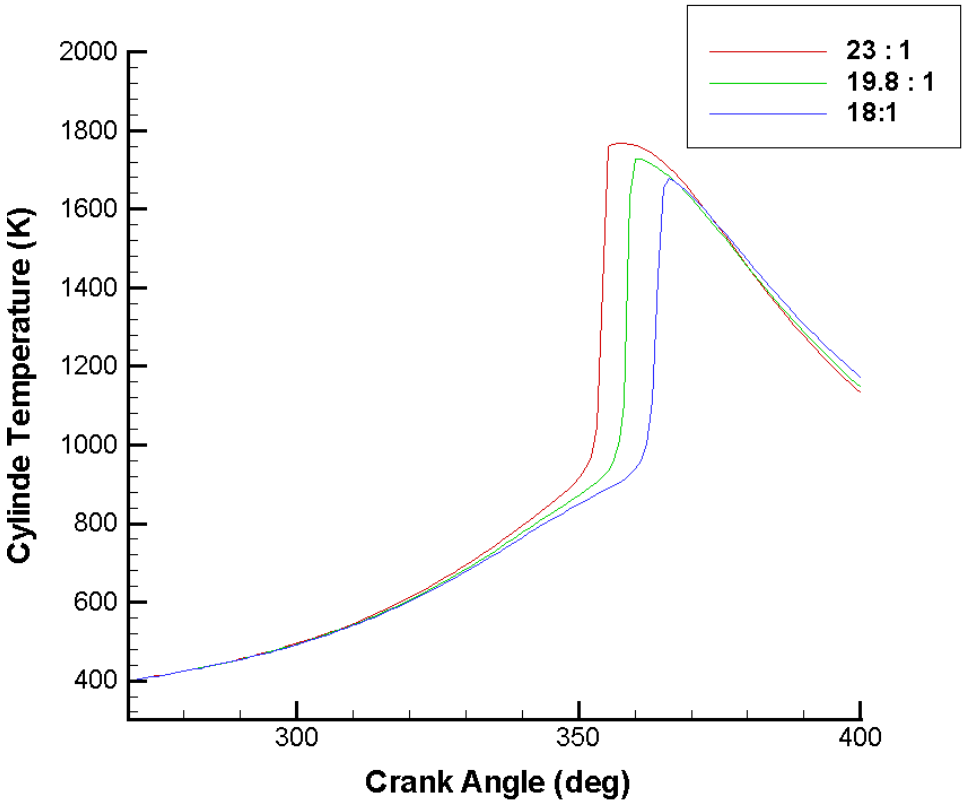


Figure 6.19. Comparison of the compression ratio effects on temperature-crank angle history

CHAPTER 7

CONCLUSION

A multi-dimensional modelling of Homogeneous Charge Compression Ignition Engines is presented via the KIVA-3V code. Both the physical and chemical modelling calculations are done by KIVA-3V code. An experimental study is taken as a reference to compare the results of simulation cycle. Releated to the experiment engine geometry a three-dimensional model is generated. For the chemical kinetic modelling a two-step kinetic mechanism is used. The first of the two global rate equations controls the disapperance of methane, and the second the oxidation of carbon monoxide.

The first part of the study included the defination of the mesh structure. Different mesh structures tested to give the best results and to make the structure independent from the calculation results. It is seen that the results taken from the simulation cycle do not change with the increasing cell numer after a limit value and the results are in good agrement with the experimental results. According to this mesh structure that includes 21337 cells and 21426 vertices defined as the modeling mesh structure.

In this study the impacts of the engine speed, intake temperature and compression ratio parameters to the HCCI combustion phase and ignition starting are also investigated. To understand the engine speed effect three different engine speed at 600 rpm, 1000rpm and 1600 rpm is simulated. It is seen that the lower kinetic reaction phase of the combustion are almost same at each speed. On the other hand, for the second stage of the combustion, when it is considered in real time in seconds it is seen that the main combustion begins earlier and the combustion duration decreases as the engine speed increase. It is also seen from these investigations that, the pressure and the temperatures at the end of the compression stroke are high at low engine speeds.

The intake temperature parameter which is commonly used for controlling HCCI engine combustion is investigated in three different values. Because of that

simulation cycle begins at 90 CAD ABDC, the initial temperatures adjusted to conform the intake temperature. The simulation performed at 400K, 450K and 500K initial temperatures. It is known that in all cases, the effect of increasing inlet charge temperature is to advance auto-ignition timing and decrease combustion duration. This study is in good agreement in this decision. Both the low temperature reactions and main combustion begin earlier with increasing inlet temperatures. It is noted that increased intake temperatures also increase the cylinder temperature at the end of the compression stroke while decreasing the cylinder pressure.

Similar effects on combustion are seen in compression ratio parameter. 23:1, 19.8:1 and 18:1 compression ratios were studied. The low temperature reactions began in earlier time with increasing compression ratio. The simulated results showed that cool flames begin at 34 CAD BTDC at 23 :1, 26 CAD BTDC at 19.8:1 and 24 CAD BTDC at 18:1 compression ratios. Similar to this it is also shown that main combustion start get earlier as the compression ration increase. Main combustion began 6 CAD BTDC at 23:1, 3CAD BTDC at 19.8:1 and 2CAD ATDC at 18:1 compression ratio increased. The main combustion duration values are 8 CAD, 7 CAD, 4 CAD relative to 18:1, 19.8:1. 23:1. This means that main combustion period get shorter at high compression ratios. It is also seen that increasing compression ration causes high pressure and temperature values at the end of compression stroke.

This work shows that three-dimensional modeling of methane HCCI engine is possible with good agreement to the experimental data.

REFERENCES

[1] **Johansson, B.**, 1996. Cycle to Cycle Variations in SI Engines - The Effects of Fluid Flow and Gas Composition in the Vicinity of the Spark Plug on Early Combustion, *SAE Paper No: 9962084.*

[2] **Onishi, S., Hong Jo, S., Shoda, K., Do Jo, P. and Kato, S.**, 1979. Active Thermo-Atmosphere Combustion (ATAC) – A New Combustion Process for Internal Combustion Engines, *SAE Paper No: 790501*.

[3] **Christensen, M., Einewall, P. and Johansson, B.**, 1997. Homogeneous Charge Compression Ignition (HCCI) Using Iso-octane, Ethanol and Natural Gas- A Comparison to Spark Ignition Operation, *SAE Paper No: 972874.*

[4] **Christensen, M., Johansson, B., Amnéus, P. and Mauss, F.**, 1998. Supercharged Homogeneous Charge Compression Ignition, *SAE Paper No: 980787.*

[5] **Christensen, M. and Johansson B.**, 1998. Influence of Mixture Quality on Homogeneous Charge Compression Ignition, *SAE Paper No: 982454.*

[6] **Christensen, M. and Johansson B.**, 1999. Homogeneous Charge Compression Ignition with Water Injection, *SAE Paper No: 1999-01-0182*.

[7] **Najt, P. M. and Foster, D. E.**, 1983. Compression-Ignited Homogenous Charge Combustion, *SAE Paper No: 830264*.

[8] **Aoyama, T., Hattori, Y., Mizuta, J. and Sato, Y.**, 1996. An Experimental Study on Premixed-Charge Compression Ignition Gasoline Engine, *SAE Paper No: 960081*.

[9] **Nakano, M., Mandokoro, Y., Kubo, S. and Yamazaki, S.**, 2000. Effects of exhaust gas recirculation in homogenous charge compression ignition engines, *Int J Engine Research*, Volume 1, No. 3, pp. 269-279.

[10] **Lavy, J., Dabadie, J., Angelberger, C., Duret, P., Willand, J., Juretzka, A., Schaflein, J., Ma, T., Lendresse, Y., Satre, A., Schulz, C., Kramer, H. and Zhao, H.**, 2000. Innovative Ultra-low NOx Controlled Auto-Ignition Combustion Process for Gasoline Engines: the 4-SPACE Project, *SAE Paper No: 2000-01-1837*.

[11] **Law, D., Kemp, D. and Allen, J.,** 2001. HCCI Mode of Combustion in a Single Cylinder 4-Stroke Engine Fitted With Active Valve Train, *SAE Paper No: 2001-01-0251*.

[12] **Thring, R. H.,** 1989. Homogenous Charge Compression-Ignition (HCCI) Engines, *SAE Paper No: 892068*.

[13] **Ryan III, T. W. and Callahan, T. J.,** 1996. Homogenous Charge Compression Ignition of Diesel Fuel, *SAE Paper No: 961160*.

[14] **Lida, N.,** 1994. Combustion Analysis of Methanol-Fuelled Active Thermo-Atmosphere Combustion (ATAC) Engine Using Spectroscopic Observation, *SAE Paper No: 940684*.

[15] **Amneus, P., Nilsson, D., Mauss, F. and Christensen, M.,** 1998. Homogenous Charge Compression Ignition Engine: experiments and detailed kinetic calculations", *4th International Symposium Comodia 1998*, pp. 567-572.

[16] **Furutani, M., Ohta, Y., Kono, M. and Hasegawa, M.,** 1998. An ultra-lean premixed compression-ignition engine concept and its characteristics, *4th International Symposium Comodia 1998*, pp. 173-177.

[17] **Christensen, M., Hultqvist, A. and Johansson, B.,** 1999. Demonstrating the Multi Fuel Capability of a Homogenous Charge Compression Ignition Engine with Variable Compression Ratio, *SAE Paper No: 1999-01-3679.*

[18] **Oakley A., Zhao, H., Ladommatos, N. and Ma, T.,** 2001. Experimental Studies on Controlled Auto-Ignition (CAI) Combustion of Gasoline in a 4-Stroke Engine, *SAE Paper No: 2001-01-1030*.

[19] **Olsson, J. and Johansson, B.,** 2001. Closed Loop Control of an HCCI Engine, *SAE Paper No: 2001-01-1031*.

[20] **Noguchi, M., Tanaka, Y., Tanaka, T. and Takeuchi, Y.,** 1979. A study on gasoline engine combustion by observation of intermediate reactive products during combustion, *SAE Paper No: 790840.*

[21] **Ishibashi, Y. and Asai, M.,** 1996. Improving the exhaust emissions of two-stroke engines by applying the Activated Radical Combustion, *SAE Paper No: 960742.*

[22] **Gentilli, R., Frigo, S., Tognotti, L., Habert P. and Lavy, J.,** Experimental study on ATAC (Active Thermo Atmosphere Combustion) in a two-stroke gasoline engine, *SAE Paper No: 970363.*

[23] **Gentilli, R. and Frigo, S.,** 2000. Further insight on ATAC and GDI combination in two-stroke engines, *SAE Paper No: 2000-01-0897.*

[24] **Oppenheim, A. K.,** 1998. Quest for Controlled Combustion Engines, *SAE Paper No: 880572*.

[25] **Oppenheim , A K.,** 1984. The Knock Syndrome. Its Cures and Its Victims, *SAE Paper No: 841339.*

[26] **Kowalewicz, A.,** 1984. Combustion Systems of High Speed Piston IC Engines, *Wydawnictwa Komunikacji*, Warsaw.

[27] **Pouring, A.,** 1993. The Evolution of the Sonex Combustion System (SCS), *Sonex Research Inc*, Annapolis, Maryland.

[28] **Lu, J.**, 1994. A Preliminary Study of Chemically Enhanced Autoignition Internal Combustion Engine, *SAE Paper No: 940758*.

[29] **Shoji, H.,** 1994. Radical Behavior in Preflame Reactions Under Knocking Operation in a Spark Ignition Engine, *SAE Paper No: 942061*.

[30] **Fish, A.,** 1969. The Controlling Role of Cool Flames in Two-Stage Ignition", *Combustion and Flame*, Volume 13, PP 39-49.

[31] **Jost, W. and Martinengo,A.,** 1966. Recent Investigations of Reaction Processes by Means of Adiabatic Compression, *SAE Paper No: 660347.*

[32] **Gussak, L.A.,** 1975. High Chemical Activity of Incomplete Combustion Products and a Method of Prechamber Torch Ignition for Avalanche Activation of Combustion in Internal Combustion Engines, *SAE Paper No: 750890.*

[33] **Gussak, L.A.,** 1979. The Application of Lag-Process in Prechamber Engines, *SAE Paper No: 790692*.

[34] **Ryan,T.W. and Callahan,T.J., 1995.** Homogenous Charge Compression Ignition of Diesel Fuel, *Proceedings of 1995 KSEA International Technical Conference Part 1-Automotive Technology*, San Francisco.

[35] **Blarigan, V.P., Paradiso, N. and Goldsborough S.,** 1998. Homogeneous Charge Compression Ignition with a Free Piston: A New Approach to Ideal Otto Cycle Performance, *SAE Paper No: 982484*.

[36] **Stockinger, M., Schäpertöns, H. and Kuhlman, P.,** 1992. Versuche an einem gemischansugenden Verbrennungsmotor mit Selbstzündung, *MTZ Motortechnisches Zeitschrift*, Volume 53 , pp. 80 – 85, Feburary.

[37] **Osses, M., Andrews, G.E. and Greenhough, J.,** 1998. Diesel Fumigation Partial Premixing for Reduced Particulate Soot Fraction Emissions, *SAE Paper No: 980532*.

[38] **Suzuki, H., Koike, N., Ishii, H. and Odaka, M.,** 1997. Exhaust Purification of Diesel Engines by Homogeneous Charge with Compression Ignition Part 1: Experimental Investigation of Combustion and Exhaust Emissions Behavior Under Pre-Mixed Homogeneous Charge Compression Ignition Method, *SAE Paper No: 970313*.

[39] **Ogawa, H., Chenyu L., Tosaka, S., Fujiwara, Y. and Miyamoto, N.,** 1998. Combustion Mechanism Analysis with In-Chamber Gas Composition Measurements in a Premixed Lean Compression Ignition Engine, *Proceedings of the Fourth International Symposium Comodia 98*, pp. 167- 172.

[40] **Yokota, H., Kudo, Y., Nakajima, H., Kakegawa, T. and Suzuki T.,** 1997. A New Concepts for Low Emission Diesel Combustion, *SAE Paper No: 970891*.

[41] **Miyamoto, T., Harada, A., Sasaki, S., Shimazaki, N., Hashizume, T., Akagawa, H., Tsujimura, K. and Hayashi, A.K.,** 1998b. Numerical Simulation of Fuel-Air Mixture Formation, Ignition and Combustion in a DI Premixed Lean Diesel Combustion Engine, Paper No. IWASC9821, *Proceedings of the Second International Workshop on Advanced Spray Combustion*, Hiroshima, Japan.

[42] **Harada, A., Shimazaki, N., Satoru, S., Miyamoto, T., Akagawa, H. and Tsujimura, K.,** 1998. The Effects of Mixture Formation on Premixed Lean Diesel Combustion, *SAE Paper No: 980533*.

[43] **Wabuchi, Y., Kawai, K., Shoji, T. and Takeda, Y.,** 1999. Trial of New Concept Diesel Combustion System – Premixed Compression-Ignited Combustion, *SAE Paper No: 1999-01-0185*.

[44] **Takeda, Y. and Keiichi, N.,** 1996. Emission Characteristics of Premixed Lean Diesel Combustion with Extremely Early Staged Fuel Injection, *SAE Paper No: 961163.*

[45] **Nakagome, K., Shimazaki, N., Miimura, K. and Kobayashi, S.,** 1997. Combustion and Emissions Characteristics of Premixed Lean Diesel Combustion Engine, *SAE Paper No: 970898*.

[46] **Gray III, A.W. and Ryan III, T.W.,** 1997. Homogeneous Charge Compression Ignition (HCCI) of Diesel Fuel, *SAE Paper No: 971676*.

[47] **Stanglmaier, R. H., Li, J. and Matthews, R.D.,** 1999. The Effect of In-Cylinder Wall Wetting Location on the HC Emissions from SI Engines, *SAE Paper No: 1999-01-0502*.

[48] **Kimura, S., Matsui, Y. and Kamihara, T.,** 1997. A New Concept of Combustion Technology in Small DI Diesel Engines – 4th Report: The Effects of Fuel Injection Rates on MK Combustion, *JSAE Technical Paper No. 9738913*, Tokyo, Japan.

[49] **Kimura, S., Matsui, Y. and Koike, M.,** 1998. New Combustion Concept for Simultaneous Reduction of NOx and Particulate Emissions from Small DI Diesel Engines, Paper No. F98T132, *Proceedings of the 1998 FISITA World Automotive Congress*, Paris, France.

[50] **Aiyoshizawa, E., Muranaka, S., Kawashima, J. and Kimura, S.,** 1998. Development of a New 4-Valve/Cylinder Small DI Diesel Engine Application of the MK Combustion Concept (Report 2), *JSAE Technical Paper No. 9832116*, Tokyo, Japan.

[51] **Mase, Y., Kawashima, J., Sato, T. and Eguchi, M.,** 1998. Nissan's New Multivalve DI Diesel Engine Series, *SAE Paper No: 981039*.

[52] **Furutani, M., Ohta, Y. and Komatsu, K.,** 1993. Onset Behavior of Low-Temperature Flames Caused by Piston Compression, *JSAE Review*, Volume14, No.2, pp. 12-18, April.

[53] **Pucher, G.R., Gardiner, D.P., Bardon, M.F. and Battista, V.,** 1996. Alternative Combustion Systems for Piston Engines Involving Homogeneous Charge Compression Ignition Concepts - A Review of Studies Using Methanol, Gasoline and Diesel Fuel, *SAE Paper No: 962063*.

[54] **Green, R.M., Cernansky, N.P., Pitz, W.J. and Westbrook, C.K.,** 1987. The Role of Low Temperature Chemistry in the Autoignition on N-Butane, *SAE Paper No: 872108*.

[55] **Addargarla, S., Henig, Y., Wilk, R.D., Miller, D.L. and Cernansky, N.P.,** 1989. Effect of Fuel-Air Mixture Stressing on Preignition Heat Release in a Knock Research Engine, *SAE Paper No: 892082*.

[56] **Kong, S.C., Ayoub, N. and Reitz, R.D.,** 1992. Modeling Combustion in Compression Ignition Homogeneous Charge Engines, *SAE Paper No: 920512*.

[57] **Hashizume, T., Miyamoto, T., Akagawa, H. and Tsujimura, K.,** 1998. Combustion and Emission Characteristics of Multiple-Stage Diesel Combustion, *SAE Paper No: 980505*.

[58] **Ishii,H., Koike, N., Suzuki, H. and Odaka, M.,** 1997. Exhaust Purification of Diesel Exhaust by Homogeneous Charge with Compression Ignition – Part 2: Analysis of Combustion Phenomena and NOx Formation by Numerical Simulation With Experiment, *SAE Paper No: 970315*.

[59] **Gray III, A.W., Ryan III, T.W., Roberts, C.E. and Dodge, L.G.,** 1998. Homogeneous Charge Compression Ignition (HCCI) Emissions Formation, Paper No. 98ATE031, *presented at the 31st ISATA Symposium*, Düsseldorf, Germany.

[60] **Dodge L.G. and others,** 1998. Modeling NOx Emissions from Lean-Burn Natural Gas Engines, *SAE Paper No: 981389.*

[61] **Dickey, D.W., Roberts, C.E. and Stanglmaier, R.H.,** 1999. Simultaneous Reduction of Diesel Engine NOx and Fuel Consumption Using Homogeneous Combustion, *JSAE Paper No: 9933646*.

[62] **Roberts, C.E. and Matthews, R.D.,** 1996. Development and Application of an Improved Ring Pack Model for Hydrocarbon Emission Studies, *SAE Paper No: 961966.*

[63] **Odaka, M., Suzuki, H., Koike, N. and Ishii, H.,** 1999. Search for Optimizing Control Method of Homogeneous Charge Diesel Combustion, *SAE Paper No: 1999-01-0184.*

[64] **Heywood, J., Higgins, J., Watss, P. and Tabaczynski, R.,** 1979. Development and Use of a Cyde Simulation to Predict SI Engine Efficiency and NO_x Emissions, *SAE Paper No: 790291*.

[65] **Smith, J.R., Aceves, D.N., Westbrook, C. and Pitz, W.,** 2000. Modeling of Homogeneous Charge Compression Ignition (HCCI) of Mathane, *ASME Fall Technical Conference*, ICE-Volume 29-3.

[66] **Amneus, P., Nilsson, D., Mauss, F., Christensen, M. and Johansson, B.,** 1998. HCCI Engine: Experiments and Detailed Kinetic Calculations, *COMODIA 98*, p.567-572.

[67] **Fiveland, S.B. and Assanis, D.N.,** 2000. A Four-Stroke homogeneous charge compression ignition engine for combustion and performance studies, *SAE Technical Paper Series*, Paper Number 2000-01-0332.

[68] **Hiltner, J., Agama, R., Mauss, F. and Johansson, B.,** 2000. HCCI Operation with Natural Gas: Fuel Composition Implications, *ASME 2000 Fall Engine Technology Conference*, September 24-27, Peoria, Illinois, USA.

[69] **Flowers, D.L., Aceves, S.M., Westbrook, C.K., Smith, J.R. and Dibble, R.W.,** 1999. Sensitivity of Natural Gas HCCI Combustion to Fuel and Operating Parameters Using Detailed Kinetic Modeling, In AES-Volume 39, *Proceedings of the ASME Advanced Energy Systems Division-1999,* Edited by S.M. Aceves, S. Garimella and R. Peterson, pp. 465-473

[70] **Karim, G.A. and Liv, Z.,** 1992. A Predictive Model for Knock in Duel Fuel Engines, *SAE Paper No: 921550*.

[71] **Karim, GA. and Gao, J.,** 1993. Prediction of the Performance of Spark-Ignition Gas Engines Including Knock, *SAE Paper No: 932823.*

[72] **Karim, GA. and Attar A.A.,** 1997. An Analytical Approach For The Optimization of a Gas Fueled SI Engine Performance Including The Consideration of Knock, ICE-Volume 28-2, *1997 Spring Technical Conference*, Calgary, Albert, Canada, 65-71.

[73] **Hajizera, S., Mauss, F. and Sunden, B.,** 1997. Investigation of End Gas Temperature and Pressure Increases in Gasoline Engines and Relevance for Knock Occurrence, *SAE Paper No: 971671.*

[74] **Hajizera, S.,** 1998. Modeling Approaches for Investigation of End-Gas Thermodynamic Characteristics in SI Engines Related to Knock, *Licentiate Thesis*, Lund Institute of Technology, Lund, Sweden.

[75] **Hajizera, S.,** 1999. A There Zone Model for Investigation of Gas Behavior In the Combustion Chamber of SI Engines in Relation to Knock, *SAE Paper No: 1999-01-0219.*

[76] **Jenkin, R.J., James, E.H. and Malalasekera, W.,** 1996. Thermal Boundary Layer Modelling in Motored Spark Engine, *SAE Paper No: 961965.*

[77] **Jenkin, R.J., James, E.H. and Malalasekera, W.,** 1997. Predicting the Onset of Endgas Autoignition with a Quasi-Dimensional Spark Ignition Engine Model, *SAE Paper No: 972877.*

[78] **Natarajan, B. and Bracco, F.V.,** 1984. On Multidimensional Modeling of Autoignition in SI Engine, *Combustion and Flame*, 57, 179-197.

[79] **Schapertons, H. and Lee, W.,** 1985. Multidimensional Modeling of Knocking Combustion in SI Engines, *SAE Paper No: 850502*.

[80] **Lund, C.M.,** 1978. HCT - A General Computer Program for Calculating Time-Dependent Phenomena Involving One-Dimensional Hydrodynamics, Transport, and Detailed Chemical Kinetics, *Lawrence Livermore National Laboratory report, U*CRL-52504.

[81] **Kee, R.J., Rupley, F.M., Meeks, E. and Miller, J.A.,** 1996. CHEMKIN III: A Fortran Chemical Kinetics Package for the Analysis of Gas-Phase Chemical and Plasma Kinetics, *Sandia National Laboratories Report*, SAND96-8216, Livermore, CA, May.

[82] **Aceves, S.M., Smith, J.R., Westbrook, C. and Pitz, W.,** 1999. Compression Ratio Effect on Methane HCCI Combustion, *ASME Journal of Gas Turbines and Power*, Volume 121, pp. 569-574.

[83] **Aceves, S.M., Flowers, D.L., Westbrook, C.K., Smith, J.R., Pitz, W.J., Dibble, R., Christensen, M. and Johansson, B.,** 2000. A Multi-Zone Model for Prediction of HCCI Combustion and Emissions, *SAE Paper No: 2000-01-0327.*

[84] **Maigaard, P., Mauss, F. and Kraft, M.,** 2000. Homogeneous Charge Compression Ignition Engine: A Simulation Study on the Effects of Inhomogeneities, *Proceedings of the ASME 2000 Spring Technical Conference*, Paper No. 2000-ICE- 275, ICE-Volume 34-2, pp. 63-70.

[85] **Firas, J.M., Aceves, S.M., Flowers, D., Smith, J.R. and Dibble, R.,** 2001. Equivalence Ratio-EGR Control of HCCI Engine Operation and the Potential for Transition to Spark-Ignited Operation, *SAE Paper No: 2001-01-3613.*

[86] **Aceves, S.M., Firas, J.M., Flowers, D., Smith, J.R., Dibble, R., Wright, J.F. and Hessel, R.P.,** 2001. A Decoupled Model of Detailed Fluid Mechanics Followed by Detailed Chemical Kinetics for Prediction of Iso-Octane HCCI Combustion, *SAE Paper No: 2001-01-3612*.

[87] **Ogink, R. and Golovitchev, V.,** 2001. Gasoline HCCI Modeling: Computer Program Combining Detailed Chemistry and Gas Exchange Processes, *SAE Paper No: 2001-01-3614.*

[88] **Fiveland, S.B., Agama, R., Christensen, M., Johanson, B., Hiltner, J., Maus, F. and Assanis, D.N.,** 2001. Experimental and Simulated Results Detailing the Sensitivity of Natural Gas HCCI Engines to Fuel Composition, *SAE Paper No: 2001-01-3609.*

[89] **Frias, J.M., Aceves, S.M., Flowers, D., Smith, J.R. and Dibble, R.,** 2000. HCCI Engine Control by Thermal Management, *SAE Paper No: 2000-01-2869.*

[89] **Soyhan, H.S.,** 2000. Chemical Kinetic Modeling of Autoignition Under Conditions Relevant To Knock In Spark Ignition Engines, *Ph.D. Thesis*, Istanbul Technical University.

[90] **Soyhan, H.S., Lovas, T. and Mauss, F.,** 2001. A Stochastic Simulation Of An HCCI Engine Using An Automatically Reduced Mechanism, *ASME Fall Technical Conference*, ICE-Volume 37-2.

[91] **Warnatz, J.,** 1992. Resolution of Gas Phase and Surface Combustion Chemistry into Elementary Reactions, *24. Symposium on Combustion*, The Combustion Institute, Sydney, Australia, July 5-10, 533-579.

[92] **Wilk, R.D., Pitz, W.J., Westbrook, C.K., Addagarla, S., Miller, D.L., Cernansky, N.P. and Green, R.M.,** 1990. Combustion of n-Butane and iso-butane in an Internal Combustion Engine: A Comparison of Experimental and Modeling Results, *23. Symposium on Combustion*, The Combustion Institute, Orleans, France, July 22-27, 1047-1053.

[93] **Westbrook, C.K., Pitz, W.J. and Warnatz, J.,** 1988. A Detailed Chemical Kinetic Reaction Mechanism for the Oxidation of iso-Octane and n-Heptane Over an Extended Temperature Range and its Application to Analysis of Engine Knock, *22. Symposium on Combustion*, The Combustion Institute, Seattle, WA, USA, August 14-19, 893-901.

[94] **Smith, J.R, Green, R.M., Westbrook, C.K. and Pitz, W.J.,** 1984. An Experimental Study of Engine Knock, *20. Symposium on Combustion*, The Combustion Institute, Ann Arbor, Michigan, August 12-17, 91-100.

[95] **Blurock, E.,** 1995. Reaction : System for Modeling Chemical Reactions, *J. Chem. Info. Comp. Sci.*, 35, 607-616.

[96] **Tomlin, A.S., Turanyi, T. and Pilling, M.J.,** 1997. Mathematical Tools for Construction, Investigation, and Reduction of Combustion mechanism, in Low Temperature Combustion and Autoignition, *Comprehensive Chemical Kinetics*, pp.293-437, Elsevier, Amsterdam.

[97] **Come, G., Warth, V., Glaude, A., Fournet, R., Leclerc, F.B. and Scacchi, G.,** 1996. Computer Aided Design of Gas-Phase Oxidation Mechanism Application to the Modeling of n-Heptane and iso-Octane Oxidation, *20. Symposium on Combustion*, The Combustion Institute, Napoli, Campi Phlearaci , Italy, July 28-August 2, 755-762.

[98] **Curran, H.J., Pitz, W.J., Westbrook, C.K., Gaffuri, P. and Leppard, W.R.,** 1996. Autoignition Chemistry in a Motored Engine: An Experimental and Kinetic Modeling Study, *20. Symposium on Combustion*, The Combustion Institute, Napoli, Campi Phlearaci , Italy, July 28-August 2, 2669-2677

[99] **Kojima, S.,** 1994. Detail Modelling of n-Butane Autoignition Chemistry, *Combustion And Flame*, 99, 87-136.

[100] **Warnatz, J.,** 1981. The structure of Laminar Alkane-, Alkene-, and Acetylene Flames, *18. Symposium on Combustion*, The Combustion Institute, Waterloo, Canada, August 17-22, 369-383.

[101] **Soyhan, H., Amneus, P., Mauss, F. and Sorusbay, C.,** 1999b. A Skeletal Kinetic Mechanism for the Oxidation of Iso-Octane and n-heptane Validated under Engine Knock Conditions, *SAE Paper No: 1999-01-3484*.

[102] **Soyhan, H., Amneus, P., Lovas, T., Nilsson, D., Maigaard, P., Mauss, F. and Sorusbay, C.,** 2000. Automatic Reduction of Detailed Chemical Reduction Mechanisms for Autoignition under SI Engine Conditions, *SAE Paper No: 960827*.

[103] **Massias, A., Diamantis, D., Masorakos, E. and Goussis, D.,** 1999. An Algorithm for the Construction of Global Reduced Mechanisms with CSP Data, *Combustion and Flame*, 117, 685-708.

[104] **Griffiths, J.F.,** 1994. Reduced Kinetic Models and their Application to Practical Combustion Systems, *Progress Energy Combustion Science*, 21, 25-107.

[105] **Halstead, M., Kirsch, L. and Quinn, C.,** 1977. The Autoignition of Hydrocarbon Fuels at High Temperatures and Pressure-Fitting of a Mathematical Model, *Combustion and Flame*, 30, 45-60.

[106] **Cox, R. and Cole, J.,** 1985. Chemical Aspects of the Autoignition of Hydrocarbon Air Mixture, *Combustion and Flame*, 60, 109-123.

[107] **Hu, H. and Keck, J.,** 1987. Autoignition of Adiabatically Compressed Combustible Gas Mixture, *SAE Paper No: 872110*.

[108] **Benson, S.W.,** 1986. Combustion, A Chemical and Kinetic View, *21. Symposium on Combustion*, The Combustion Institute, Munich, Germany, August 3-8, 703-711.

[110] **Chun, K.M. and Heywood, J.B.,** 1989. A Knock Anticipating Strategy Basing on the Real-Time Combustion Mode Analysis, *SAE Paper No: 890882*.

[111] **Brussovansky, S., Heywood, J.B. and Keck, J.C.,** 1992. Predicting The Effects of Air and Coolant Temperature, Deposits, Spark Timing and Speed on Knock in Spark Ignition Engines, *SAE Paper No: 922324*.

[112] **Cowart, J., Haghgooie, M., Newman, C., Davis, G., Pitz, W. and Westbrook, C.,** 1992. The Intensity of Knock in an Internal Combustion Engine: An Experimental and Modeling Study, *SAE Paper No: 922327*.

[113] **Li, H., Miller, D.L. and Cernansky, N.P.,** 1992. A Study on the Application of a Reduced Chemical Reduction Model to Motored Engines for Heat Release Prediction, *SAE Paper No: 922328*.

[114] **Paczko, G., Lefdal, P.M. and Peters, N.,** 1986. Reduced Reaction Schemes for Methane, Methanol and Propane Flames, *21. Symposium on Combustion Institute*, The Combustion Institute, Munich, Germany, August 3-8, 739-748.

[115] **Glarborg, P., Lilleheie, I., Bygtoyl, S., Magnusen, F., Kilpinen, P. and Hupo, M.,** 1992. A Reduced Mechanism for Nitrogen Chemistry in Methane Combustion, *24. Symposium on Combustion*, The Combustion Institute, Sydney, Australia, July 5-10, 889-898.

[116] **Nakano, M., Nakahara, S., Akihima, K., Kubo, S. and Yamazahi, S.,** 1995. Predictions of the Knock Onset and the Effects of Heat Release Pattern and Unburned Gas Temperature on Torque at Knock Limit in S.I. Engines, *SAE Paper No: 952408*.

[117] **Wang, S., Miller, D.L. and Cernansky, N.P.,** 1996a. Prediction of Preignition Reactivity for n-Butane Blends Using A Reduced Chemical Kinetic Model, *SAE Paper No: 961154*.

[118] **Li, H., Miller, D.L. and Cernansky, N.P.,** 1996. Development of a Reduced Chemical Kinetic Model for Prediction Reactivity and Autoignition of Primary Reference Fuels, *SAE Paper No: 960498*.

[119] **Wang, S., Miller, D.L. and Cernansky, N.P.,** 1996b. A Reduced Chemical Kinetic Model for Autoignition of The Butanes, *SAE Paper No: 962106*.

[120] **Roberts, C.E., Matthews, R.D. and Leppard, W.R.,** 1996. Development of a Semi-Detailed Kinetics Mechanism for the Autoignition of iso-Octane, *SAE Paper No: 962107*.

[121] **Griffiths, J.F., Hughes, K.J., Schreiber , M. and Poppe, C.,** 1994. A Unified Approach to the Reduced Kinetic Modeling of Alkane Combustion, *Combustion and Flame*, 99, 533-540.

[122] **Grouset, D., Plion, P., Znaty, E. and Galany, S.,** 1986. Development of a Variational Method for Chemical Kinetic Sensitivity Analysis, *21. Symposium on Combustion*, The Combustion Institute, Munich, Germany, August 3-8, 795-807.

[123] **Chevalier, C., Pitz, W.J., Warnatz, J., Westbrook, C.K. and Melenk, H.,** 1992. Hydrocarbon Ignition: Automatic Generation of Reaction Mechanism and Applications to Modeling of Engine Knock, *24. Symposium on Combustion*, The Combustion Institute, Sydney, Australia, July 5-10, 93-101.

[124] **Neshe, M., Warnatz, J. and Chevalier, C.,** 1996. KineticModeling of the Oxidation of Large Aliphatic Hydrocarbons, *26. Symposium on Combustion*, The Combustion Institute, Napoli, Campi Phlearaci, Italy, July 28 - August 2, 1-18.

[125] **Somers, L.M.T. and Goey, L.P.H.,** 1994. Analysis of a Systematical Reduction Technique, *25. Symposium on Combustion Institute*, Irvine, California, July31- August 5, 957-963.

[126] **Soyhan, H., Amneus, P., Mauss, F. and Sorusbay, C.,** 1999a. A Skeletal Kinetic Mechanism for Natural Gas Fuelled SI Engine, *ULIBTK'99 Conference on Thermal Sciences and Technologies*, Volume 1, Sakarya, Turkey, February 28-29, 204-209.

[127] **Nilson, D.,** 2000. Analysis and Reduction of Fuel and Pollutant Chemistry in Combustion Systems, *Licentiate Thesis*, Lund Institute of Technology, Lund, Sweden.

[128] **Nilsson, D., Lovas, T., Amneus, P. and Mauss, F.,** 1999. Reduction of Complex Fuel Chemistry for Simulation of Combustion in an HCCI Engine, *VDI-Berichte 1492*, VDI Verlag, Tagung Dresden, Germany, September 14-15, 511-516.

[129] **Lovas, T., Nilsson, D. nad Mauss, F.,** 1999. Development of Reduced Chemical Mechanisms for Nitrogen Containing Fuels, *Proceedings of 5. International Conference on Technologies and Combustion for a Clean Environment*, Portuguese Section of the Combustion Institute, Lisbon, Potugal, July 12-15, 139-143.

[130] **Eggels, R.L. and Goey, L.P.,** 1995. Mathematically Reduced Reaction Mechanisms Applied to Adiabatic Hydrogen/Air Flames, *Combustion and Flame*, 100,559-570.

[131] **Turanyi, T.,** 1994. Application of Repro-Modeling for the Reduction of Combustion Mechanisms, *25. Symposium on Combustion*, The Combustion Institute, Irvine, California, July 31 – August 5, 949-955.

[132] **Maas, U. and Warnatz, J.,** 1988. Ignition Processes in Hydrogen-Oxygen Mixtures, *Combustion and Flame*, 74, 53-69.

[133] **Niemann, H., Schmidt, D. and Maas, U.,** 1996. An Efficient Storage Scheme for Reduced Chemical Kinetics Based on Orthogonal Polynomials, *Konrad Zuse Zentrum fur Informationtechnik*, Berlin, Germany, Preprint SC. 96-18.

[134] **Tomlin, A.S., Pilling, M.J., Turanyi, T., Merkin J.H. and Brindley, J.,** 1992. Mechanism Reduction for the Oscillatory Oxidation of Hydrogen: Sensitivity and Quasi-Steady-State Analyses, *Combustion and Flame*, 91, 107.

[135] **Westbrook, C.K. and Dryer, F.L.,** 1981. Chemical Kinetics and Modeling of Combustion Process, *18. Symposium on Combustion*, The Combustion Institute, Waterloo, Canada, August 17-22, 749-767.

[136] **Hirt, C.W., Amsden, A.A. and Cook, J.L.,** 1974. *J. Comput. Phys. 14*,227..

[137] **Pracht, W.E.,** *1975. J. Comput. Phys. 17,132.*

[138] **Roache, P.J.,** 1982. *Computational Fluid Dynamics,* Hermosa Publishers, Albuquerque, New Mexico.

[139] **Leer B. van,** 1979. *J. Comput. Phys. 32*, 101.

[140] **Ramshaw, J.D., O'Rourke, P.J. and Stein, L.R.,** 1985. *J. Comput. Phys. 58*, 361.

[141] **Tsao, K.C. and Han, Z.,** 1993**.** An Exploratory Study on Combustion Modeling and Chamber Design of Natural Gas Engines, *SAE Paper No: 962107.*

[142] **Christensen, M., Hultqvist, A., Johansson, B.,** 1999**.** Demonstrating the Multi Fuel Capability of a Homogeneous Charge Compression

Ignition Engine with Variable Compression Ratio, *SAE Paper No: 1999-01-3679*

CURRICULUM VITAE

Mr. Alper Kutluata is graduated with a B.Sc. Degree in Mechanical Engineering from the Istanbul Technical University in 2000. He has been working on his M.Sc. degree at the division of Automotive Engineering at the same university since 2000.